

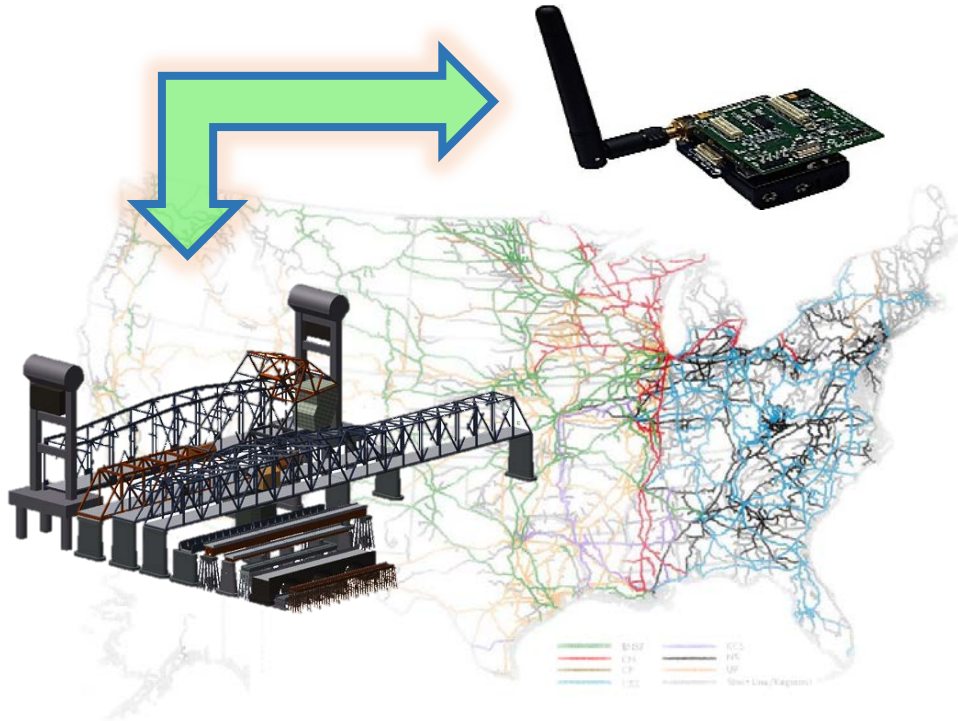


U.S. Department of
Transportation

**Federal Railroad
Administration**

Campaign Monitoring of Railroad Bridges in High-Speed Rail Shared Corridors using Wireless Smart Sensors

Office of Research,
Development,
and Technology
Washington, DC 20590



NOTICE

This document is disseminated under the sponsorship of the Department of Transportation in the interest of information exchange. The United States Government assumes no liability for its contents or use thereof. Any opinions, findings and conclusions, or recommendations expressed in this material do not necessarily reflect the views or policies of the United States Government, nor does mention of trade names, commercial products, or organizations imply endorsement by the United States Government. The United States Government assumes no liability for the content or use of the material contained in this document.

NOTICE

The United States Government does not endorse products or manufacturers. Trade or manufacturers' names appear herein solely because they are considered essential to the objective of this report.

| REPORT DOCUMENTATION PAGE | | | <i>Form Approved</i> <i>OMB No. 0704-0188</i> |
|--|--|---|--|
| Public reporting burden for this collection of information is estimated to average 1 hour per response, including the time for reviewing instructions, searching existing data sources, gathering and maintaining the data needed, and completing and reviewing the collection of information. Send comments regarding this burden estimate or any other aspect of this collection of information, including suggestions for reducing this burden, to Washington Headquarters Services, Directorate for Information Operations and Reports, 1215 Jefferson Davis Highway, Suite 1204, Arlington, VA 22202-4302, and to the Office of Management and Budget, Paperwork Reduction Project (0704-0188), Washington, DC 20503. | | | |
| 1. AGENCY USE ONLY (Leave blank) | 2. REPORT DATE June 2015 | 3. REPORT TYPE AND DATES COVERED Technical Report – July 2014 | |
| 4. TITLE AND SUBTITLE Campaign Monitoring of Railroad Bridges in High-Speed Rail Shared Corridors using Wireless Smart Sensors | | 5. FUNDING NUMBERS | |
| 6. AUTHOR(S) B.F. Spencer, F. Moreu, R. Kim | | | |
| 7. PERFORMING ORGANIZATION NAME(S) AND ADDRESS(ES) University of Illinois at Urbana-Champaign Smart Structures Technology Laboratory Department of Civil and Environmental Engineering 205 N. Matthews Ave. Urbana, IL 61801 | | 8. PERFORMING ORGANIZATION REPORT NUMBER | |
| 9. SPONSORING/MONITORING AGENCY NAME(S) AND ADDRESS(ES) U.S. Department of Transportation Federal Railroad Administration Office of Railroad Policy and Development Office of Research and Development Washington, DC 20590 | | 10. SPONSORING/MONITORING AGENCY REPORT NUMBER DOT/FRA/ORD-15/19 | |
| 11. SUPPLEMENTARY NOTES COTR: Cameron Stuart | | | |
| 12a. DISTRIBUTION/AVAILABILITY STATEMENT This document is available to the public through the FRA Web site at http://www.fra.dot.gov . | | 12b. DISTRIBUTION CODE | |
| 13. ABSTRACT (Maximum 200 words) This research project used wireless smart sensors to develop a cost-effective and practical portable structural health monitoring system for railroad bridges in North America. The system is designed for periodic deployment rather than as a permanent installation to enable campaign-style bridge response monitoring under in-service conditions. This research project measured bridge responses from a 310 feet long steel truss bridge using wireless sensors and developed a finite element (FE) model to obtain global bridge responses under varied train loads and speeds. Additionally, this project developed a new simple beam model that predicts critical speeds and resonances based on train traffic properties. The results from this pilot project provide a technological foundation to develop campaign monitoring sensor technology as an important tool with which to manage railroad bridge assets. | | | |
| 14. SUBJECT TERMS Railroad bridge safety, bridge performance monitoring, wireless sensors, campaign monitoring | | 15. NUMBER OF PAGES 78 | 16. PRICE CODE |
| 17. SECURITY CLASSIFICATION OF REPORT Unclassified | 18. SECURITY CLASSIFICATION OF THIS PAGE Unclassified | 19. SECURITY CLASSIFICATION OF ABSTRACT Unclassified | 20. LIMITATION OF ABSTRACT |

METRIC/ENGLISH CONVERSION FACTORS

ENGLISH TO METRIC

LENGTH (APPROXIMATE)

- 1 inch (in) = 2.5 centimeters (cm)
- 1 foot (ft) = 30 centimeters (cm)
- 1 yard (yd) = 0.9 meter (m)
- 1 mile (mi) = 1.6 kilometers (km)

AREA (APPROXIMATE)

- 1 square inch (sq in, in²) = 6.5 square centimeters (cm²)
- 1 square foot (sq ft, ft²) = 0.09 square meter (m²)
- 1 square yard (sq yd, yd²) = 0.8 square meter (m²)
- 1 square mile (sq mi, mi²) = 2.6 square kilometers (km²)
- 1 acre = 0.4 hectare (he) = 4,000 square meters (m²)

MASS - WEIGHT (APPROXIMATE)

- 1 ounce (oz) = 28 grams (gm)
- 1 pound (lb) = 0.45 kilogram (kg)
- 1 short ton = 2,000 pounds (lb) = 0.9 tonne (t)

VOLUME (APPROXIMATE)

- 1 teaspoon (tsp) = 5 milliliters (ml)
- 1 tablespoon (tbsp) = 15 milliliters (ml)
- 1 fluid ounce (fl oz) = 30 milliliters (ml)
- 1 cup (c) = 0.24 liter (l)
- 1 pint (pt) = 0.47 liter (l)
- 1 quart (qt) = 0.96 liter (l)
- 1 gallon (gal) = 3.8 liters (l)
- 1 cubic foot (cu ft, ft³) = 0.03 cubic meter (m³)
- 1 cubic yard (cu yd, yd³) = 0.76 cubic meter (m³)

TEMPERATURE (EXACT)

$$[(x-32)(5/9)] \text{ } ^\circ\text{F} = y \text{ } ^\circ\text{C}$$

METRIC TO ENGLISH

LENGTH (APPROXIMATE)

- 1 millimeter (mm) = 0.04 inch (in)
- 1 centimeter (cm) = 0.4 inch (in)
- 1 meter (m) = 3.3 feet (ft)
- 1 meter (m) = 1.1 yards (yd)
- 1 kilometer (km) = 0.6 mile (mi)

AREA (APPROXIMATE)

- 1 square centimeter (cm²) = 0.16 square inch (sq in, in²)
- 1 square meter (m²) = 1.2 square yards (sq yd, yd²)
- 1 square kilometer (km²) = 0.4 square mile (sq mi, mi²)
- 10,000 square meters (m²) = 1 hectare (ha) = 2.5 acres

MASS - WEIGHT (APPROXIMATE)

- 1 gram (gm) = 0.036 ounce (oz)
- 1 kilogram (kg) = 2.2 pounds (lb)
- 1 tonne (t) = 1,000 kilograms (kg) = 1.1 short tons

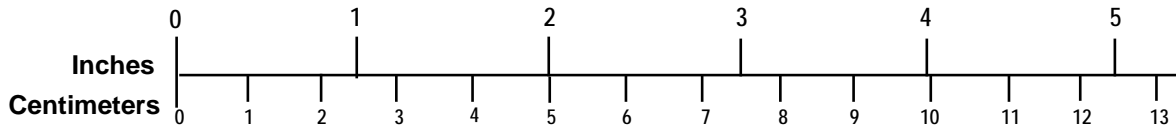
VOLUME (APPROXIMATE)

- 1 milliliter (ml) = 0.03 fluid ounce (fl oz)
- 1 liter (l) = 2.1 pints (pt)
- 1 liter (l) = 1.06 quarts (qt)
- 1 liter (l) = 0.26 gallon (gal)
- 1 cubic meter (m³) = 36 cubic feet (cu ft, ft³)
- 1 cubic meter (m³) = 1.3 cubic yards (cu yd, yd³)

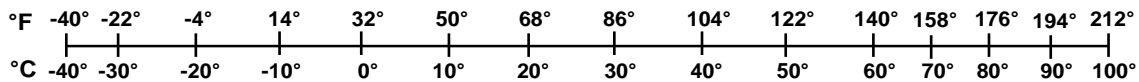
TEMPERATURE (EXACT)

$$[(9/5) y + 32] \text{ } ^\circ\text{C} = x \text{ } ^\circ\text{F}$$

QUICK INCH - CENTIMETER LENGTH CONVERSION



QUICK FAHRENHEIT - CELSIUS TEMPERATURE CONVERSION



For more exact and or other conversion factors, see NIST Miscellaneous Publication 286, Units of Weights and Measures. Price \$2.50 SD Catalog No. C13 10286

Updated 6/17/98

Acknowledgements

The Smart Structures Technology Laboratory (SSTL) and the Rail Transportation and Engineering Center (RailTEC), both located at the University of Illinois at Urbana - Champaign, thank Canadian National Railway (CN) for providing access to the test site railroad bridge, technical support, and for arranging the work train equipment needed to support the research reported herein. In particular, we thank the following CN personnel: Sandro Scola (Chief Bridge Engineer for the US) for general coordination, Alan Craine (Southern Region Chief Engineer) for support during bridge access and coordination, Hoat Le (bridge testing team director) and David Roberts (bridge testing senior engineer) for technical support and advice during the different stages of this project, Matt Gann (track manager) for access to the bridge and general coordination with work train testing with on-going traffic over the bridge, and Cliff Holdren (main foreman), Kyrann Walker, and Bob Coleman for protection at the bridge during the campaign monitoring visits. Additionally, the Illinois research team thanks Norfolk Southern Corporation (NS) and bridge engineer Nila Jackson for information about the NS traffic that researchers used for wireless strain sensor calibration. Finally, the research team thanks the Bridge & Structure Laboratory of the Department of Civil Engineering at the University of Tokyo at Japan and Dr. Tomonori Nagayama for providing magnetic strain checkers and wireless strain sensor boards for the campaign monitoring tests in this project.

Contents

| | |
|---|-------------|
| Acknowledgements | iii |
| List of Figures | v |
| List of Tables | viii |
| EXECUTIVE SUMMARY | 1 |
| 1. INTRODUCTION | 2 |
| 1.1 Background | 2 |
| 1.2 Technology Assessment | 2 |
| 1.3 Organization of the Report | 5 |
| 2. PROJECT DESCRIPTION | 7 |
| 2.1 Project Objectives | 7 |
| 2.2 Technical Approach | 8 |
| 2.3 Industry Participation | 9 |
| 3. MONITORING SYSTEM DEPLOYMENT | 13 |
| 3.1 Finite Element Model | 13 |
| 3.2 Sensor Layout | 14 |
| 3.3 Data Collected under Regular Traffic | 17 |
| 3.4 Data Collected during Work Train Tests | 24 |
| 3.5 Data Collected from Remote Monitoring | 33 |
| 4. RESULTS | 35 |
| 4.1 Bridge FE Model Updating | 35 |
| 4.2 Simple Beam Model | 42 |
| 4.3 Bridge Resonance | 46 |
| 4.4 Reference-Free Displacement Estimation | 53 |
| 4.5 Sample Analysis of Autonomously Collected Data | 56 |
| 4.6 Prioritization of Railroad Bridge Repairs and Replacement | 59 |
| 5. CONCLUSIONS | 61 |
| 5.1 Summary of Achievements | 61 |
| 5.2 Gap Analysis | 62 |
| 6. VISION FOR THE FUTURE | 64 |
| 6.1 Background | 64 |
| 6.2 Recommendations | 65 |
| 6.3 Proposed Research Tasks | 66 |
| APPENDIX: Abbreviations and Acronyms | 68 |

List of Figures

| | |
|---|----|
| Figure 1.1 Campaign monitoring using wireless smart sensors | 3 |
| Figure 1.2 (a) Imote2 with antenna and sacked on battery board, (b) SHM-A sensor board | 4 |
| Figure 1.3 SHM-S sensor board (left), with SHM-DAQ (right)..... | 5 |
| Figure 2.1 Concept of proposed wireless sensing system..... | 7 |
| Figure 2.2 Technical approach for research..... | 9 |
| Figure 2.3 Bridge over the Little Calumet River (near Chicago, IL) | 10 |
| Figure 3.1 Bridge 3D FE model..... | 13 |
| Figure 3.2 (a) Floor system modeling, (b) details of the floor system..... | 14 |
| Figure 3.3 GUI for the FE model..... | 14 |
| Figure 3.4 General layout of the sensors installed at the bridge..... | 15 |
| Figure 3.5 Layout of the rail sensors at the bridge and vicinity | 15 |
| Figure 3.6 (a) Magnet strain checker, (b) magnet strain checker installed at rail..... | 16 |
| Figure 3.7 Train sensors setup | 16 |
| Figure 3.8 Base station for remote wireless sensing monitoring of RR bridges..... | 17 |
| Figure 3.9 Tee-Rosette strain gage rail sensing data | 18 |
| Figure 3.10 Train speed estimation using two wireless strain gages | 18 |
| Figure 3.11 Comparison between conventional and magnetic rail strain..... | 18 |
| Figure 3.12 Estimation of car loadings using wireless smart sensors..... | 19 |
| Figure 3.13 Acceleration measurements at both structure and rail via Auto-Monitor | 20 |
| Figure 3.14 Rail shear strain at LW and structural strain at L4-U5..... | 20 |
| Figure 3.15 LVDT deployment under regular traffic | 21 |
| Figure 3.16 Transverse displacement under freight train | 21 |
| Figure 3.17 Transient transverse displacement under Amtrak train for damping (ζ) estimation . | 22 |
| Figure 3.18 LVDT frequency analysis comparison with accelerometers analysis..... | 22 |
| Figure 3.19 Bridge response under different trains | 23 |
| Figure 3.20 Test data after Amtrak (a) time history, (b) PSD | 24 |
| Figure 3.21 Work train wheel loading scheme | 25 |
| Figure 3.22 Strain measurements at multiple locations under work train | 26 |
| Figure 3.23 Estimated wheel load and work strain wheel load at 5 MPH..... | 26 |
| Figure 3.24 Rail shear strain comparison for all NB work train experiments | 27 |

| | |
|--|----|
| Figure 3.25 IF estimation for both magnetic and conventional strain of a diagonal truss element under different train speeds..... | 28 |
| Figure 3.26 Acceleration comparison (a) L4EH, (b) L4WH..... | 29 |
| Figure 3.27 RMS comparison (a) longitudinal axis, (b) vertical axis, and (c) lateral axis..... | 29 |
| Figure 3.28 Train response comparison (a) idling on track, (b) running on track..... | 31 |
| Figure 3.29 Train response comparisons (a) idling on the bridge, (b) running on the bridge..... | 32 |
| Figure 3.30 Acceleration RMS comparison (a) longitudinal axis, (b) vertical axis, and (c) lateral axis..... | 32 |
| Figure 3.31 Accelerations captured during remote sensing..... | 33 |
| Figure 3.32 Strains collected during remote sensing..... | 34 |
| Figure 3.33 Example of battery voltage monitoring..... | 34 |
| Figure 4.1 Model update validation..... | 35 |
| Figure 4.2 Bridge additional mass elements (a) track system details, (b) element lacing..... | 36 |
| Figure 4.3 Comparison of experimentally identified and model modes and frequencies..... | 37 |
| Figure 4.4 Strain comparisons from measured data and model predictions..... | 38 |
| Figure 4.5 Strain map predicted by the FE model for the work train..... | 41 |
| Figure 4.6 Predicted stress under multiple train loading (a) truss element labeling, (b) stress assessment..... | 42 |
| Figure 4.7 Bridge and train model (a) FE model, (b) simplified beam and moving distributed-mass model, and (c) simplified beam and moving point-mass model..... | 44 |
| Figure 4.8 Distributed-mass model and Point-mass model comparison..... | 45 |
| Figure 4.9 Strain estimation from the beam-mass model (a) instrumented element location, (b) strain comparison..... | 46 |
| Figure 4.10 Examples of time history at mid-span of bridge at certain train speeds (Moving mass model); (a) train speeds at 5 MPH, (b) 50 MPH, (c) 91 MPH (Resonance speed), (d) 100 MPH, (e) 150 MPH..... | 48 |
| Figure 4.11 Vertical bridge response (RMS of acceleration) at mid-span of bridge for the work train..... | 49 |
| Figure 4.12 Vertical bridge response (maximum absolute displacement) at mid-span of bridge for the work train..... | 49 |
| Figure 4.13 Vertical bridge response (maximum dynamic displacement) at mid-span of bridge for the work train..... | 49 |
| Figure 4.14 Maximum lateral displacement of the beam-mass model under various speeds at mid-span of bridge for the work train..... | 50 |
| Figure 4.15 Lateral response of the beam-mass model under the test train (RMS of acceleration)..... | 51 |

| | |
|--|----|
| Figure 4.16 Maximum vertical bridge response under Amtrak trains: (a) vertical, (b) lateral.... | 51 |
| Figure 4.17 Loading distances potentially generating resonance in the bridge..... | 52 |
| Figure 4.18 Car diagram for work train vehicle | 52 |
| Figure 4.19 V_{cr} comparison for resonance under work train (a) vertical, (b) lateral | 53 |
| Figure 4.20 KF estimator | 54 |
| Figure 4.21 KF estimation | 55 |
| Figure 4.22 Simple beam model for KF displacement estimation..... | 55 |
| Figure 4.23 KF numerical example results | 56 |
| Figure 4.24 Auto Monitoring validation (a) NB train 9 MPH, (b) SB train 33 MPH | 57 |
| Figure 4.25 Truss element labeling..... | 58 |
| Figure 4.26 Predicted stresses percentages under open regular traffic (a) one train on West track, (b) two trains | 59 |
| Figure 4.27 Simplified bridge campaign monitoring of railroad bridges | 60 |
| Figure 6.1 Railroad corridor capacities level of service: (a) in 2007 and (b) in 2035..... | 64 |
| Figure 6.2 ASCE 2025 Vision | 65 |
| Figure 6.3 Railroad bridge classification towards campaign monitoring | 66 |

List of Tables

| | |
|---|----|
| Table 1.1 Monitoring objectives and sensing strategies | 5 |
| Table 2.1 Description of typical daily traffic on bridge..... | 12 |
| Table 3.1 Work train experiment speeds and directions..... | 25 |
| Table 3.2 Work train properties | 25 |
| Table 3.3 IF estimation from rail shear strain at different speeds | 28 |
| Table 4.1 Comparisons of significant modes between the preliminary FE model and experimental modal analysis..... | 36 |
| Table 4.2 Comparisons of significant modes between the updated FE model and experimental modal analysis..... | 38 |

EXECUTIVE SUMMARY

This research project provides a strong foundation for developing a simplified and effective approach to campaign monitoring of railroad bridge structural health with wireless smart sensors. University of Illinois researchers designed, developed and deployed a wireless structural health monitoring system to assess the dynamic performance of an in-service railroad bridge. Researchers used this data to calibrate and refine a set of numeric models that predict the performance of the bridge under various loads and speeds. Furthermore, the Illinois research team used a simple moving-mass beam model developed as part of this project, to estimate the resonances of the truss bridge and identify the critical speeds under two different train load scenarios: freight trains and Amtrak trains. Combining the use of models and campaign monitoring using only two wireless sensor nodes will allow railroad personnel to estimate critical speeds for similar types of bridges.

North America's railroad bridge structural engineering community has ranked studying and addressing the impact of High-Speed Rail (HSR) traffic on existing bridges as one of their top research priorities.¹ To estimate bridge performance and safe operating conditions for new service conditions (including higher loads and speeds), a well-calibrated numerical model is required. Engineers quantify a bridge's safe load capacity, assess its performance, and calibrate/update related numerical models by monitoring bridge behavior in the field under various service loads and speeds. With a well-calibrated numerical model, one can estimate bridge performance and the safe operating conditions for new service conditions including higher loads and speeds. New monitoring technology can provide railroad operators objective information about the in-service performance of their bridges that can enhance inspection quality, improve railroad safety, reduce maintenance costs, and improve prioritization of bridge repairs and replacements.

Wireless smart sensors are a promising new technology that can potentially reduce the cost and complexity of bridge assessment tasks. These sensors feature wireless communication capabilities, battery power, small size, easy deployment and retrieval, low cost, and onboard computing abilities. Under contract with the Federal Railroad Administration (FRA), University of Illinois researchers developed and validated a portable and cost-effective Structural Health Monitoring (SHM) system for railroad bridges. The system was field-tested on a Canadian National Railway (CN) railroad bridge in Illinois.

¹ Moreu, F. & LaFave, J. M. (2012). Current Research Topics: Railroad Bridges and Structural Engineering. Newmark Structural Engineering Laboratory Report Series, No. 032 (Also see: <http://hdl.handle.net/2142/34749>).

1. INTRODUCTION

1.1 Background

In 2009, the U.S. Government announced a new vision for High-Speed and Intercity Passenger Rail. Since then, the U.S. Department of Transportation has supported the development of shared corridors in which existing passenger trains would run at higher speeds, sharing the same track with freight traffic. Adapting current bridges for HSR shared corridor operations will bring unique challenges due to the operational requirements and constraints associated with North American railroad infrastructure. According to the Transportation Research Board and the Association of American Railroads, expanding the nation's infrastructure to match projected growth from 2007-2035 will cost an estimated \$148 billion (in 2007 dollars).² It is predicted that freight carried by North American railroads will double.³ Amtrak marked its highest year of ridership in 2012 with 31.2 million passengers (double since 2000) and expects a 400% increase in passengers in the North East Corridor by 2040.⁴ Maintaining adequate track capacity to address expanding passenger and freight needs is one of the largest challenges in creating a competitive rail network.

Bridges are a critical component of railroad infrastructure. Currently, the only general guide to railroad bridge inspection practices is the American Railway Engineering and Maintenance-of-Way Association (AREMA) Inspection Handbook.⁵ This book lists the different inspection requirements for each railroad bridge type, indicating signs of bridge decay, common defects, inspection checklists, and emergency recommendations. This publication recommends observing the behavior of railroad bridges under live load (“noting excessive deflection, sway, or any other abnormal condition”). However, railroad bridge inspectors currently lack the tools to measure bridge responses under trains easily and effectively.

Analytical studies on the in-service response of bridges due to train loads⁶ have been conducted with the goal of gaining a deeper understanding of the critical speeds and loads for specific bridges. Experimental validation of these models has received little attention, limiting their predictive power. The scarcity of experimental results has been due, in part, to the high cost of instrumenting a bridge. Inspectors need new campaign-monitoring tools that are cost effective, easily deployed and recovered, and can enable real-time assessment of the bridge performance under in-service loads.

1.2 Technology Assessment

Unlike traditional hard-wired monitoring systems, wireless smart sensors can be quickly and easily installed, used, and removed for use on other bridges. Portable sensors and equipment are the key elements of campaign monitoring (Figure 1.1). Additionally, the wireless-based system

² Cambridge Systematics, Inc. (2007). National Rail Freight Infrastructure Capacity and Investment Study.

³ Thompson, L. (2010). A Vision for Railways in 2050. International Transport Forum.

⁴ ASCE. (2013). Report Card for America's Infrastructure.

⁵ AREMA. (2008). Bridge Inspection Handbook© 2008.

⁶ Yang, Y.B., Yau, J.D. & Wu, Y.S. (2004). Vehicle-Bridge Interaction Dynamics with Applications to High-Speed Railways. World Scientific, 2004.

can provide data and information in real time due to the onboard computing capabilities of the sensor nodes. Unlike traditional, hard-wired monitoring approaches, these systems are portable and can be deployed as need, where needed.



Figure 1.1 Campaign monitoring using wireless smart sensors

Wireless smart sensors offer an attractive alternative to traditional wired systems. However, commercially available wireless sensor nodes are typically designed for low sampling and data throughput rates, which limits their utility for structural health monitoring (SHM). The Imote2 (see Figure 1.2a), developed by Intel, is a wireless sensor platform designed for data intensive applications such as SHM. The Imote2 includes a high-performance X-scale processor (PXA27x), with adjustable speed based on application demands and power management (from 13MHz to 416MHz). It has 256K SRAM, 32MB Flash RAM, and 32MB SDRAM, which enables the intense onboard calculations required for SHM applications and allows the user to store more measurements. Sensor boards are stacked on the Imote2 via two connectors to facilitate sensing with the Imote2 (see Figure 1.2b).

While the large memory and powerful processor make the Imote2 attractive, the sensor hardware available from Intel was inadequate for SHM applications. Moreover, the software was not capable of supporting data intensive applications. Therefore, Illinois researchers developed several SHM-specific sensor boards and software for the Imote2. SSTL researchers developed a general-purpose accelerometer board,⁷ a high-sensitivity accelerometer board,⁸ and a strain sensor board⁹ for the Imote2 (see Figure 1.3). The Illinois researchers refer to them as SHM-

⁷ Rice, J.A. & Spencer, Jr., B.F. (2009). Flexible Smart Sensor Framework for Autonomous Full-scale Structural Health Monitoring. NSEL Report Series, No. 18, University of Illinois at Urbana-Champaign. (Also see: <http://hdl.handle.net/2142/13635>).

⁸ Jo, H., Rice, J.A., Spencer, Jr., B.F., & Nagayama, T. (2010). Development of a High-sensitivity Accelerometer Board for Structural Health Monitoring, Proceedings of the SPIE Smart Structures/NDE Conference, Vol.7647.

⁹ Jo, H, Park, J.W., B.F. Spencer, Jr., Jung, H-J. (2012) Design and validation of high-precision wireless strain sensors for structural health monitoring of steel structures. Proceedings of the SPIE Smart Structures/NDE Conf.

Acceleration (SHM-A), SHM High-sensitivity (SHM-H), and SHM-Strain (SHM-S) sensors, respectively. As part of the technology assessment justification, Table 1.1 lists the bridge types along with the information that is collected, the sensors for collecting the information, and the sensor locations for each type. This wireless sensor hardware meets the needs of railroad bridge monitoring.

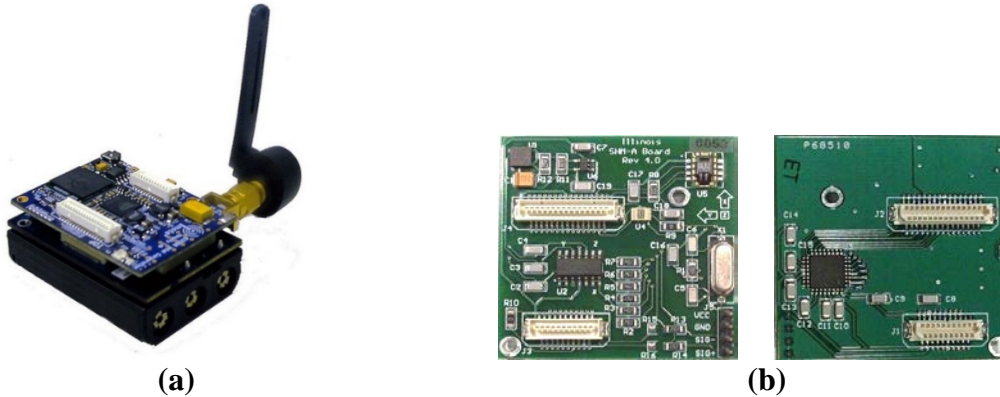


Figure 1.2 (a) Imote2 with antenna and sacked on battery board, (b) SHM-A sensor board

As part of the Illinois Structural Health Monitoring Project (ISHMP), a collaborative effort in civil engineering and computer science at the University of Illinois at Urbana-Champaign, researchers developed the ISHMP Services Toolsuite. The Toolsuite provides a software framework for continuous and reliable monitoring of civil infrastructure using wireless smart sensors. This software is available as open source for research purposes at <http://shm.cs.uiuc.edu/software.html>.

Illinois researchers have demonstrated this wireless sensor technology for monitoring highway bridges. For example, the 2nd Jindo Bridge¹⁰ deployment in Korea, which consists of 113 wireless sensors with 669 sensing channels, is the world largest full-scale wireless smart sensor network. The Government Bridge,¹¹ a swing-bridge in Illinois, is another example of full-scale and long-term monitoring deployment. Both of these deployments employ the same Imote2 wireless smart sensor that was used for this project. These hardware and software innovations form a flexible smart sensor framework for full-scale, autonomous SHM that is employed in this research (<http://sstl.cee.illinois.edu>).

¹⁰ Spencer, Jr., B.F., Cho, S., & Sim, S-H. (October 2011) Wireless Monitoring of Civil Infrastructure Comes of Age. Structures Magazine, pp. 12-15. (Also see: <http://www.structuremag.org/Archives/2011-10/C-Technology-Spencer-Oct11.pdf>).

¹¹ Giles, R.K., Kim, R., Sweeney, S.C., Spencer, Jr., B.F., L.A. Bergman, C.K. Shield, and S. Olsen, “Multimetric Monitoring of a Historic Swing Bridge.” Proceedings of the ASCE Structures Congress, 2012. (Also see: http://dl.dropbox.com/u/9924653/249_Giles_MultimetricMonitoringHistoricSwingBridge_Final.pdf).

Table 1.1 Monitoring objectives and sensing strategies

| Objective | Information | Sensor type | Bridge location | Notes |
|---------------------------------|--------------------------------|-------------------------|---|--|
| <i>Loading properties</i> | Rail strain | Wireless strain sensors | Both inside and outside the bridge | Collect data from bridge approaches |
| <i>Dynamic properties</i> | Accelerations | Wireless accelerometers | Main nodes (both planes) | Also 10 feet from the ground for 3D dynamics |
| | High Sensitivity Accelerations | Wireless accelerometers | At few nodal points (both planes) | Cost-effectively reduce entire noise level |
| <i>Pseudo-static properties</i> | Structural strain | Wireless strain sensors | Members both in tension and compression | Test magnetic strain checker for campaign monitoring |

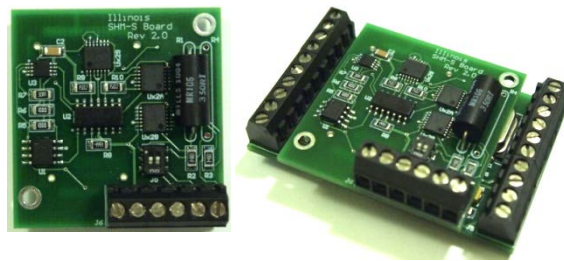


Figure 1.3 SHM-S sensor board (left), with SHM-DAQ (right)

1.3 Organization of the Report

This report discusses the use of wireless smart sensors for monitoring in-service responses of railroad bridges. Chapter 2 describes the overall project objectives and expected benefits, as well as the technical approach for this research, while Chapter 3 describes the preliminary finite element (FE) model of the bridge, the deployed monitoring system, and the data collected. Chapter 4 summarizes the main results of this research, including the creation of predicted strain maps under in-service loads, the development of the simple beam model used for bridge resonance studies, and reference-free estimation of bridge displacements under in-service loads. Chapter 5 presents the achievements of this research and compares these achievements against the goals laid out in the original proposal. Finally, Chapter 6 describes a vision for using wireless smart sensors as an important tool to manage railroad bridges in North America and discusses the research needed to realize this vision.

The goal of this research is to provide railroads with new objective information about the in-service performance of their bridges that addresses, but is not limited to, the following current needs:

- Safety - Regular campaign monitoring of bridges increases the safety of railroad operations.
- Bridge Management - Bridge replacement prioritization requires quantifiable data about the bridge population to enable rationale decision-making and budget allocation.
- Planning and Transportation - The railroad can better identifying the current structural capacity of the bridges within the network.
- Institutional - Regulatory recommendations, incentives, and penalties associated with bridge management (and liability consequences) to improve the safety of railroad operations¹².

¹² FRA. (2010, July 15). Bridge Safety Standards.

2. PROJECT DESCRIPTION

This chapter describes the objectives of this project, the technical approach taken by the researchers, and the industry partnership that was established (including the bridge that was chosen to validate the wireless system).

2.1 Project Objectives

The primary objective of this research project was to develop and validate a portable, cost-effective, and practical structural health monitoring system for railroad bridges in North America using wireless smart sensors (Figure 2.1). The system adapted wireless sensor technology developed at the University of Illinois as part of the ISHMP. This research demonstrated that railroad bridge load response data can be efficiently collected using wireless smart sensors, and this data was used to predict structural responses of the bridge under trains running at different loads and at higher speeds. To prove this concept within the railroad environment, Illinois partnered with the Canadian National (CN) Railway to execute the technical aspects of this research. Ultimately, this research will provide railroads with new objective information about the in-service performance of its bridges, which can enhance inspection quality, improve safety, reduce maintenance costs, and help prioritize bridge repairs and replacements.

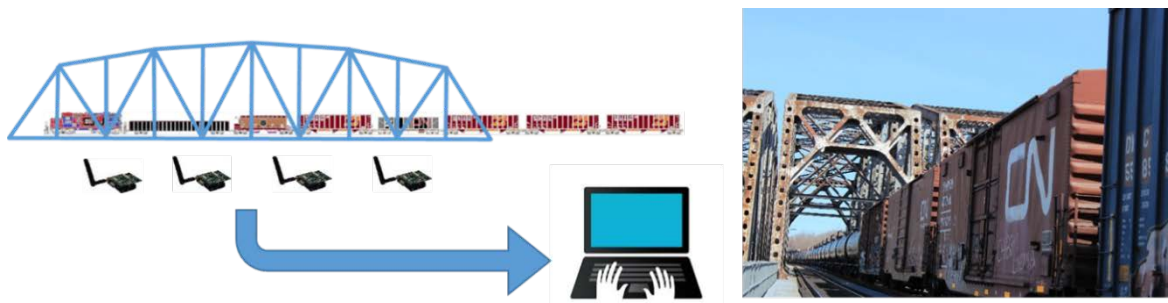


Figure 2.1 Concept of proposed wireless sensing system

The project demonstrated that campaign monitoring with wireless smart sensors has the following benefits:

- The ability to identify the fundamental issues affecting the dynamic behavior of existing bridge structures in response to the vehicle loads at various speeds
- The ability to harvest objective information about the in-service performance of bridges, improving the assessment of safety and reliability and laying a foundation for providing early warning regarding evolving hazards
- The potential to improve prioritization of bridge repairs and replacement in order to speed up the enabling of HSR in shared corridors
- The ability to experimentally calibrate/validate current numerical approaches for assessing bridge performance, turning these models from explanatory in nature to having powerful predictive capabilities

Chapter 5 assesses our success in achieving these goals and realizing these benefits.

2.2 Technical Approach

To achieve the goals of this project, researchers identified seven critical tasks carried out over the project's 12-month duration (see Figure 2.2):

- 1. Develop an analytical model of the bridge response to various loads/speeds**
Researchers developed a basic analytical model for the CN bridge over the Little Calumet River at MP 16.9 on the south side of Chicago. The model's results pinpointed sensor locations that characterize the live bridge performance and predict the critical speeds and loads for the structure.
- 2. Instrument designated CN bridge and approach track**
Based on the results from Task 1, the Illinois research team deployed the wireless smart sensors on the CN bridge. A minimum of 10 wireless sensor nodes were installed on the bridge and track, including vertical load strain sensors to the approach rails (which would measure wheel loads and train speeds). CN coordinated Illinois field visits to the bridge before, during, and after monitoring. The company also provided access and track protection for the Illinois research team members while on CN property.
- 3. Conduct experiments using CN work train collecting bridge response data**
Researchers collected in-service response data from the bridge under various speed, load, and direction conditions using a dedicated work train.
- 4. Compare data collected with analytical model results**
Engineers used the bridge performance data to update the analytical model developed in Task 1. Two subsequent monitoring campaigns verified and calibrated the model. Also, the sensor locations were optimized to yield the most important information with a fixed number of sensors.
- 5. Continue to monitor the designated bridge during normal traffic for project duration**
For the duration of the project, the system collected data under revenue service conditions to maximize the experience gained from the deployment. Illinois researchers removed the system at the end of the project in coordination with CN.
- 6. Develop a quantitative basis for assessing the value of using wireless sensors for railroad bridge campaign monitoring**
Researchers analyzed all the gathered data to quantify the value of wireless sensors for railroad bridge campaign monitoring, as well as other railroad applications.
- 7. Report and presentation to industry**
Research publications are available in the [Newmark Structural Engineering Laboratory Report Series](#), which is archived in Illinois' digital repository.

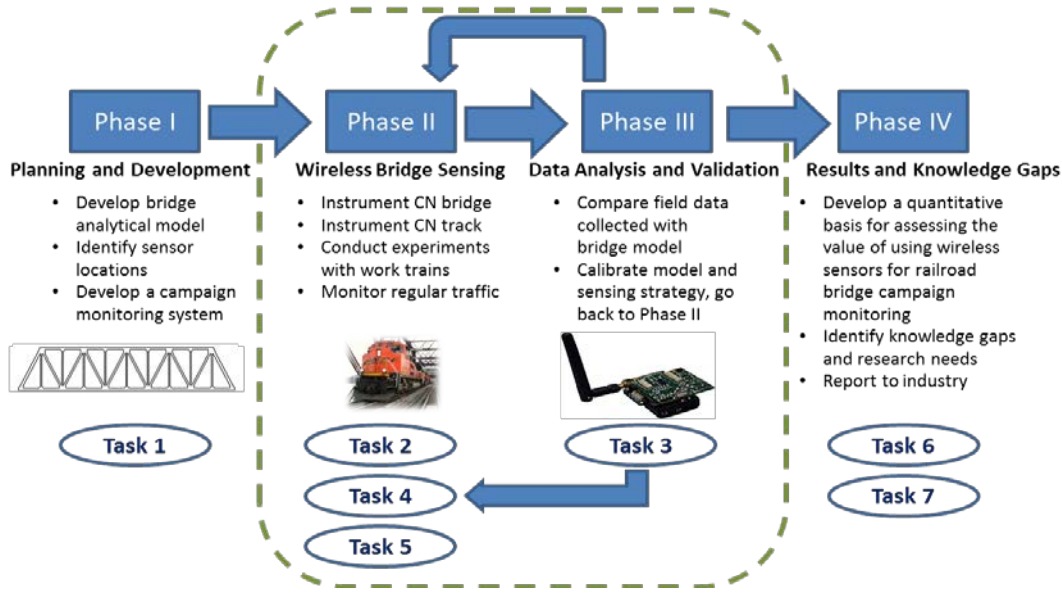


Figure 2.2 Technical approach for research

2.3 Industry Participation

CN Railroad was a critical partner in this research. The company identified a two-track steel truss bridge for instrumentation and testing which was within 2 hours distance of UIUC and within 30 minutes driving distance of the CN Railroad Headquarters office in Homewood, IL (Figure 2.3). CN provided access, coordination assistance, and in-kind resources for sensor installation and monitoring of this bridge. It also provided invaluable guidance regarding issues of importance to the CN.

The Illinois research team deemed this bridge to be well-suited for this project for several reasons:

1. According to the Federal Railroad Administration (FRA),¹³ 53% of the railroad bridge inventory in North America is made of steel.
2. This bridge is deemed to be in excellent structural conditions, so it can serve as a reference for FE model development and calibration.
3. Three identical steel trusses are located next to each other, so three bridges potentially can be monitored for nearly the same effort.
4. Displacements can be collected from adjacent trusses from a fixed location for reference-free displacement estimation validation.
5. This bridge is on a congested line, so many trains will be crossing the bridge on a regular basis.

¹³ FRA. (2008). Railroad bridge superstructures materials by length.

2.3.1 Bridge Description

The selected bridge is located on the south side of Chicago at MP 16.9 over the Little Calumet River. The focus of this research was the intermediate steel truss (tracks CN1 and CN2 – Figure 2.3), a 310'-4" span with both passenger and freight traffic in both directions: North Bound (NB) and South Bound (SB).

The bridge was designed in 1960, following the 1956 American Railway Engineering Association recommended practices and specifications for steel railroad bridges. The following technical specifications were used:

- Dead load estimated with deck and track weight of 510 lbs. linear foot of track
- Live load under Cooper E-72 load (for each track)
- Impact load under locomotives with a hammer blow
- Riveted steel conforming to current standard American Society for Testing and Materials (ASTM) A502-65 Grade I
- Unit Stresses for Axial Tension, Net Section – Carbon Steel: 18,000 psi
- Unit Stresses for Axial Compression, Gross Section – Carbon Steel: 15,000 – 0.25 (L/r) psi, where L/r is the slenderness of the member under consideration

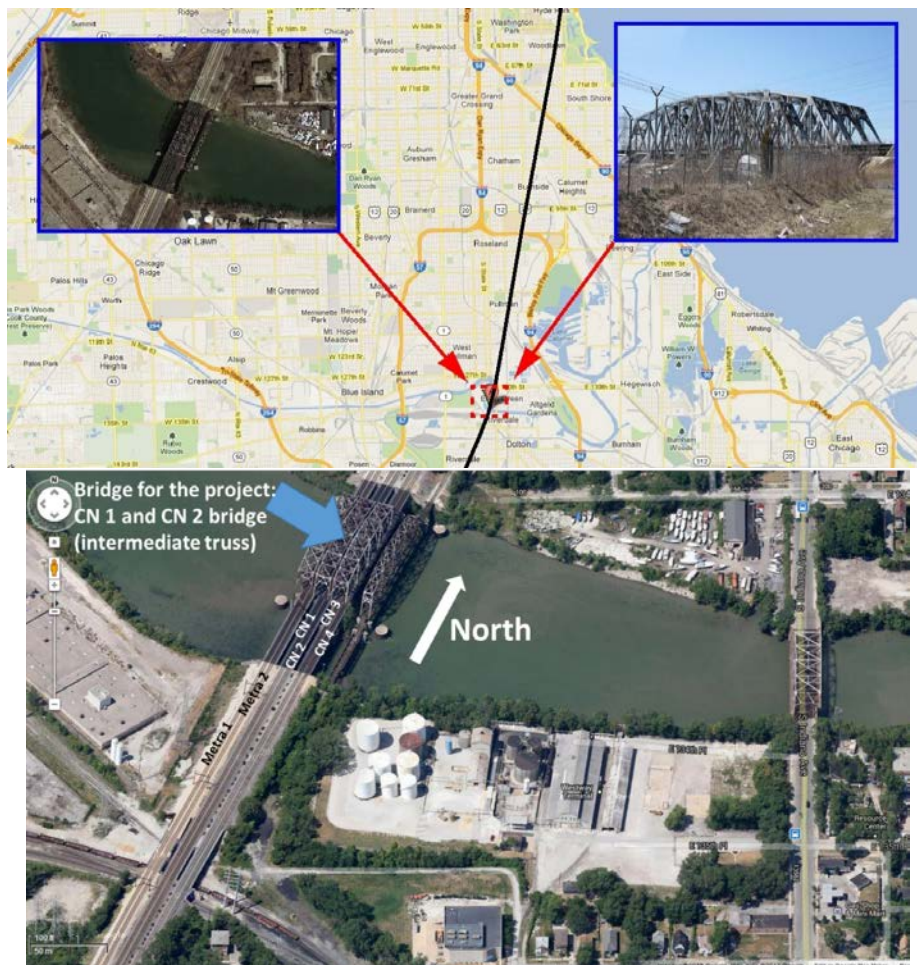






Figure 2.3 Bridge over the Little Calumet River (near Chicago, IL)

The truss foundation consists of two forty-five feet tall reinforced concrete piers on each end of the span. The piers provide bearing for the three spans, supported by thirty-inch drilled caissons with steel core driven to the bedrock. CN built the bridge in 1971 with an expected life of 100 years. CN stated that this bridge was in excellent condition at the time this research took place, and the company provided the most recent inspection reports of this bridge to the Illinois research team to support their assessment.

2.3.2 Regular Traffic

The bridge experiences different types of regular traffic during normal operation, as listed in Table 2.1. The large amount of traffic on this bridge provided a unique test-bed with which to achieve the objectives of this research as described in Chapter 1.

Table 2.1 Description of typical daily traffic on bridge.

| View | Type | Trains/day | Track |
|---|---------|--------------|--------------|
|  | Amtrak | 6 | CN1 |
|  | Freight | ~ 10 | CN1, CN2 |
|  | Metra | > 20 | Metra tracks |
|  | Other | Very unusual | Any track |

3. MONITORING SYSTEM DEPLOYMENT

This chapter discusses the preliminary finite element model that was developed to support the sensor placement task, presents the monitoring system, and describes the data that was collected.

3.1 Finite Element Model

Researchers developed a preliminary analytical model of the bridge based on the original construction drawings, and used this model to pinpoint the locations for the sensors. The team used Matlab® to build the model (see Figure 3.1), which had 25 different section properties (extracted from the CN shop drawings) and 724 elements in total.

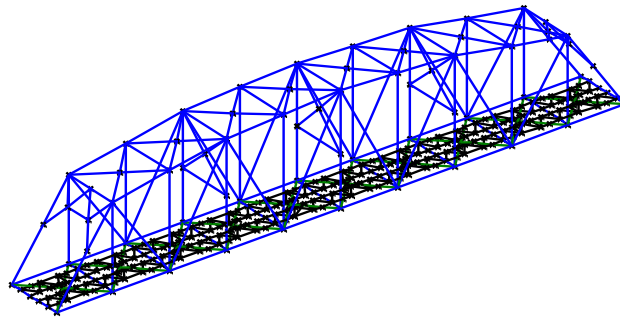
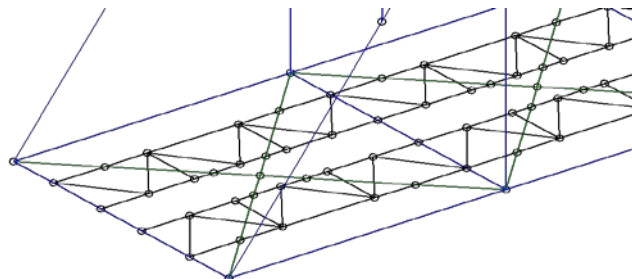


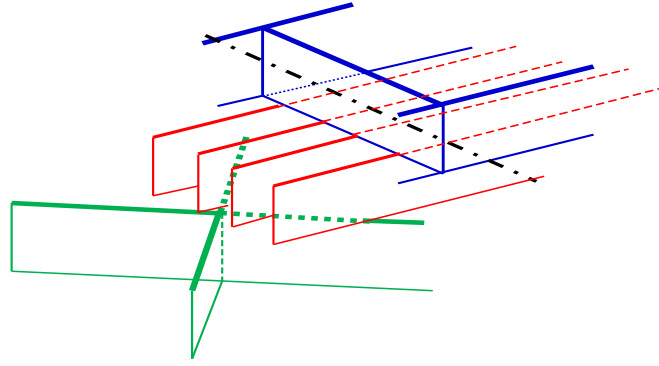
Figure 3.1 Bridge 3D FE model

The floor system of the bridge is very rigid. Lower chords, floor beams, stringers and bottom lateral bracings form the floor system. The Illinois research team accounted for this rigidity in the FE model by treating all the floor layers as one floor system and calculating the moment of inertia about the reference axis at the center of lower chords. Figure 3.2 illustrates the different layers forming the floor system.

The Illinois research team also developed a Graphical User Interface (GUI) for convenient data representation to the user (see Figure 3.3). The program can plot the nominal model of the bridge and plot mode shapes at a user-selected frequency. The model and GUI were used to understand the dynamic response of the bridge and to determine the locations for sensors so that the desired information could be harvested and so that spatial aliasing would be minimized.



(a)



(b)

Figure 3.2 (a) Floor system modeling, (b) details of the floor system

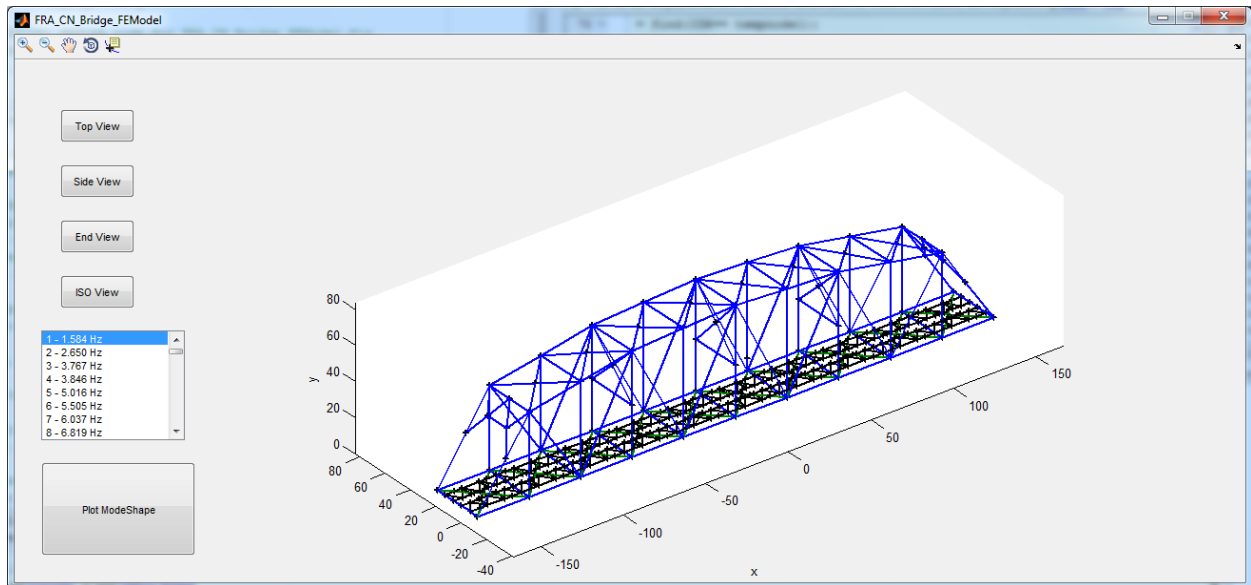


Figure 3.3 GUI for the FE model

3.2 Sensor Layout

This section describes where the sensors were deployed on the bridge and track. It also specifies where the sensors were installed in the locomotive during the work train experiments.

3.2.1 Bridge and Track Sensors

Figure 3.4 shows the general sensor deployment, including wireless accelerometers, wireless strain gages (both conventional and magnetic), and wired Linear Variable Differential Transformers (LVDT) for measuring transverse displacements. Both SHM-A (measures up to 2g) and SHM-H (measures up to 200 mg with 10 times higher sensitivity) accelerometers are used. Figure 3.5 shows the layout for the strain sensors installed in the rail. For the purpose of this research, the research team decided to install strain sensors on the rail both within the main truss and outside of the CN bridge, approximately 2 ft. away from the North back wall.

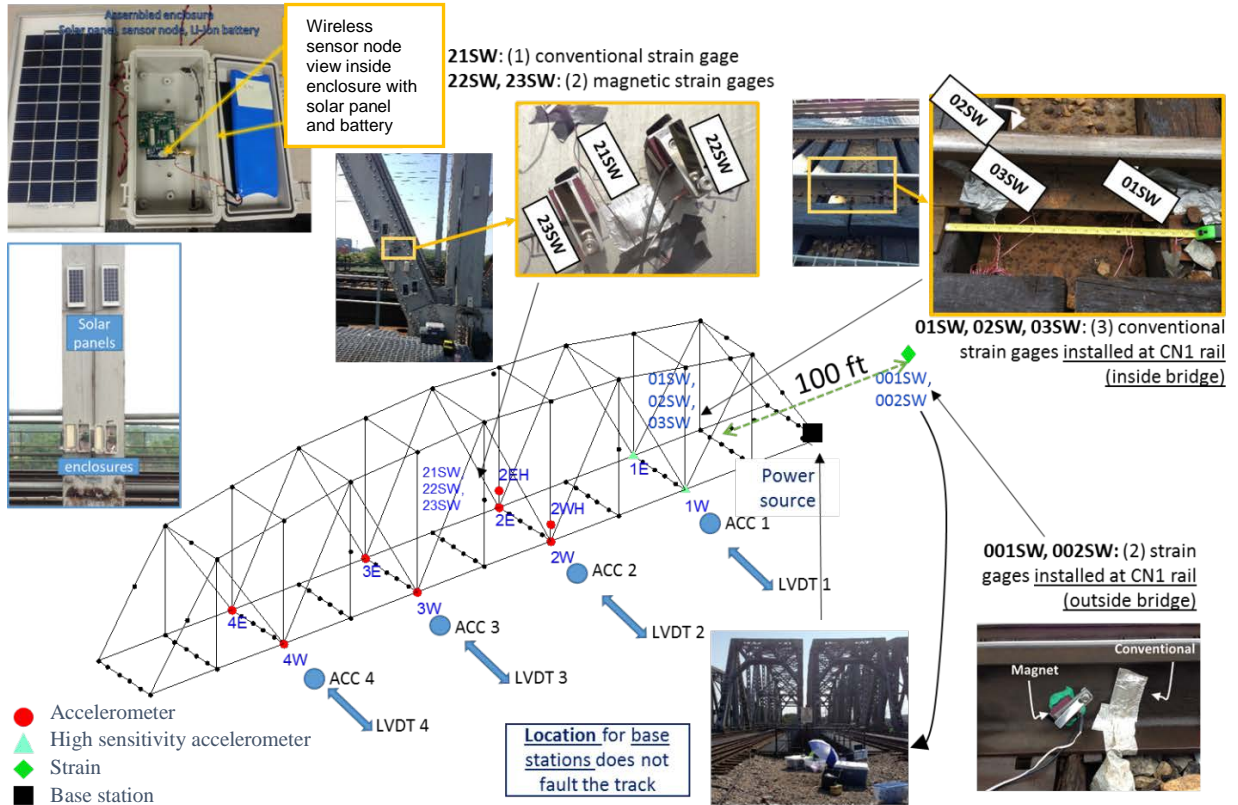


Figure 3.4 General layout of the sensors installed at the bridge

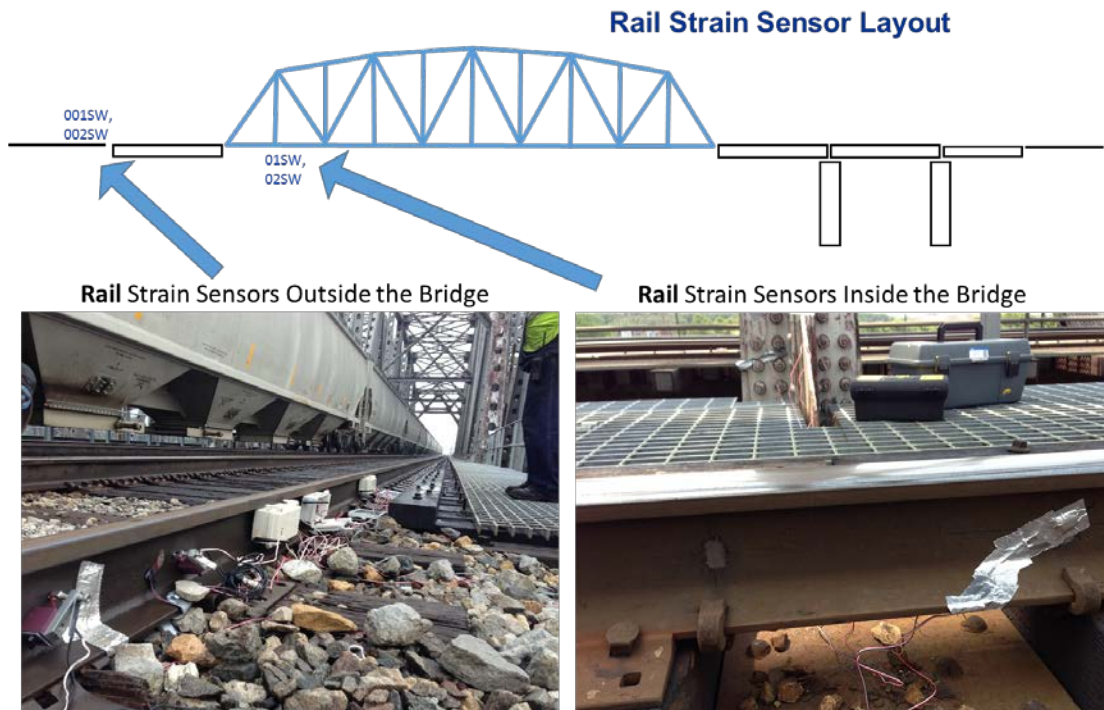


Figure 3.5 Layout of the rail sensors at the bridge and vicinity

To make strain measurement easier and simpler, the Illinois research team used a magnetic strain checker (see Figure 3.6a). The magnetic strain checker (frictional strain gauge) model FGMH-2A from Tokyo Sokki Kenkyujo Co., Ltd was used. Researchers applied conventional modeling clay around the sensors (see Figure 3.6b) to limit the effect of impact forces due to the very high frequencies induced by fast trains (Amtrak).

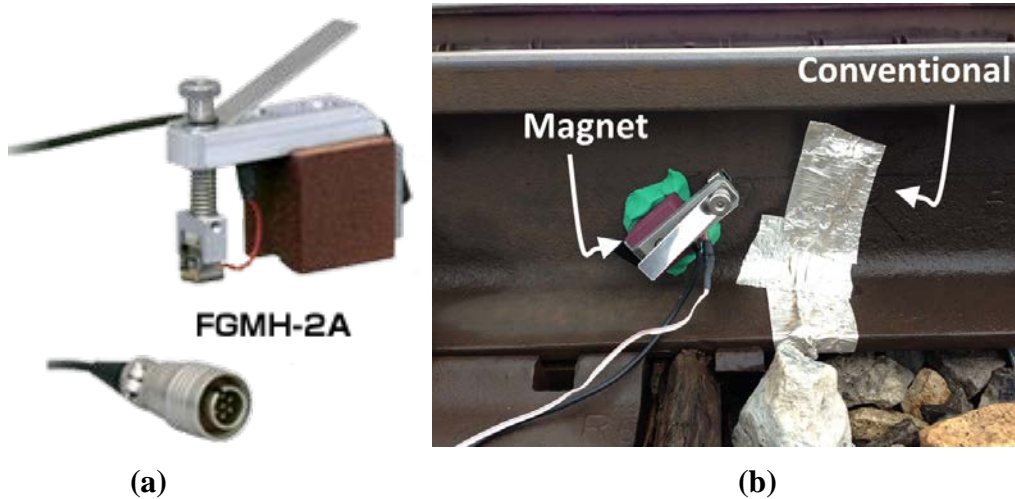


Figure 3.6 (a) Magnet strain checker, (b) magnet strain checker installed at rail

3.2.2 Train Sensors

The research team installed wireless smart sensors on the locomotive to obtain the train response during the tests. Because the train starts approximately a mile away from the bridge, a laptop inside the engine controlled the train sensors. The sensors shown in Figure 3.7 captured the responses of the front and rear bogie, as well as the response of the car body.

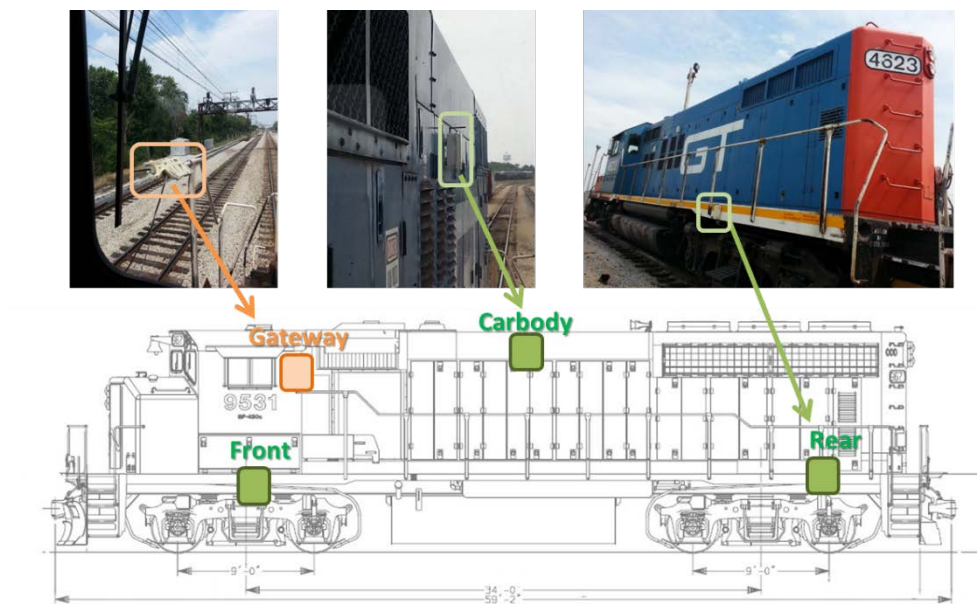


Figure 3.7 Train sensors setup

3.2.3 Base Station

The Illinois research team installed a permanent base station PC with a cellular internet connection at the bridge to collect data throughout the project (see Figure 3.8). The base station collected the response of the bridge under regular traffic and sent it remotely to the University of Illinois. The research team installed all the software needed to control remotely all the wireless smart sensors at the bridge and provide email notification of anomalous bridge responses.

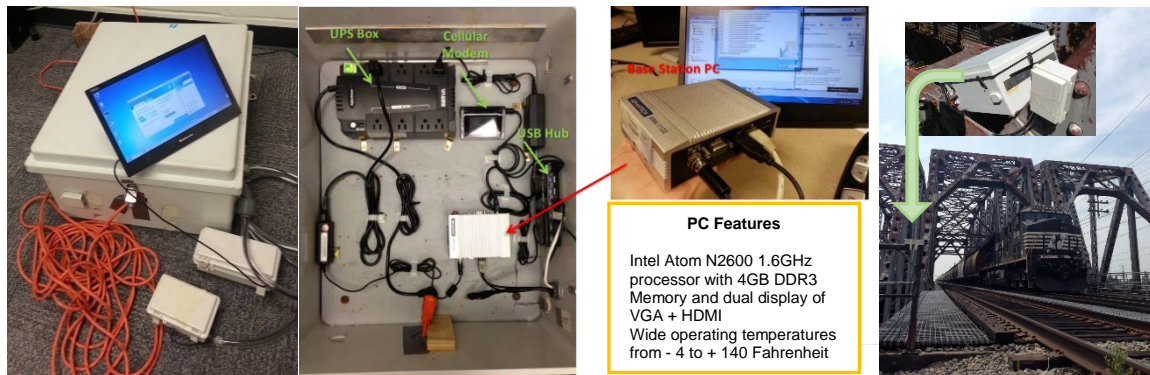


Figure 3.8 Base station for remote wireless sensing monitoring of RR bridges

3.3 Data Collected under Regular Traffic

The Illinois research team collected several sets of data under regular train traffic during multiple campaign monitoring trips to the bridge and during remote monitoring of the bridge.

3.3.1 Track Monitoring (Rail)

Figure 3.9 shows a typical time history of the bridge's strain data. The peaks correspond to each axle of an Amtrak train crossing the bridge at 65 miles per hour (MPH). Figure 3.10 shows the strain at two different locations within the bridge used to estimate train speed.

Magnetic strain checker

Figure 3.11 shows the comparison between the two measurements (magnet and conventional rail strain under Amtrak train). Researchers calibrated the magnetic strain sensor by using multiple measurements of known loads and measuring the difference in magnitudes between the uniaxial magnetic strain and the conventional Tee-Rosette strain. Once the magnetic strain was calibrated, researchers used it independently for rapid strain monitoring of unknown loads.

Load estimation using rail shear strain

Using the 136 lb/yard rail properties and the measured strains from the strain gage, the Illinois research team estimated the vertical loads on the rail as the wheels passed over the strain gage. If a set of known loads crossed the bridge, researchers re-calibrated the strain measurements for higher accuracy. For example, the Illinois research team measured the rail shear strain of a Norfolk Southern (NS) freight train. NS provided the train manifest that describes the geometry and weight of each car, as well as the wheel loads. Comparison of the wheel loads from NS to the estimated wheel loads from the measured strains for this train allowed the researchers to calibrate the system. As shown in Figure 3.12, wheel loads estimated from the measured strains match well with actual wheel loads.

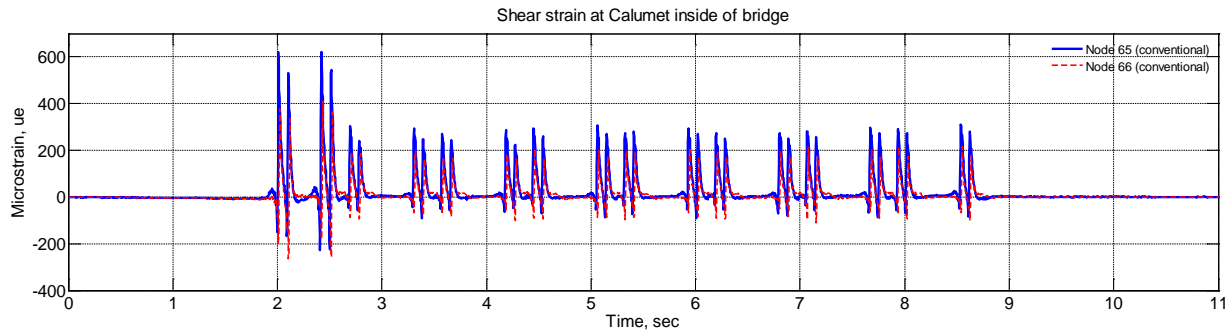


Figure 3.9 Tee-Rosette strain gage rail sensing data

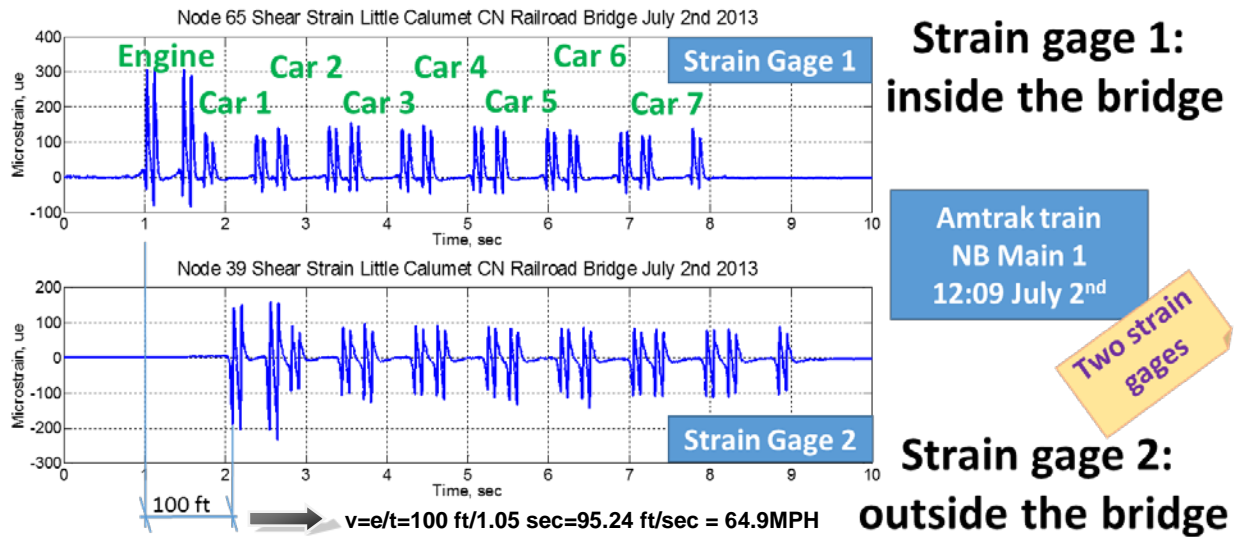


Figure 3.10 Train speed estimation using two wireless strain gages

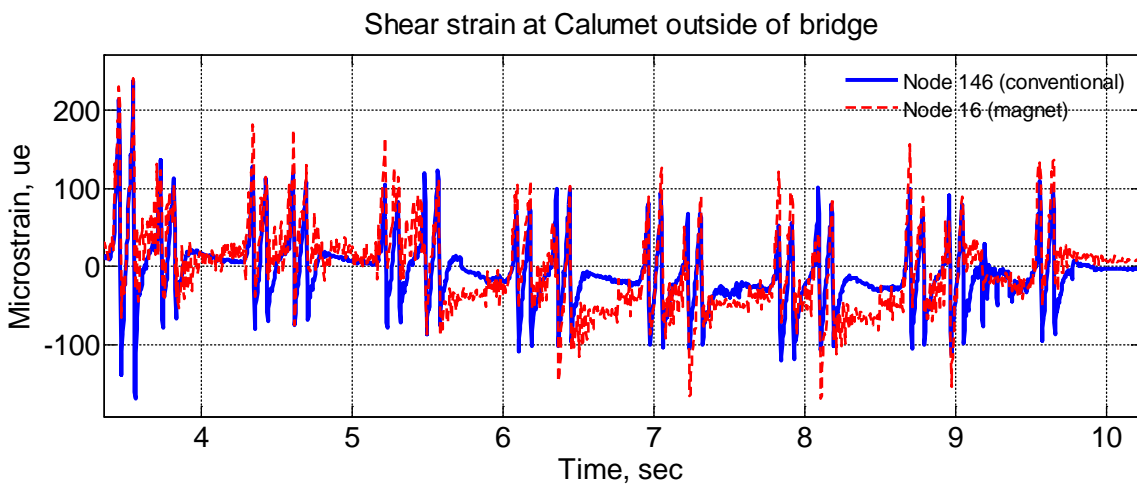


Figure 3.11 Comparison between conventional and magnetic rail strain

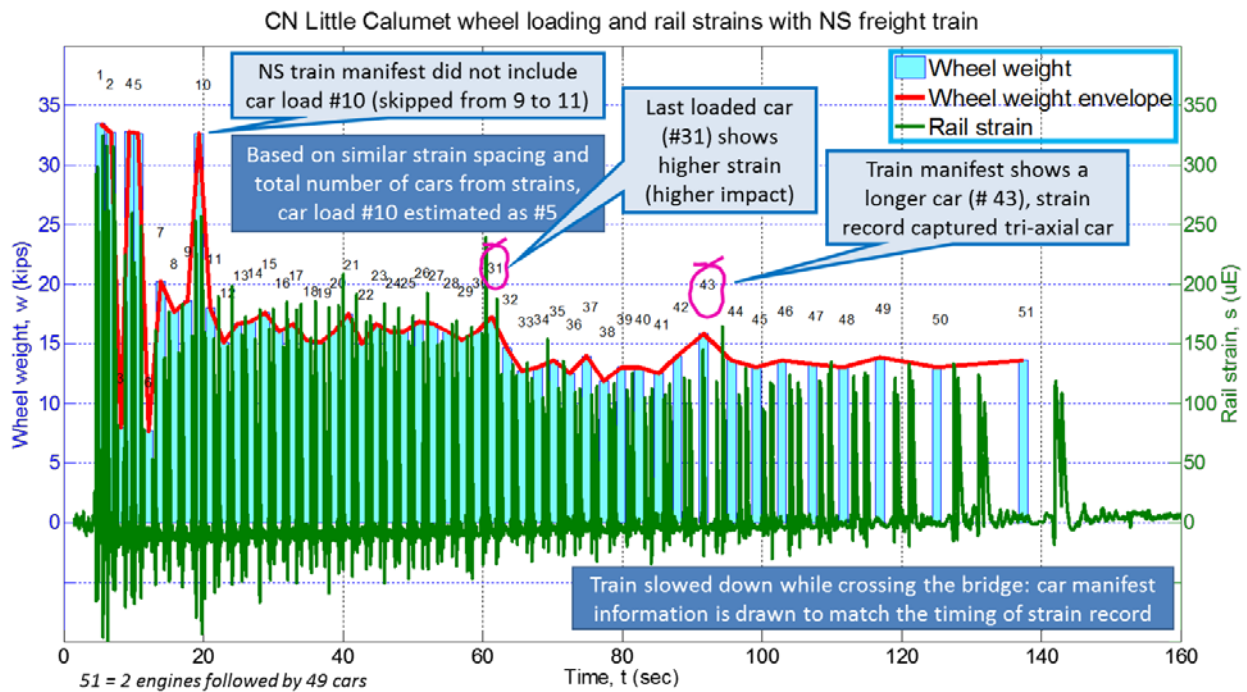


Figure 3.12 Estimation of car loadings using wireless smart sensors

Acceleration measurements at the rail

In addition to the shear strain measurements, the Illinois research team measured accelerations from the rail under trains. Rail accelerations at the bridge approaches have higher amplitudes than the accelerations at the structural elements (see Figure 3.13). During future research projects, long-term monitoring will obtain additional acceleration data from the rail at the approaches and at the rail in multiple locations throughout the bridge. In this way, researchers can collect the input loads and speeds of multiple trains and compare changes in the rail loading throughout the length of the bridge and outside the bridge. In particular, railroad bridge managers are interested in characterizing and monitoring the changes in the response of railroad bridge approaches over time.

3.3.2 Structural Strain Monitoring

The Illinois research team selected the L4-U5 element for collecting structural strain under regular freight train traffic, because elements L4-U5 and L6-U5 are the only two elements in the truss that undergo significant levels of tension and compression due to trains crossing the bridge. Element L4-U5 was closer to the north end of the truss, which is the safe area that CN selected for the Illinois research team while trains were crossing. Figure 3.14 shows a plot of the time history of the structural strain together with the rail strain measurements (at the L1 location) under the same train.

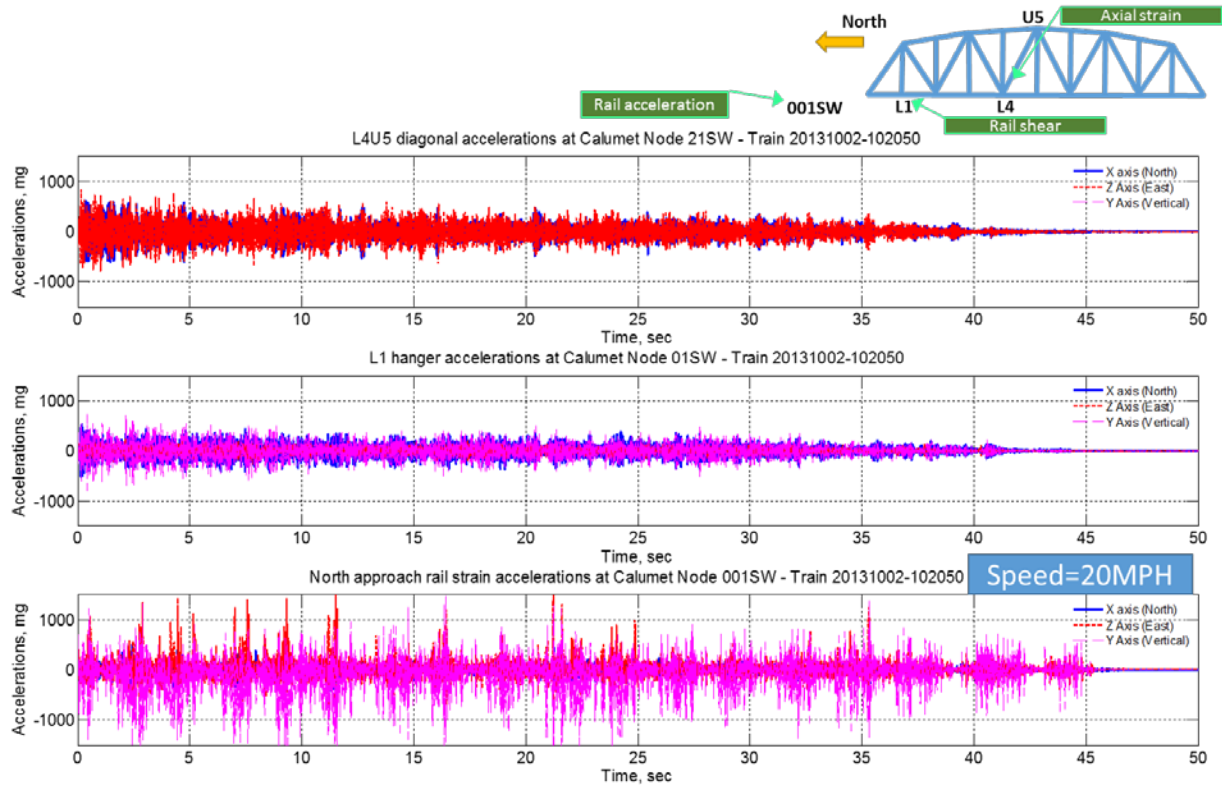


Figure 3.13 Acceleration measurements at both structure and rail via Auto-Monitor

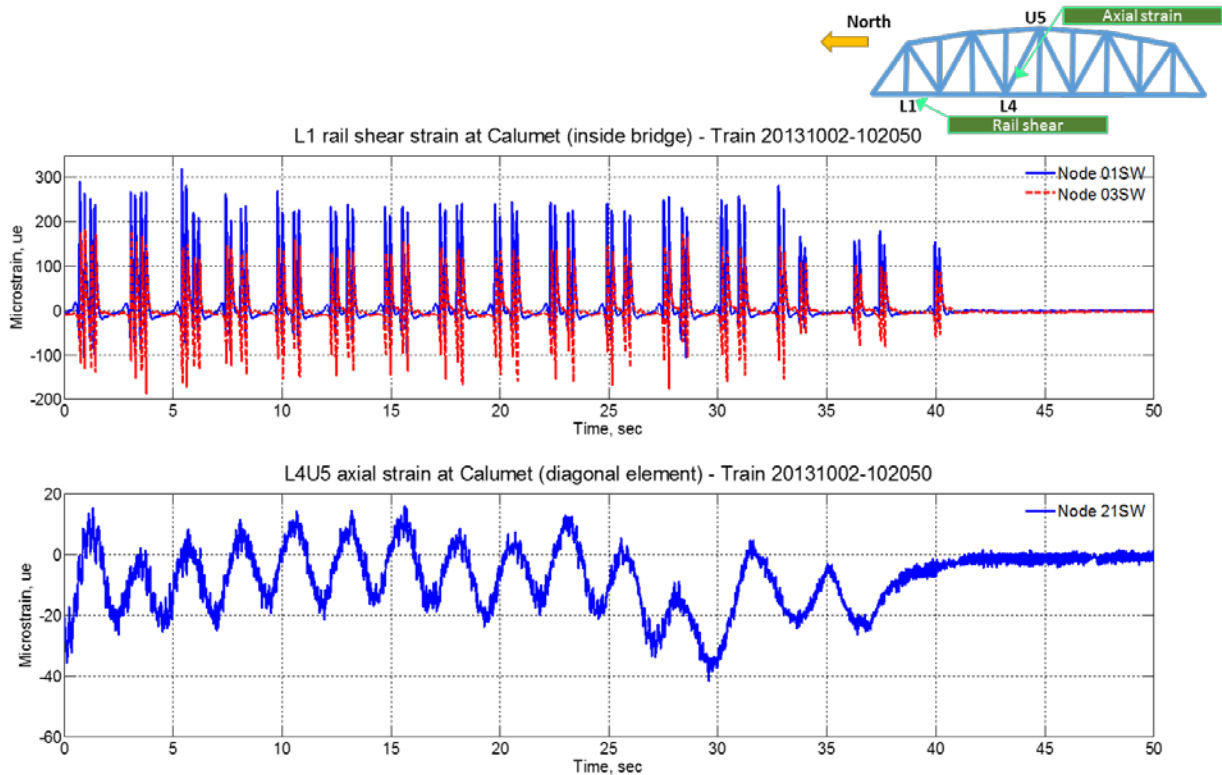


Figure 3.14 Rail shear strain at LW and structural strain at L4-U5

The research team used the displacement data for the dynamic assessment of the bridge responses (see Figure 3.15). Figure 3.16 shows transverse displacements at 2/5th span under a freight train. Examining the free-vibration response after the train crossed the bridge (see Figure 3.16) showed the damping in the first mode of the unloaded bridge to be 0.3% of critical damping. Additionally, the LVDTs captured the lower frequency response of the bridge, allowing confirmation of frequency components estimates from the high sensitivity accelerometers (see Figure 3.18). The next section provides a more detailed discussion of the accelerations collected at the bridge.

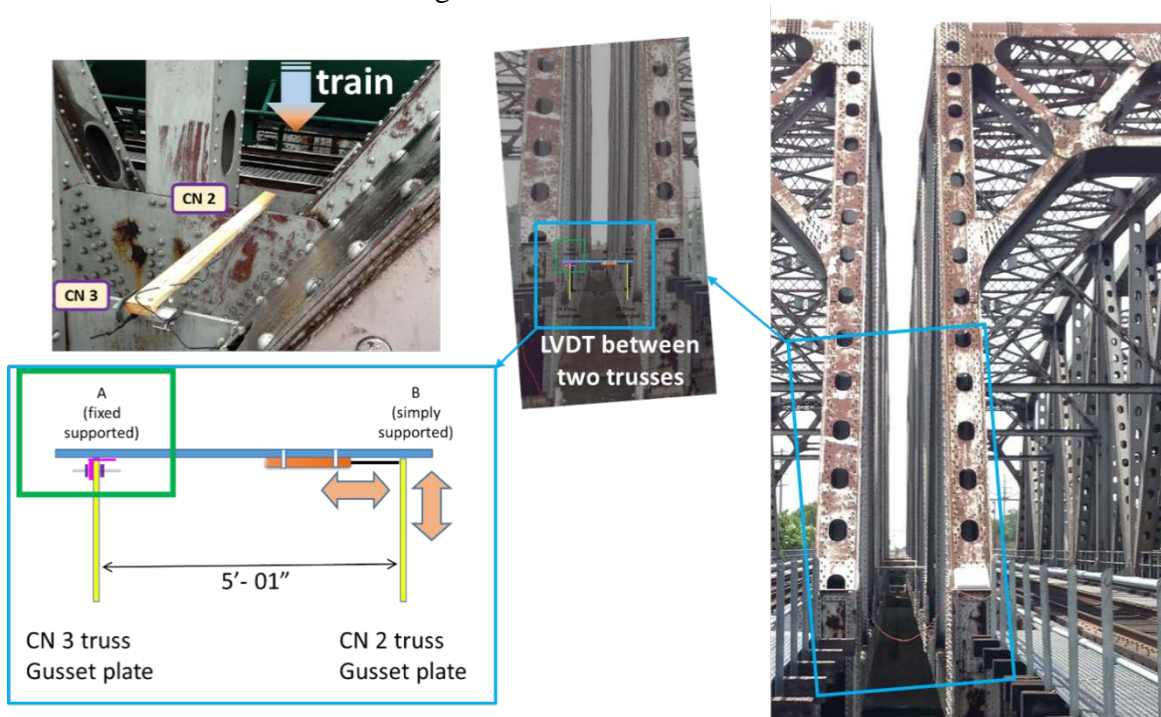


Figure 3.15 LVDT deployment under regular traffic

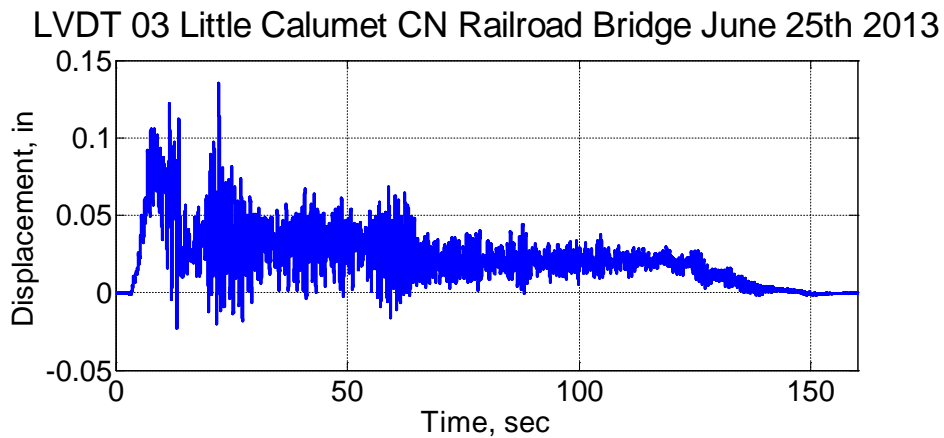


Figure 3.16 Transverse displacement under a freight train

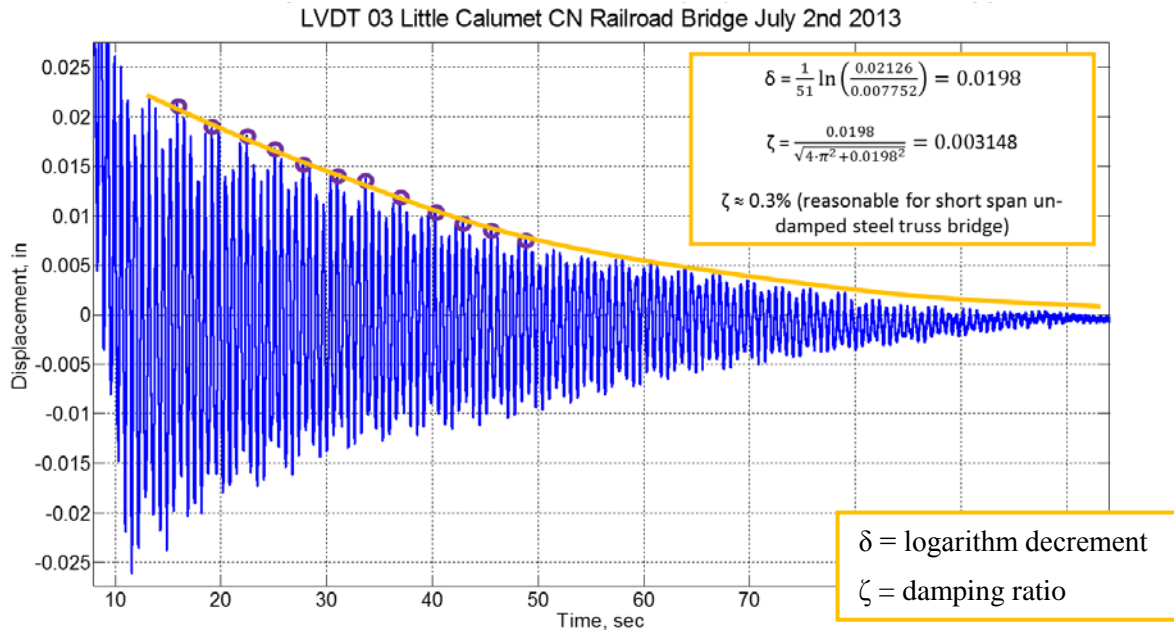


Figure 3.17 Transient transverse displacement under Amtrak train for damping (ζ) estimation

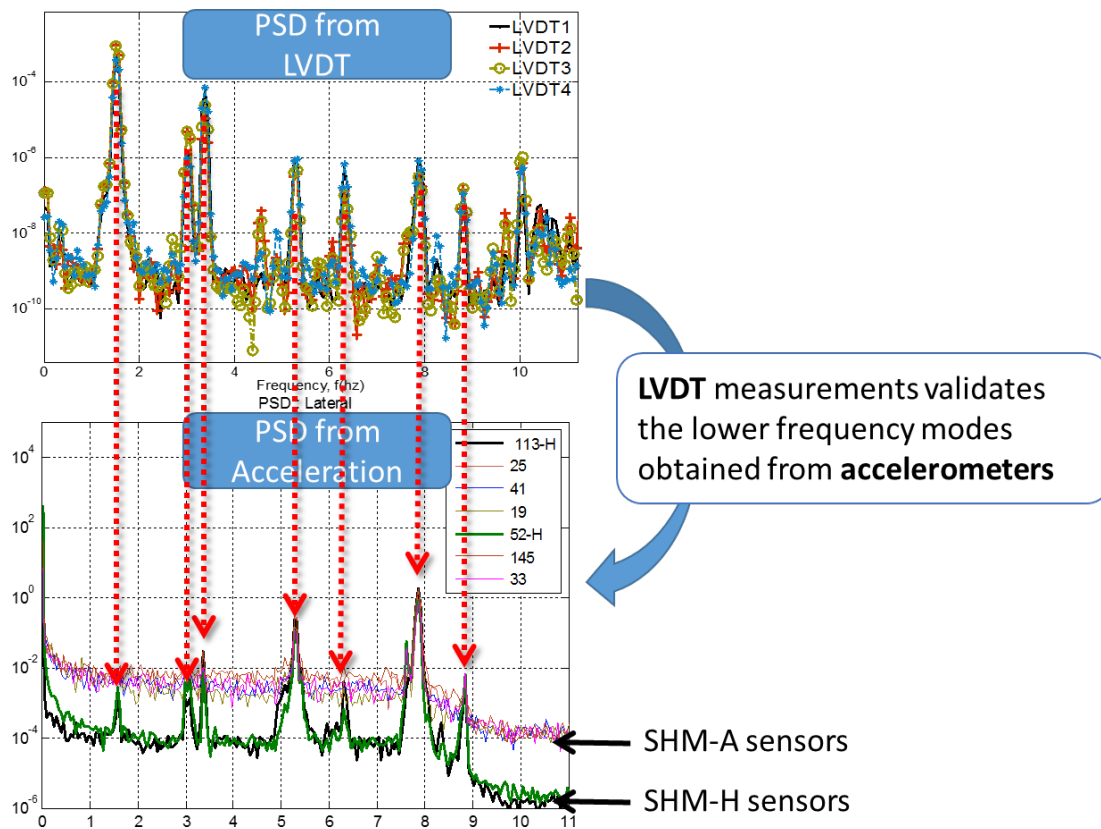


Figure 3.18 LVDT frequency analysis comparison with accelerometers analysis

3.3.3 Structural Acceleration Response Monitoring

The Illinois research team collected a number of bridge responses from multiple campaign monitoring trips to the bridge. The duration of the measurements depended on the type of train and when sensing was triggered to start. Figure 3.19 shows examples of this data. Dataset 1 (collected on June 25th) contains a NB Amtrak train on CN1 track (at $t = 200$ seconds, Figure 3.19a), and a short SB freight train on CN1 track (at $t = 800$ seconds, Figure 3.19a). Dataset 2 from July 2nd contains a long NB freight train on CN2 track (at $t = 750$ seconds, Figure 3.19b). The small peaks prior to the freight train (at $t = 250$ seconds, Figure 3.19b) correspond to the bridge response under Metra trains (the Metra track is located at the West side of the test bridge, as shown in Figure 2.3). Such bridge responses are unique, because the train is on a different track on a different span and it does not affect the total weight of the bridge.

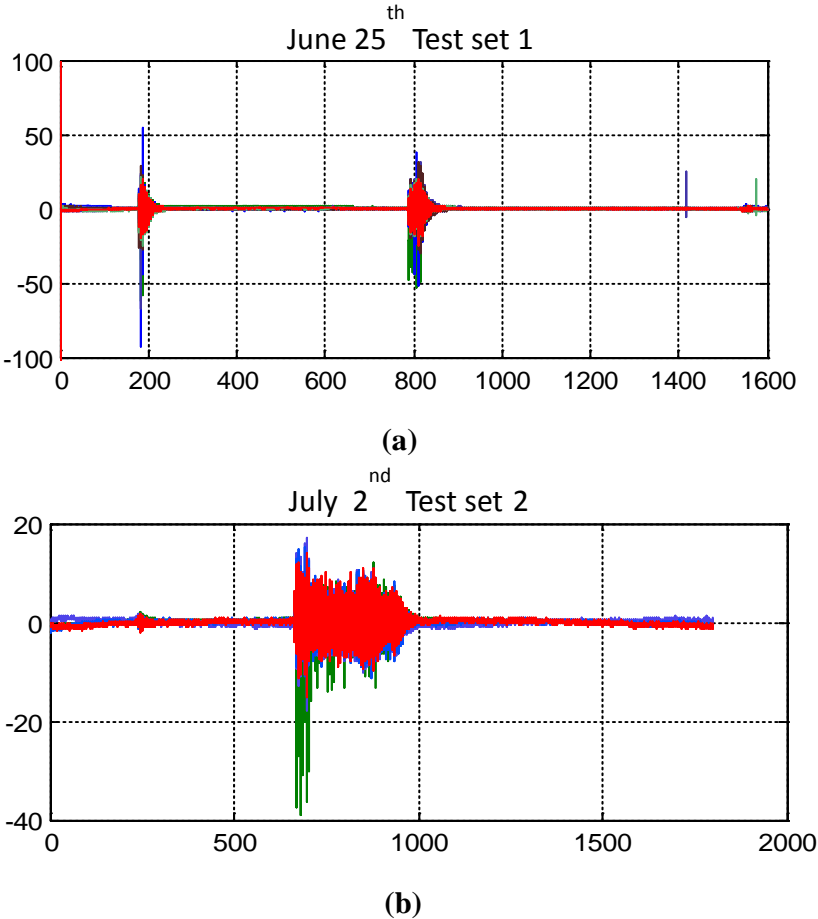


Figure 3.19 Bridge response under different trains

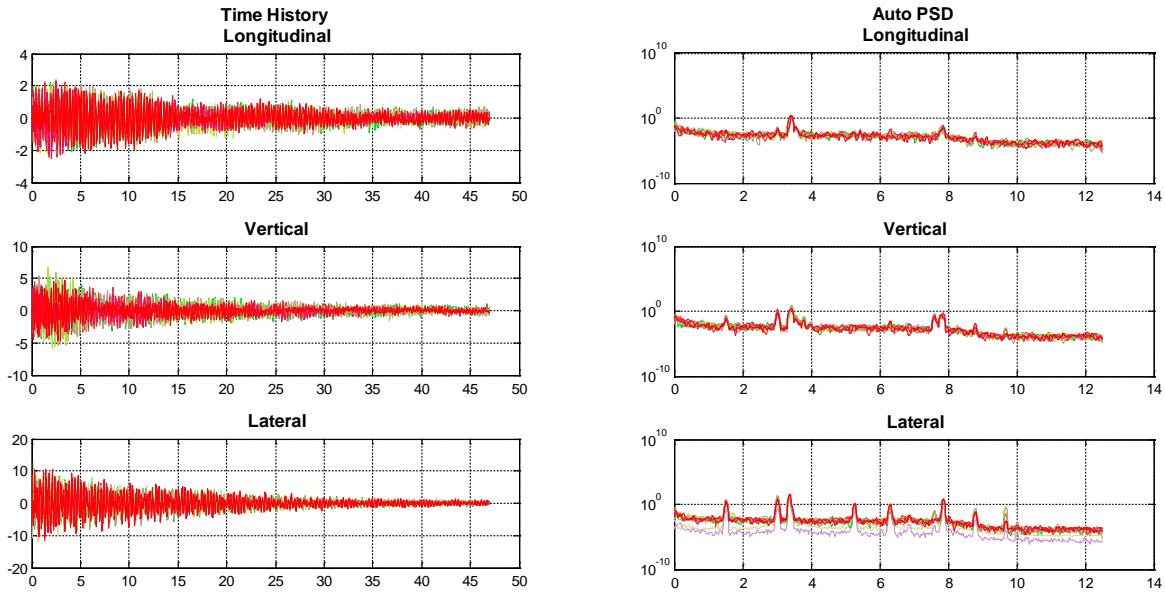


Figure 3.20 Test data after Amtrak (a) time history, (b) PSD

The research team used the transient response of the bridge under the Amtrak train after it crossed the bridge for system identification of the bridge (from the August 26th campaign). The researchers adapted the peak-picking method based on the cross Power Spectral Density (PSD) functions; natural frequencies were calculated from the record in which the peak was best seen. Amtrak runs relatively fast on the bridge (over 50 MPH) which results in larger accelerations, as compared to the slower freight trains. Figure 3.20a and Figure 3.20b shows the time history and PSD, respectively, for all sensors (see Figure 3.4). The PSD shows that the Amtrak train excited the bridge at a wide range of frequencies.

3.4 Data Collected During Work Train Tests

This section describes the experiments using work trains that were conducted by the Illinois research team in collaboration with CN. It describes the main characteristics of the work train, the experiments, and the data that researchers collected during the experiment. CN coordinated and provided the work train to the Illinois research team on August 26, 2013.

3.4.1 Work Train Description

CN provided a work train for measurements of changes of bridge responses under various train speeds. Figure 3.21 depicts the wheel loads and distribution. Table 3.1 summarizes the train speeds and directions for each test. Table 3.2 shows the general properties of the work train cars weight and geometry.

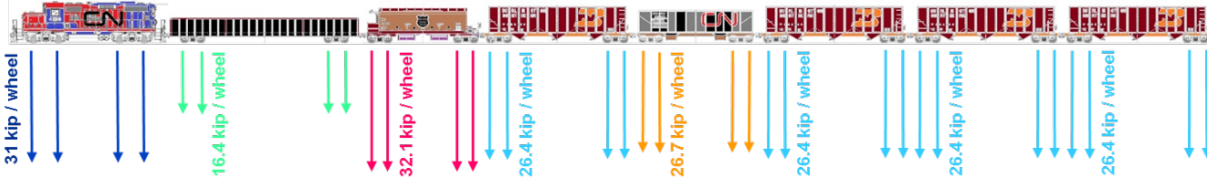


Figure 3.21 Work train wheel loading scheme

Table 3.1 Work train experiment speeds and directions

| Time | Direction | Speed, s (mph) | Operated Speed, s (mph) |
|-------|-----------|----------------|-------------------------|
| 13:20 | NB | 50 | 46 |
| 13:55 | SB | 30 | 30 |
| 14:20 | NB | 40 | 42 |
| 15:20 | SB | 25 | NA |
| 15:45 | NB | 5 | 5 |
| 15:50 | SB | 5 | 5 (ended at 0) |
| 16:10 | NB | 25 | 27 |

Table 3.2 Work train properties

| | Weight [Tons] | Length [feet] |
|--------------|---------------|---------------|
| Locomotive | 124 | 57 |
| Cars (7) | 701 | 334 |
| Total | 825 | 391 |

3.4.2 Structural Strain Monitoring Under Work Train Traffic

Figure 3.22 shows the strain measurements at both the structural elements and the rail under one of the work train experiments (work train NB at 50 MPH). The research team estimated train wheel loads from the rail strain measurements (lower figure). The upper figure compares both conventional and magnetic strain measurements at the structural element, and the results show that they are nearly identical.

Figure 3.23 shows the estimated wheel loads from the strain measurements at the rail. As shown under open traffic previously, the shear strain can successfully estimate wheel loads from rail measurements. The comparison between the known wheel loads and the estimated wheel loads provides evidence so researchers can subsequently use the load predictions from rail strain measurements as input loads for bridge response analysis.

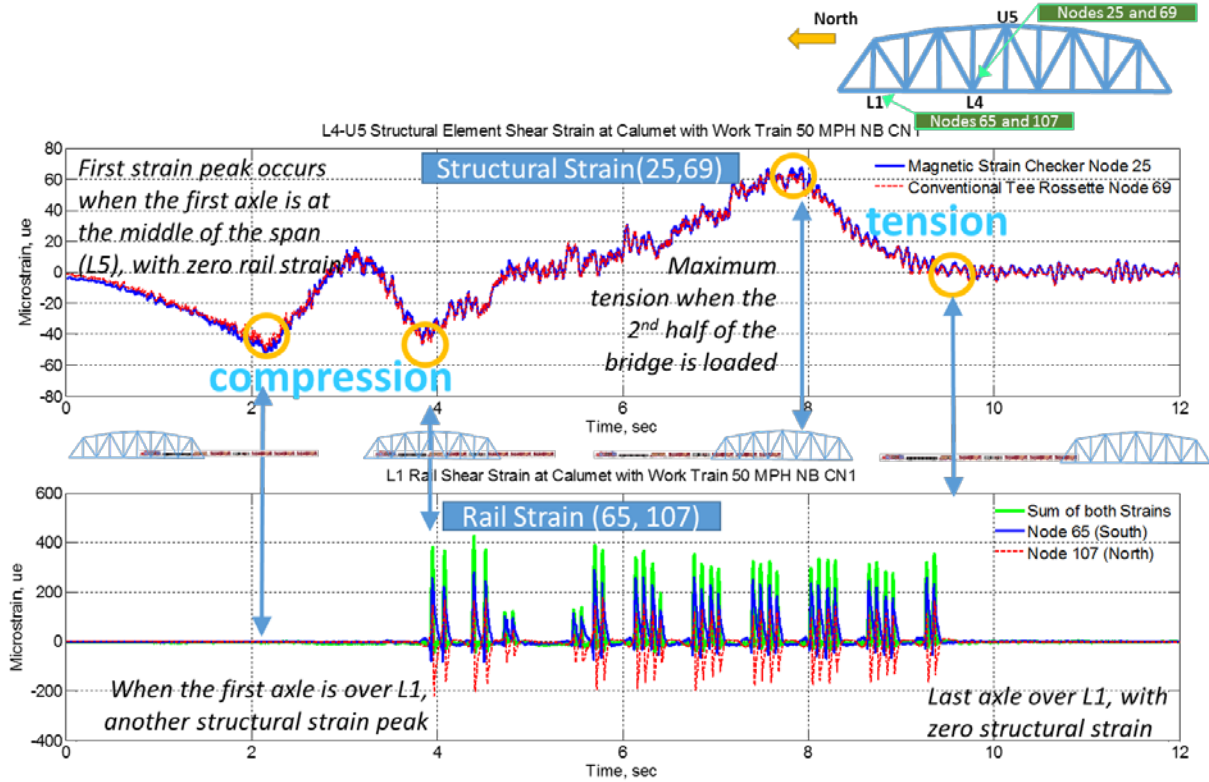


Figure 3.22 Strain measurements at multiple locations under work train

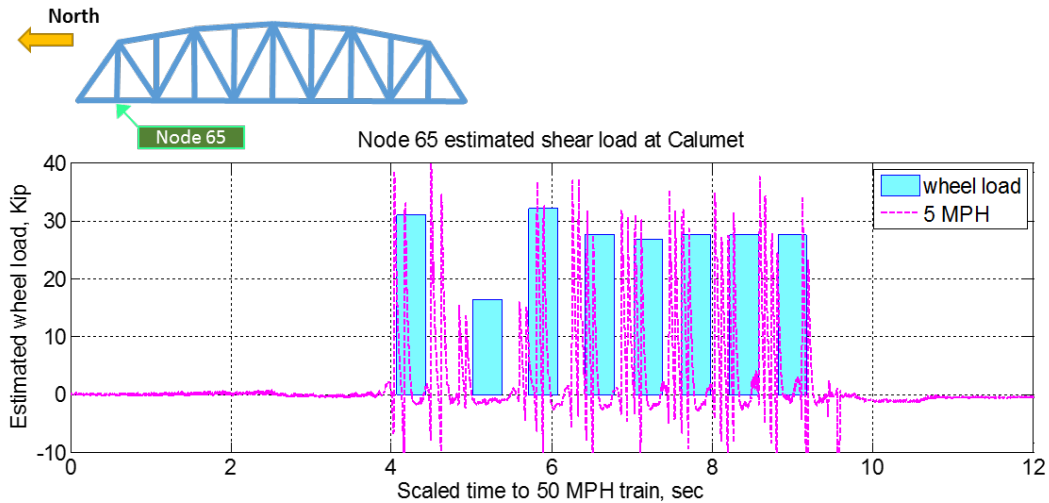


Figure 3.23 Estimated wheel load and work strain wheel load at 5 MPH

Impact Factor estimation

The American Railway Engineering and Maintenance-of-Way Association (AREMA) determines the Impact Factor (IF) for steel railroad bridges as a sum of two effects: vehicle rocking (RE), and the vertical effects due to superstructure-vehicle interaction (IV), therefore $IF=RE+IV$ ¹⁴. Both terms are empirical. For design, AREMA determines RE as 20% of the wheel without impact. Equation (1) shows the AREMA's IV formula for a steel truss.

$$IV' = 15 + \frac{4000}{(L + 25)} \quad (1)$$

The steel truss spans 310'-4", consequently, the IV is calculated in Equation (2)

$$IV = 15 + \frac{4000}{(310.42 + 25)} = 26.92\% \quad (2)$$

Figure 3.24 compares the shear strains at different speeds scaled to the recorded time under the 50 MPH train. Table 3.3 shows the maximum magnitudes under each car and the estimated IF, defined as the increment of load with speed over the "pseudo-static" load (5 MPH for this study). The measured IF at the rail is lower than the designed IF for structural elements. The reason for these differences is that these are readings at the rail level and the IF refers to structural elements. Figure 3.25 shows the effects of speed to the IF in the structural elements. Based on the two analyses, both rail and structural strains increase with higher speeds. However, the speed level results for this experiment cannot indicate a clear or significant relation between the increase of speed and the increase of strain. The change in the dynamic strain levels for these speeds is relatively small compared to the pseudo-static strain levels.

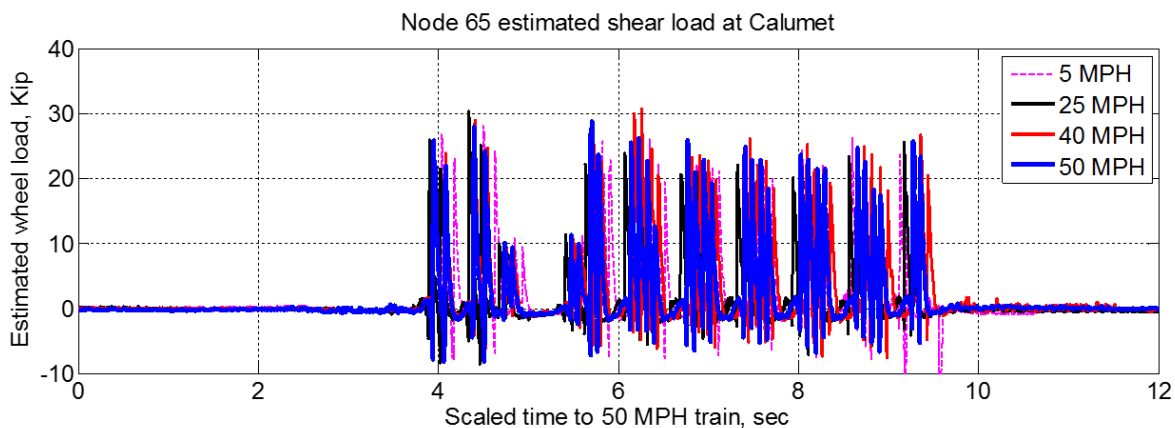
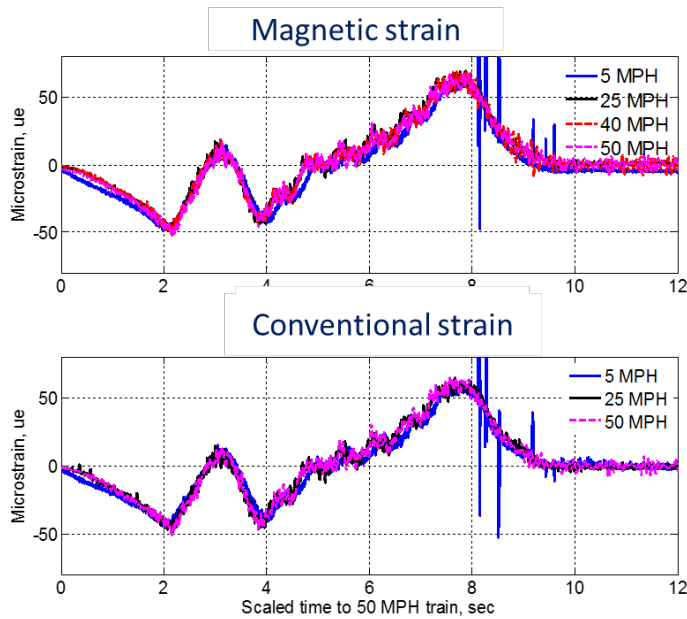
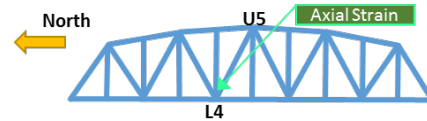


Figure 3.24 Rail shear strain comparison for all NB work train experiments

¹⁴ AREMA Manual, 2013.

Table 3.3 IF estimation from rail shear strain at different speeds

| Speed, s (MPH) | Engine | Gondola | Car 1 | Car 2 | Car 3 | Car 4 | Car 5 | Car 6 |
|----------------|--------|---------|------------|------------|-------|-------------|-------|-------|
| 5 | NA | NA | NA | NA | NA | NA | NA | NA |
| 25 | 8% | 3% | -7% | -7% | -12% | -17% | -5% | 8% |
| 40 | 3% | -2% | 19% | 11% | 5% | 3% | 2% | 13% |
| 50 | -1% | 5% | 12% | 17% | 1% | -3% | 1% | 9% |



| Speed, s (MPH) | Strain, e (ue) | IF |
|----------------|----------------|-----|
| 5 | 61.48 | NA |
| 25 | 69.48 | 13% |
| 40 | 68.74 | 12% |
| 50 | 67.72 | 10% |

| Speed, s (MPH) | Strain, e (ue) | IF |
|----------------|----------------|----|
| 5 | 59.68 | NA |
| 25 | 64.98 | 9% |
| 40 | NA | NA |
| 50 | 64.74 | 8% |

Figure 3.25 IF estimation for both magnetic and conventional strain of a diagonal truss element under different train speeds

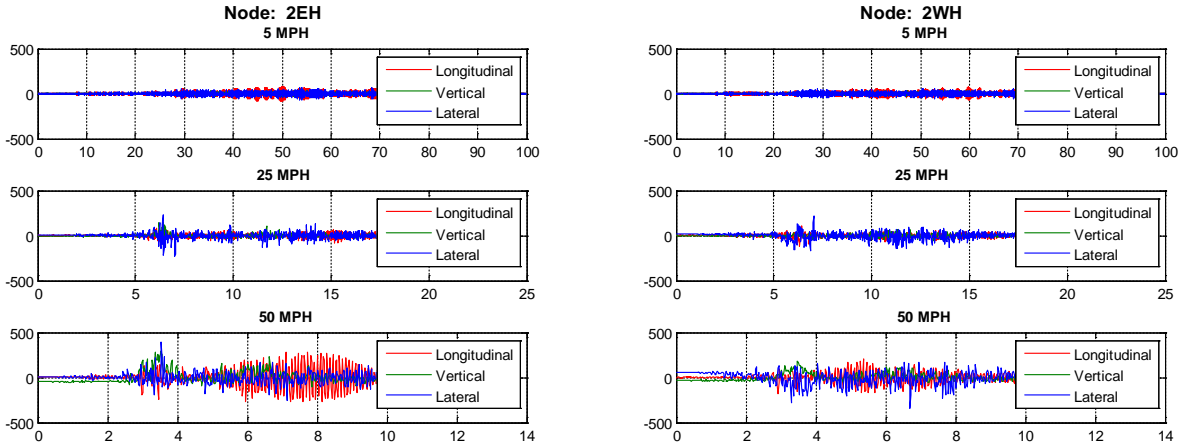


Figure 3.26 Acceleration comparison (a) L4EH, (b) L4WH

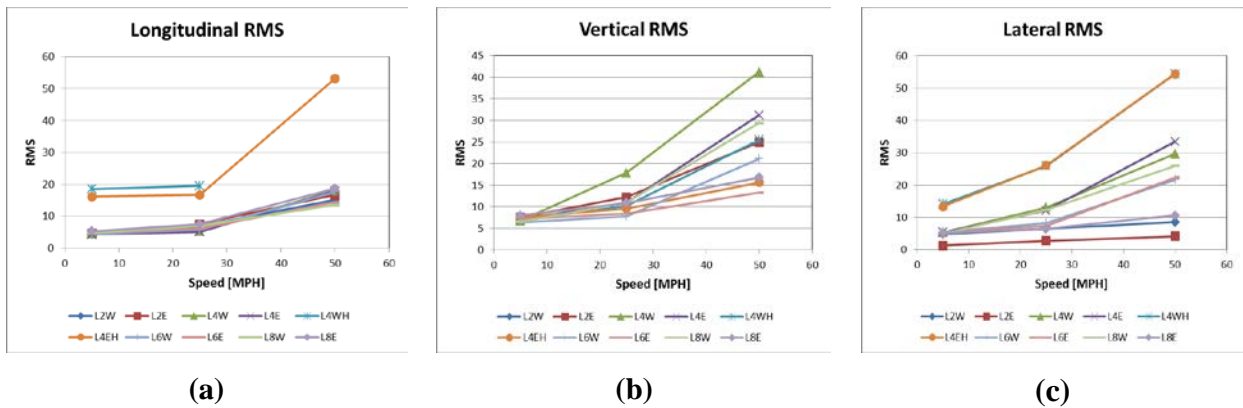


Figure 3.27 RMS comparison (a) longitudinal axis, (b) vertical axis, and (c) lateral axis

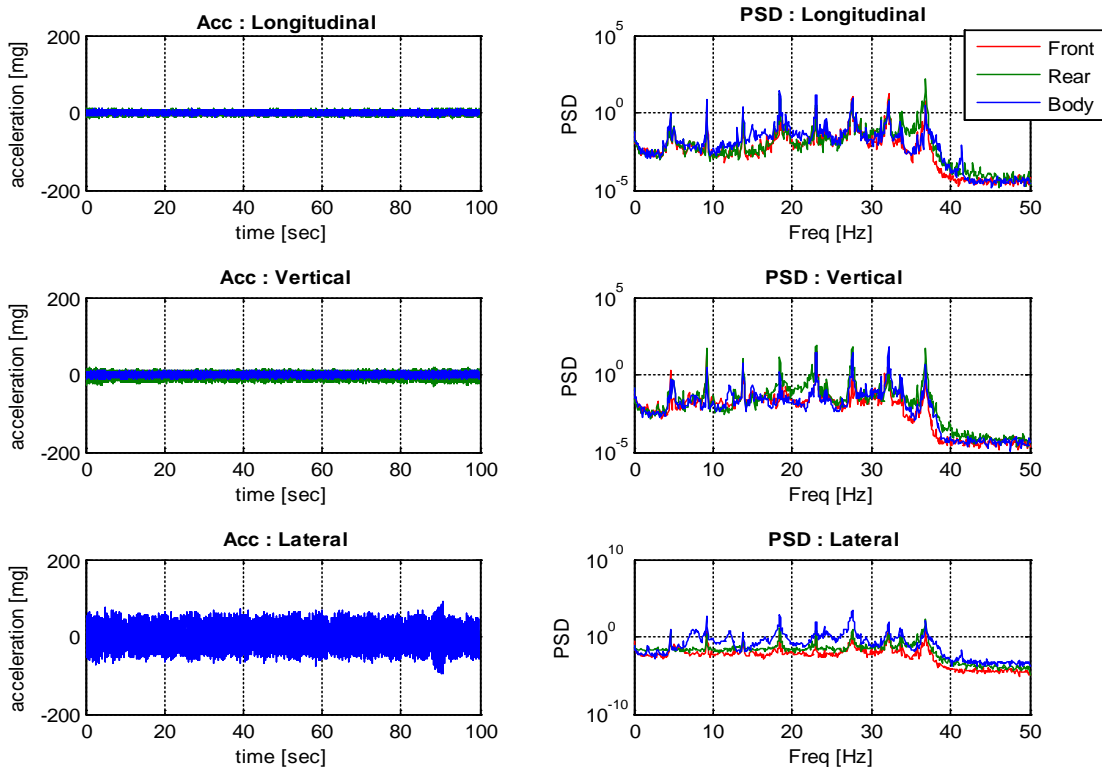
3.4.3 Structural Acceleration Monitoring Under Work Train Traffic

The Illinois research team investigated the effect of the train speeds on the bridge response as part of the work train tests by collecting bridge responses during each train run. The highest peak accelerations, in all directions, occurred in the L4EH and L4WH sensors. Figure 3.26 shows accelerations recorded at those two sensor locations from the NB test at 5, 25, and 50 MPH. The increased response at 50 MPH indicates that the bridge is more excited in all three directions under trains running at higher speeds. Figure 3.27 compares the Root Mean Square (RMS) from all acceleration records, which all increased with speed.

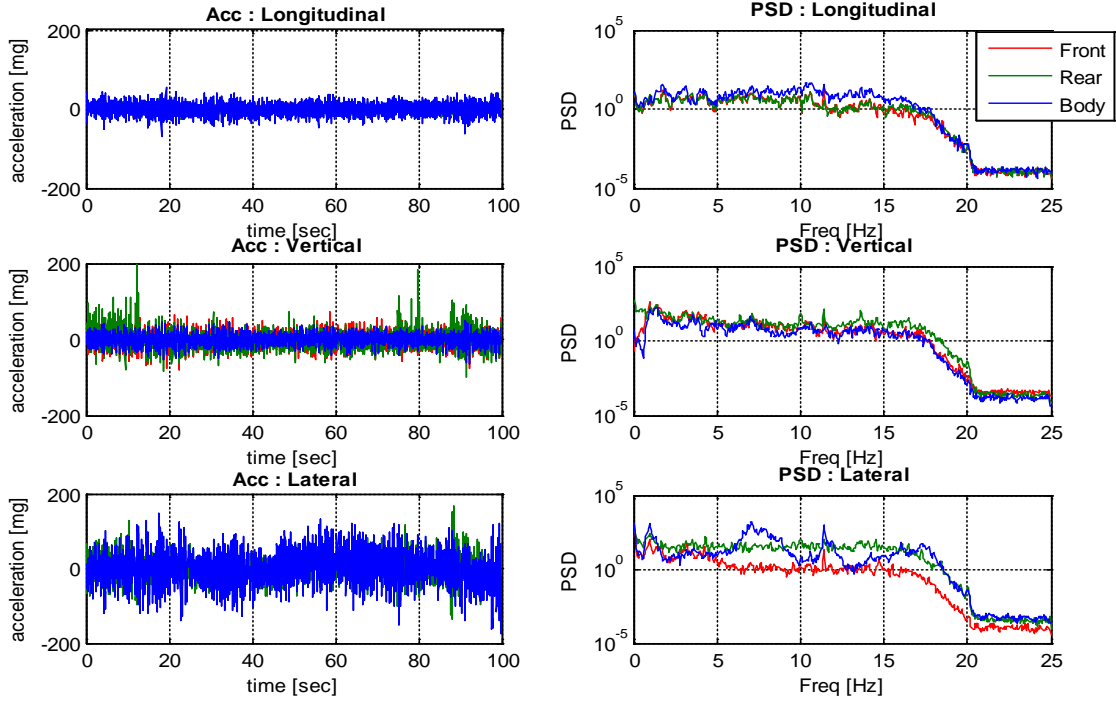
3.4.4 Train Acceleration Monitoring

The Illinois research team investigated the main characteristics of the locomotive—train idling on the track, train running on the track, train idling on the bridge, and train running the bridge—by collecting train responses at different train locations. Figure 3.28a shows idle status of the train in time and frequency domain. Accelerations of the front and rear bogies are relatively small (± 10 mg). The PSD plots show periodic peaks, which are due to engine torque pulses.

When the train is running on the track, the amplitudes of the front and rear bogie accelerations are almost 1000 mg (see Figure 3.28b). The engine-induced vibration is no longer visible while the train is running on the track. Figure 3.29a shows the train response while the test train is idling on the bridge. Response levels are smaller (5 mg) then when the train was idling on the track. In the frequency domain, the periodic response at 4.9 Hz, 9.8 Hz is again visible. The train acceleration levels while running on the bridge at 25 MPH reach ± 200 mg (see Figure 3.29b). The results consistently show that the train acceleration responses on the bridge are smaller than the train acceleration responses on the track.

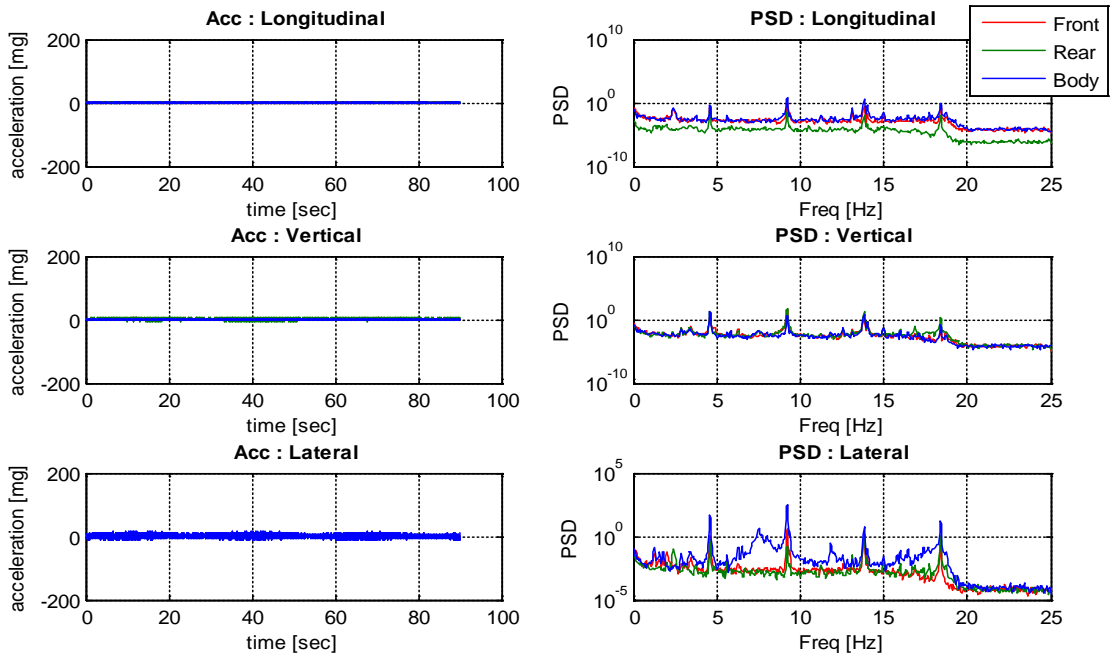


(a)

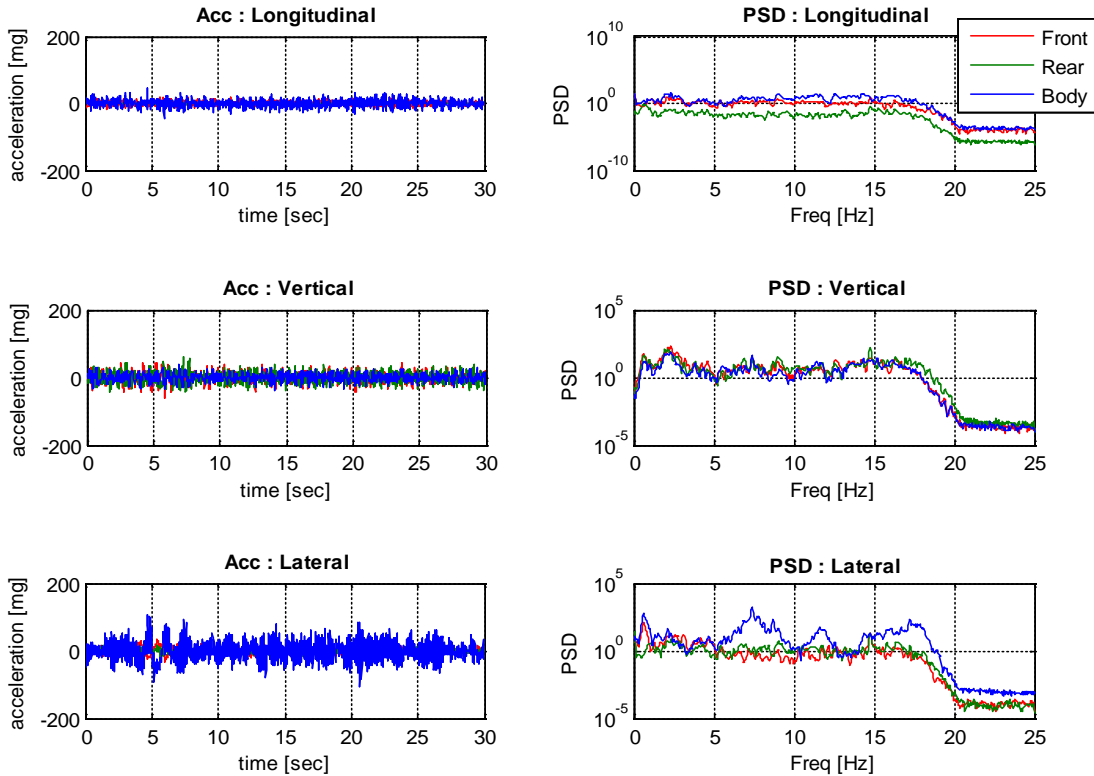


(b)

Figure 3.28 Train response comparison (a) idling on track, (b) running on track

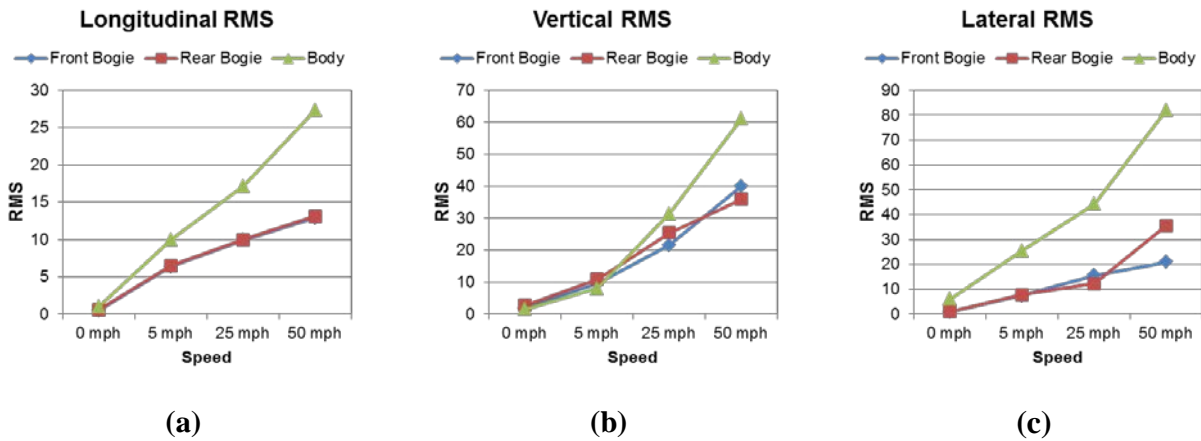


(a)



(b)

Figure 3.29 Train response comparisons (a) idling on the bridge, (b) running on the bridge



(a)

(b)

(c)

Figure 3.30 Acceleration RMS comparison (a) longitudinal axis, (b) vertical axis, and (c) lateral axis

The Illinois research team compared the RMS of the train at various speeds (see Figure 3.30). As the speed increased, the responses in front and rear bogie and car body increased linearly. In the future, researchers plan to use these measurements to characterize the train responses under interactions between vehicle (train), track and bridge (or Vehicle-Track-Bridge Interactions).

3.5 Data Collected from Remote Monitoring

Auto-Monitor, the application that remotely monitors the wireless sensor network, ran daily for over two months. The Auto-Monitor service includes: (1) Threshold check, (2) Remote sensing, and (3) Auto-Util check. The threshold check functionality measures a short period of acceleration and decides whether to start the remote sensing application.

During the period of August 26 and September 27, over 30 remote sensing events were automatically initiated. The Auto-Monitor application captured bridge responses under various trains crossing the bridge (see Figure 3.31) and the team used the collected data to update the bridge modal analysis. Additionally, the Auto-Monitor application collected both structural and rail strain data, which was used to estimate the loading characteristics of the train crossing the bridge and the structural responses to that load. Figure 3.32 shows the rail strain collected remotely on October 24 (intermodal train). The above figure shows green peaks indicating the separation of the wheels, and the strain amplitude estimates the input load under each wheel. The lower figure shows the structural strain collected with remote monitoring at L4-U5 diagonal member.

The Auto-Util check function included voltage level check in all sensor nodes to ensure that the service remained sustainable. Over a month, the batteries were charging constantly through solar panel and showed over 4V (Figure 3.33). These results show that the system is highly sustainable and reliable.

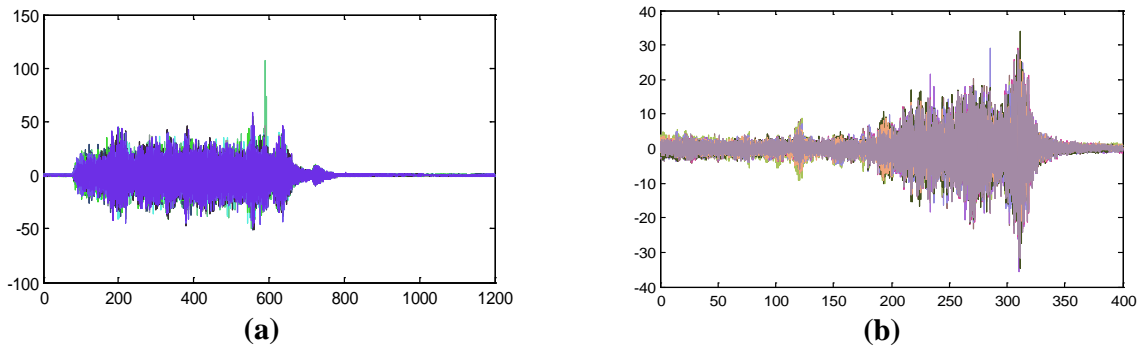


Figure 3.31 Accelerations captured during remote sensing

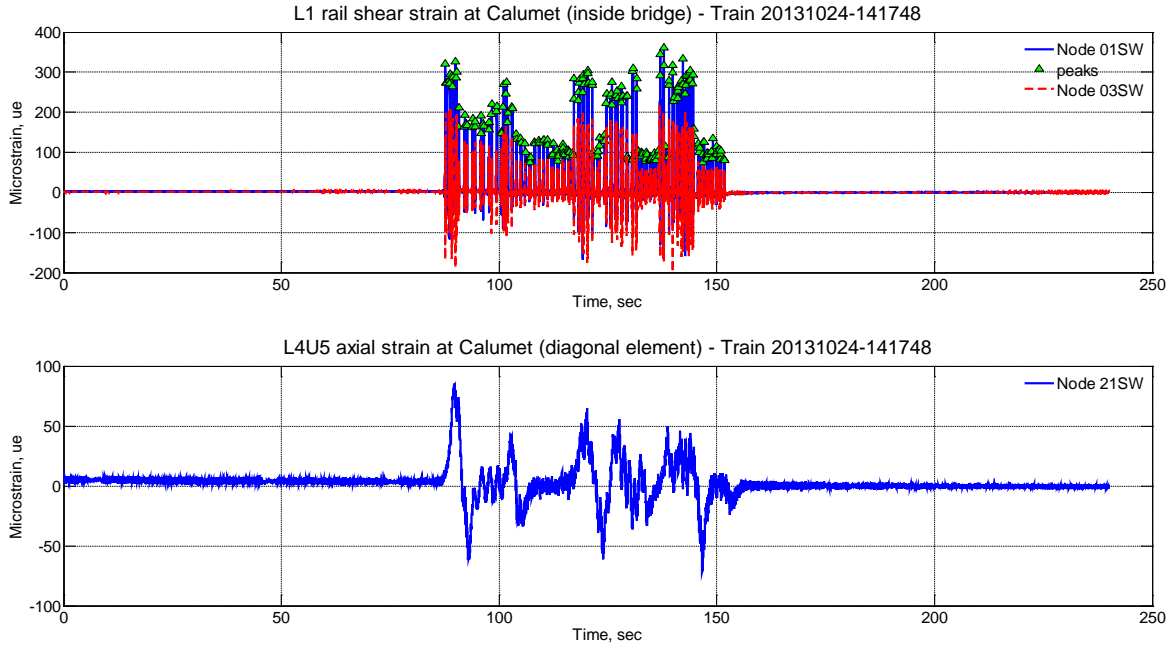


Figure 3.32 Strains collected during remote sensing

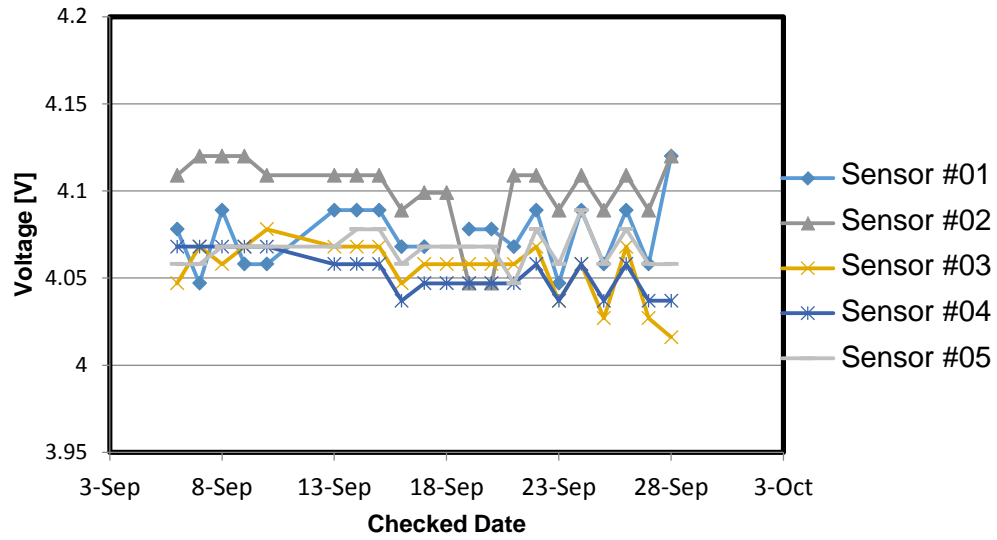


Figure 3.33 Example of battery voltage monitoring

4. RESULTS

This section summarizes the results of this project, which includes: validating and updating of the bridge's FE model, conducting a strain analysis of the bridge, developing and validating a simple beam model for estimating bridge resonance, and creating reference-free bridge displacement estimations. Also, a sample analysis of the autonomously collected data is presented.

4.1 Bridge FE Model Updating

4.1.1 Preliminary Results

Figure 4.1 shows the modal analysis results of the first four fundamental modes. The bridge is more flexible in the lateral direction, with the first, second and third lateral modes at 1.58 Hz, 2.70 Hz and 3.77 Hz, respectively. The first vertical mode is at 3.85 Hz.

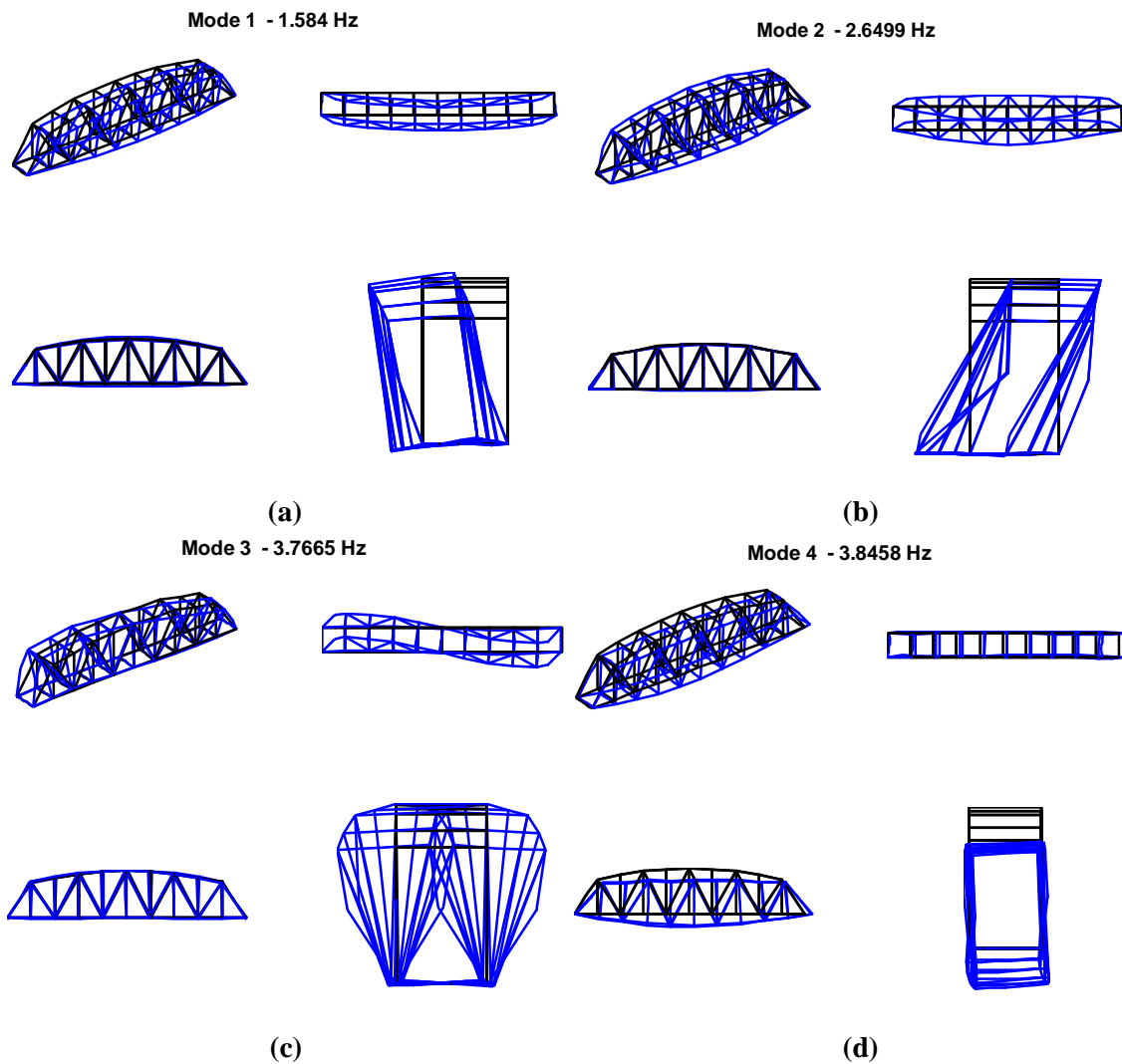


Figure 4.1 Model update validation

Table 4.1 compares the modal frequencies identified from the FE model with the experimentally determined modal frequencies. While the first lateral mode in the FE model matches well with those identified experimental data, the other modes differ from the test data by about 10%. Updating the model brings it into closer agreement with the measured data.

Table 4.1 Comparisons of significant modes between the preliminary FE model and experimental modal analysis

| Mode Name | FE model (Hz) | WSS System ID (Hz) | Difference (%) |
|--------------------------|---------------|--------------------|----------------|
| 1 st Lateral | 1.58 | 1.54 | 2.60 |
| 2 nd Lateral | 2.70 | 3.01 | 10.30 |
| 3 rd Lateral | 3.76 | 3.39 | 10.91 |
| 1 st Vertical | 3.86 | 3.59 | 7.52 |

4.1.2 Updated Parameters

The shop drawings provided by the CN indicated that the total mass of the bridge should be approximately 2,500 kips, which was larger than the weight of the initial model. The model had underestimated the mass associated with the track system (tie and rail), lacing, and utilities (see Figure 4.2), and the research team updated it to accommodate this mass. In addition, the maximum total mass of the work train on the span is approximately 1,200 kips, which represents approximately 40% of the weight of the bridge structure; the weight of the Amtrak train is about half of the weight of the work train, or 20% of the weight of the bridge.



(a)

(b)

Figure 4.2 Bridge additional mass elements (a) track system details, (b) element lacing

4.1.3 Validation of FE Model Against Measured Data

This section compares the measured modal properties and strains with the model's predictions. Figure 4.3 compares the modes and frequencies of the updated FE model against the modes and

frequencies identified from the measured data. The blue/black models (i.e., the first two columns) show the mode shapes and frequencies from the FE model. The red/gray models (i.e., the third column) show the mode shapes and frequencies from the data. The middle column (blue/black) shows the modes of the FE model at the sensor locations.

Comparing the updated model and the experimentally derived data shows excellent agreement (Table 4.2), with an error of less than 5% in the frequencies for all modes. These results indicate that the model could be a predictive tool that determines bridge responses under different loadings.

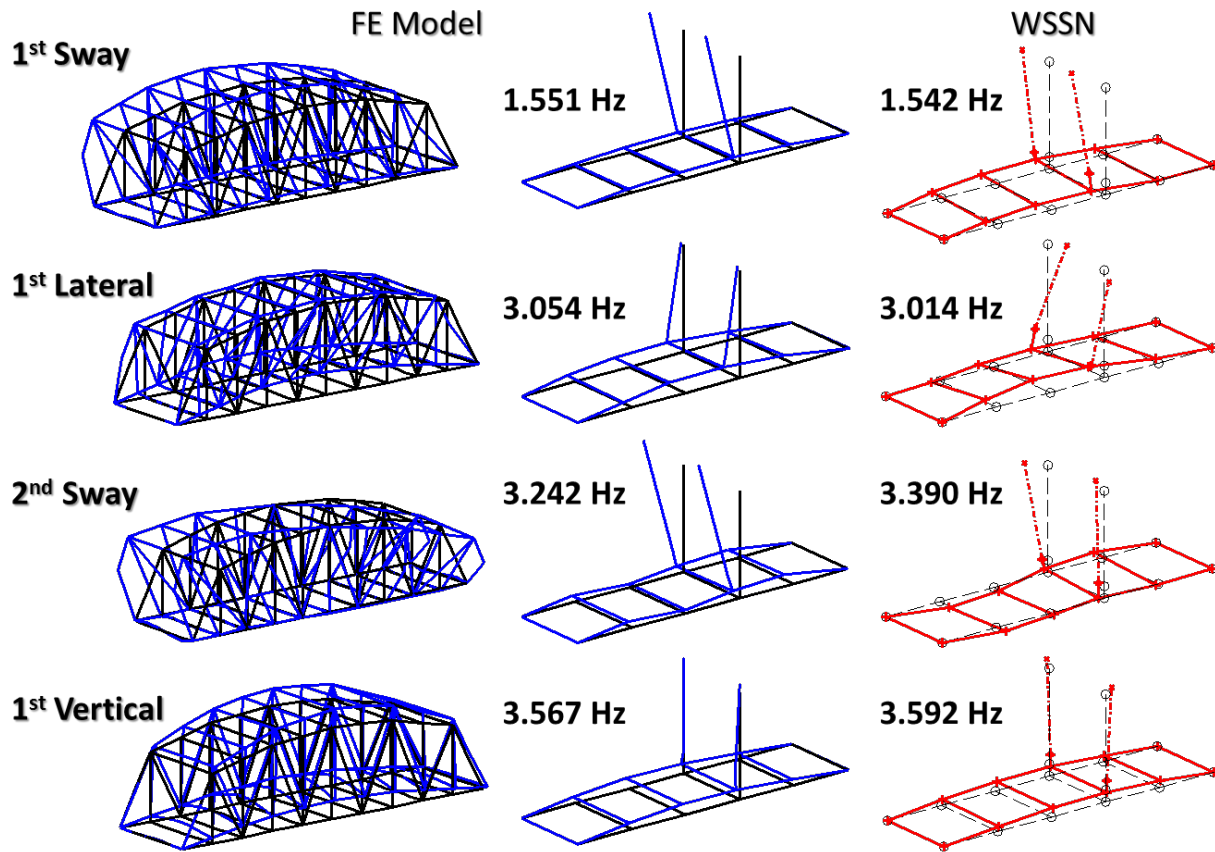


Figure 4.3 Comparison of experimentally identified and model modes and frequencies

Researchers compared the measured strains under trains to the estimated strain from the model. The Illinois research team installed both a wireless strain checker and a conventional strain gage on the L4-U5 element and collected strains under work train tests. Earlier studies found that the dynamic component of the strain is small at the speeds for which we collected data. Therefore, the Illinois research team performed a series of static analyses of the FE model condition as a train crosses the bridge and compared the results. The strain collected in the field was also validated using hand calculations of the strains under the given work train loading.

Table 4.2 Comparisons of significant modes between the updated FE model and experimental modal analysis

| Mode Name | FE model (Hz) | WSS System ID (Hz) | Difference (%) |
|--------------------------|---------------|--------------------|----------------|
| 1 st Lateral | 1.55 | 1.54 | 0.65 |
| 2 nd Lateral | 3.05 | 3.01 | 1.33 |
| 3 rd Lateral | 3.24 | 3.39 | 4.42 |
| 1 st Vertical | 3.57 | 3.59 | 0.56 |

The measured strain matches the predicted strain model using static analysis of the FE model (Figure 4.4). These results demonstrate the predictive power of the FE model and show that it is a good tool for understanding the behavior of the bridge under in-service loads.

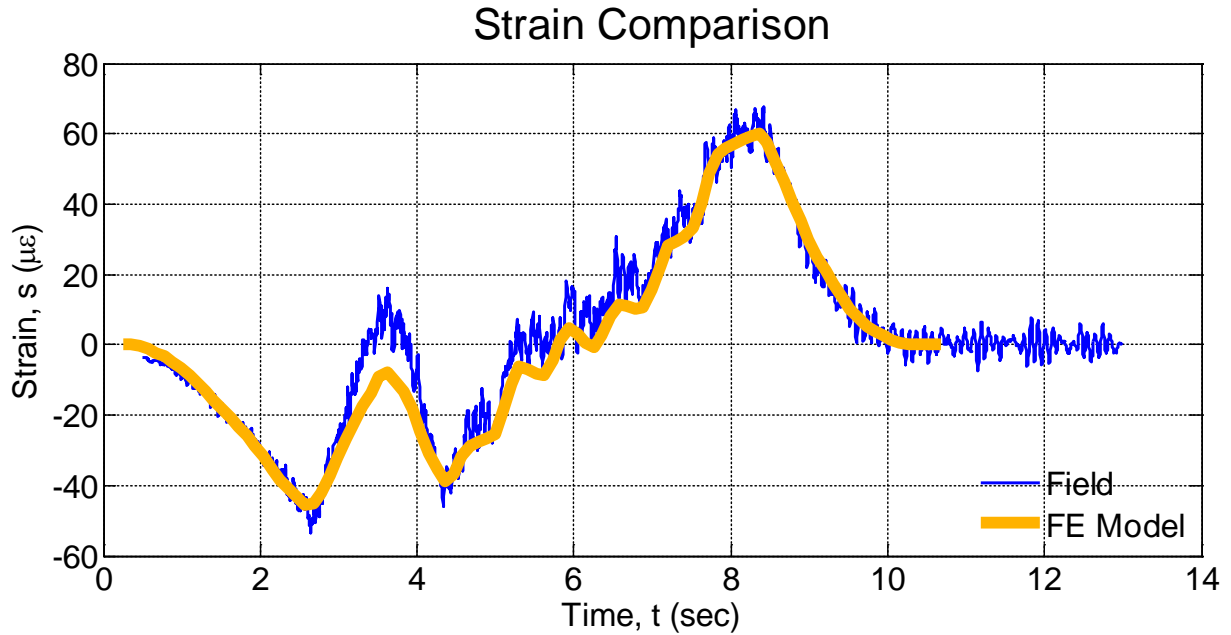


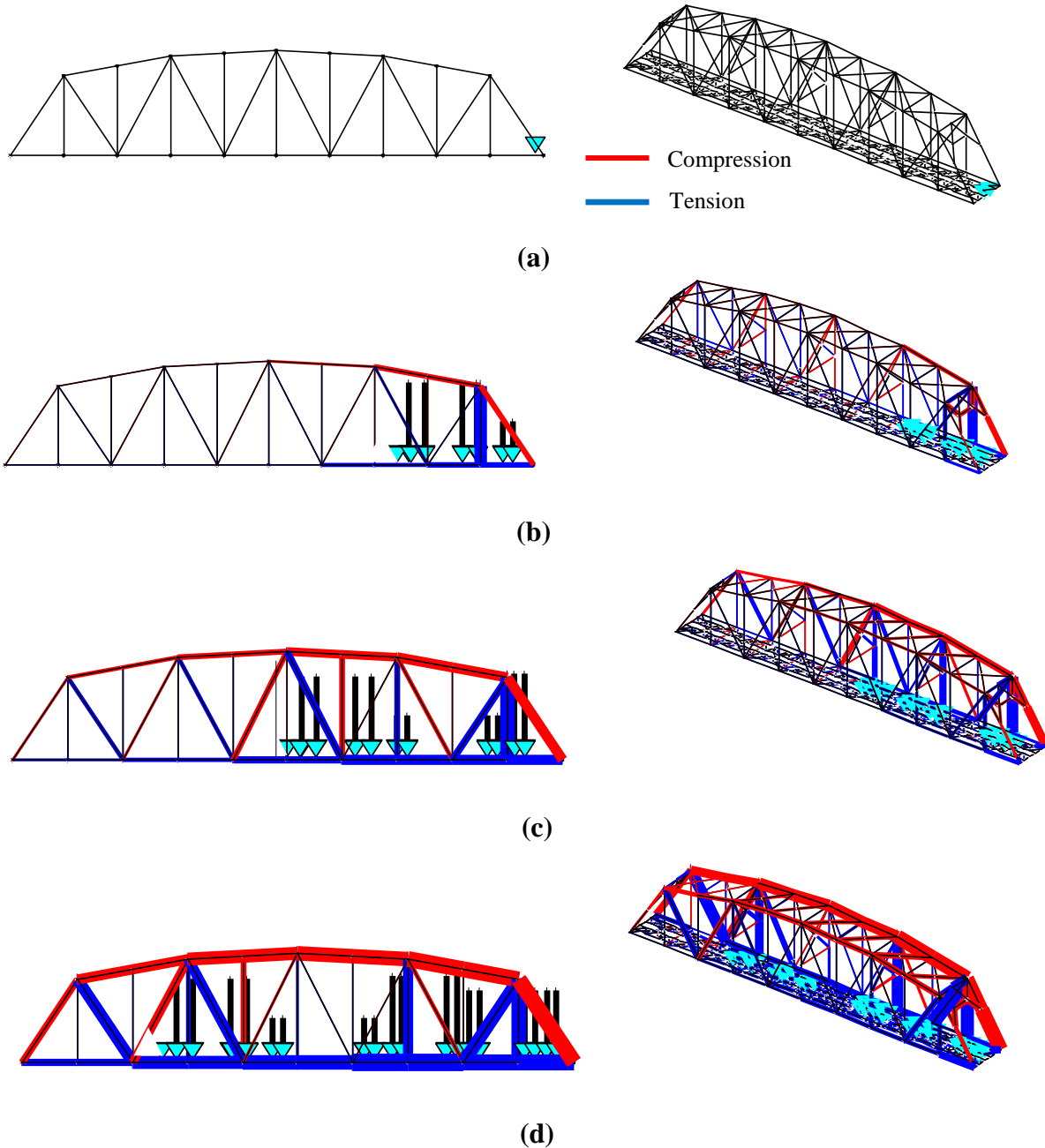
Figure 4.4 Strain comparisons from measured data and model predictions

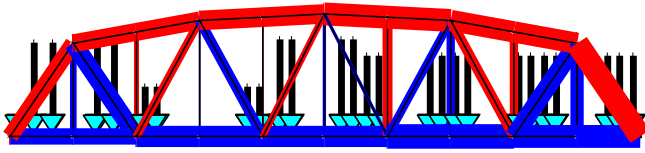
4.1.4 Strain Map for the Structure

This section demonstrates how the FE model, combined with measured data, can develop a strain map for the entire structure. As mentioned previously, the dynamic component of the strain at the observed speeds is small; consequently, combining the wheel loads determined from the instrumented rail with the FE model of the bridge can provide an estimate of the strains and stresses experienced at arbitrary locations on the bridge.

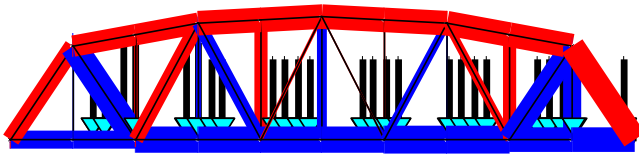
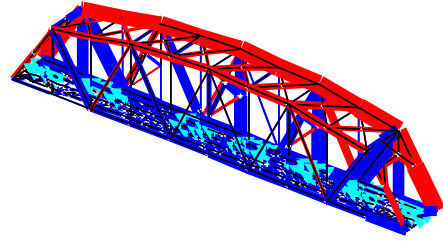
Figure 4.5 provides the evolution of the strain map as the work train crosses the bridge. The left corresponds to north in the figure. The cyan triangle indicates the locations of the wheels as the work train crosses the bridge. The length of the black lines above the cyan triangles indicates the

magnitude of the wheel loads. Members in tension are marked in red and members in compression are marked in blue. The thickness of the colored elements indicates the relative magnitude of the strain in each element. For those elements with strain levels under a specified tolerance limit, the element is marked with a thin black line. The right column of this figure also shows the 3-D view of the strain distribution. The asymmetric strain distribution between the West and the East truss planes are due to only one train loading the double-tracked bridge. The information provided by this analysis can verify designs, monitor damage, and assess the fatigue life of bridges under in-service loads. An animation of the evolution of the strain map as the train crosses the bridge is at the following link: <http://sstl.cee.illinois.edu/BridgeStrainVideo.html>.

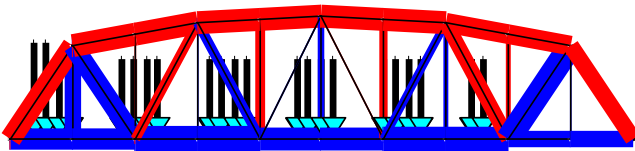
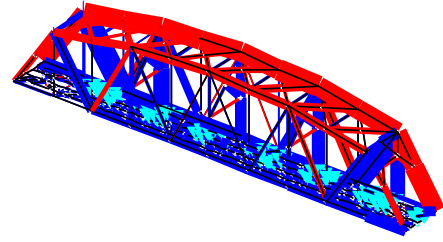




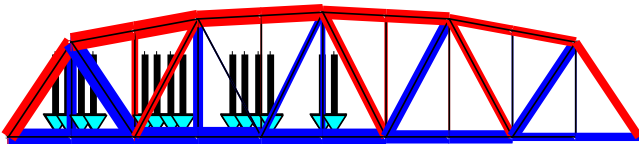
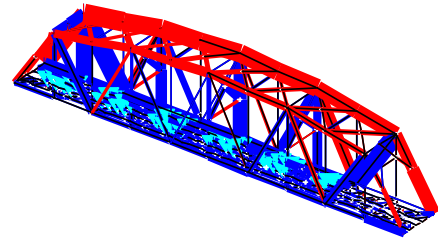
(e)



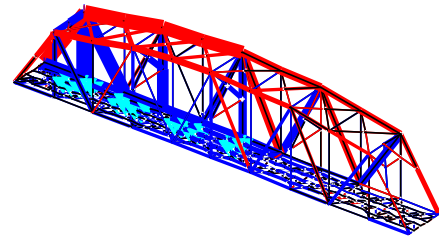
(f)

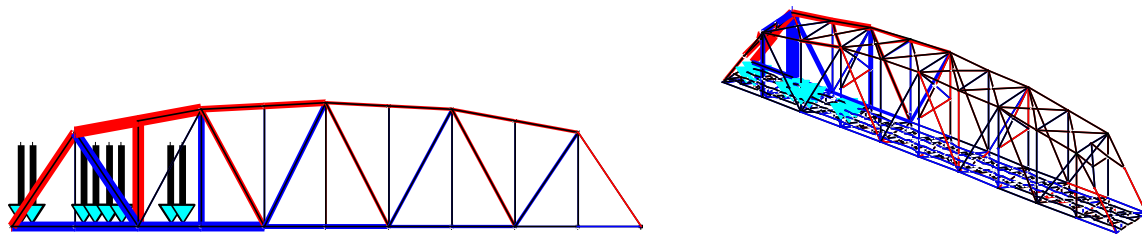


(g)

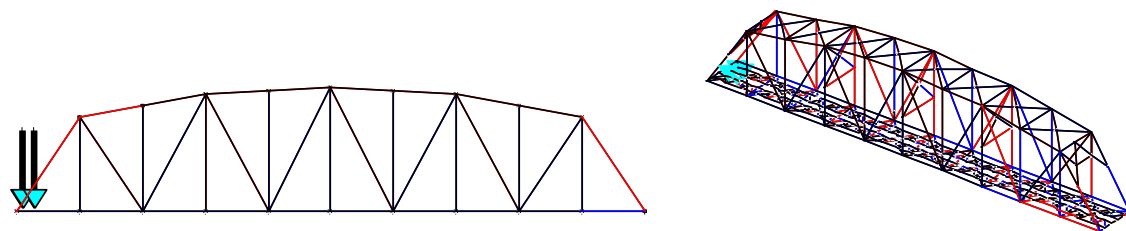


(h)





(i)

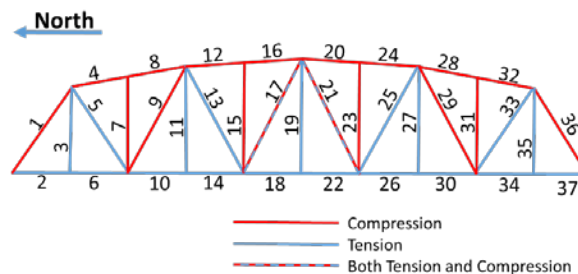


(j)

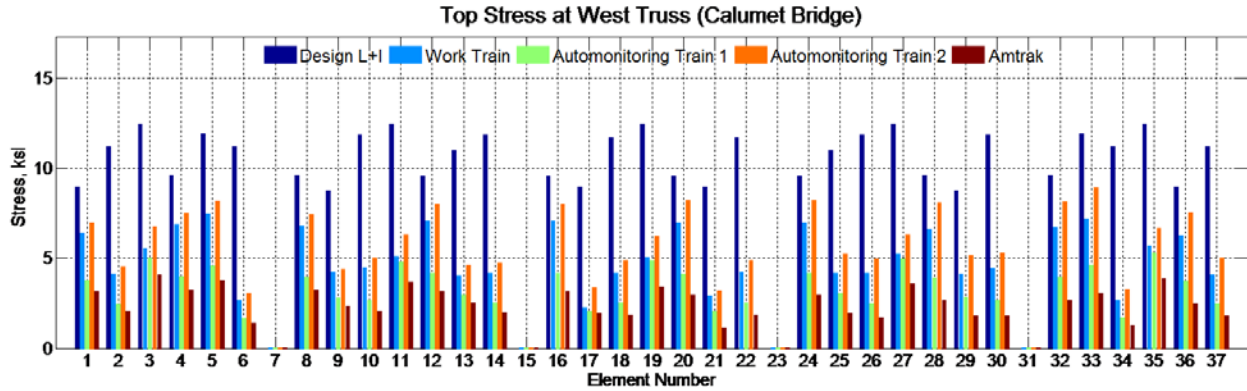
Figure 4.5 Strain map predicted by the FE model for the work train

4.1.5 Fatigue Assessment

This research uses the strain data to make a global fatigue assessment of the bridge. Researchers used the FE model to predict the strain under various train-measured loadings and obtain the associated stress for each element. Figure 4.6a shows the element labeling for stress analysis and Figure 4.6b shows the FE model estimates of stresses for all the truss elements in the bridge under different trains loading the bridge (assuming two tracks loaded at the same time), as compared to the design stresses. As shown, the stress levels are lower than the design stresses. The endurance limit is the amplitude of cyclic stress that a member can undergo without experiencing fatigue, which is 30 ksi for structural steel. Based on a linear analysis, the stress levels measured in the bridge and those predicted by the FE model are well under the fatigue endurance limit. In the future, the Illinois research team could develop this predictive tool to estimate the remaining life of steel trusses in situations where fatigue may be a concern.



(a)



(b)

Figure 4.6 Predicted stress under multiple train loading
 (a) truss element labeling, (b) stress assessment

4.2 Simple Beam Model

This section describes a simple model that predicts the dynamic response of the bridge to trains running at arbitrary speeds. In the past, various researchers have developed bridge/train models; however, these models require detailed parameter development for both the train and the bridge and they are often computationally demanding. As a model gets more complicated, the fundamental characteristics of the bridge’s responses become harder to discern. In this research project, an Euler-Bernoulli beam is used to represent the bridge and the train is modeled as a moving mass (i.e., vehicle-bridge interaction is neglected).

First, the Illinois research team built the model and estimated the parameters from limited sensor data. Subsequently, the research team validated the model against the measured data. Finally, the research team used the model to estimate bridge resonance. Additionally, the researchers will use the model to assist in determining bridge displacements from measured accelerations and strains. The predictive power of this simple model is substantial and to our knowledge, the model has not appeared previously in the open literature.

4.2.1 Model Formulation

The Illinois research team modeled the CN bridge as an Euler-Bernoulli beam, and the train as moving masses crossing the bridge (see Figure 4.7a). Two approaches are considered: (1) the mass of each car is distributed over its car body length (see Figure 4.7b), and (2) half the mass of each car is concentrated at the center of the front and rear bogies (see Figure 4.7c). These results are also compared against the more traditional moving load problem (i.e., the mass of the train is neglected in calculating the response of the bridge). In this model, simple assumptions and a more complete description of the problem provide powerful predictions compared to the conventional formulation that ignores the mass of the train in the vibration of the bridge.

The simplified beam model employs the Assumed-Modes Method¹⁵. The vertical displacement of the beam is:

¹⁵ Craig & Kurdilla. (2006). “Fundamentals of Structural Dynamics.” Second Edition, Wiley, New York.

$$v(x,t) = \sum_{i=1}^N \psi_i(x)q_i(t) \quad (3)$$

where $\psi_i(x)$ represents each of the assumed modes of vibration of the simplified beam model. The mass matrix for the combined bridge/train system is:

$$M=M_B+M_T(t) \quad (4)$$

where the mass of the beam, M_B , is given by:

$$M_{B_{ij}} = \int_0^L \rho A \psi_i(x) \psi_j(x) dx \quad (5)$$

the contribution of the train mass, $M_T(t)$, is:

$$M_{T_{ij}}(t) = \int_0^L m^*(x - V_0 t) \psi_i(x) \psi_j(x) dx \quad (6)$$

and $m^*(x)$ is the function defining the train mass on the bridge. The stiffness matrix and applied loads are:

$$K_{ij} = \int_0^L EI \psi_i''(x) \psi_j''(x) dx \quad (7)$$

$$P_j(t) = -g \int_0^L m^*(x - V_0 t) \psi_j(x) dx \quad (8)$$

A damping ratio of 0.5% is assumed for each mode of the bridge (without the train) based on measured bridge responses. The initial conditions are assumed to be zero. The equation of motion of the simplified beam model is then:

$$\{M + M_T(t)\} \ddot{q}(t) + C \dot{q}(t) + K q(t) = P(t) \quad (9)$$

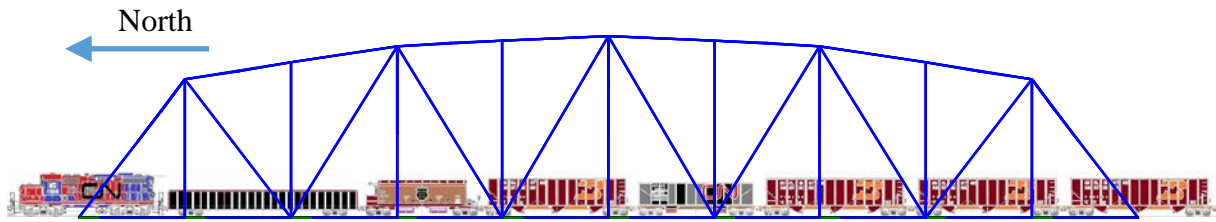
4.2.2 Model Parameter Estimation

The construction drawings provided the mass of the bridge and the measured data determined the first vertical and lateral natural frequencies of the bridge. The equation relating the mass and the frequency is:

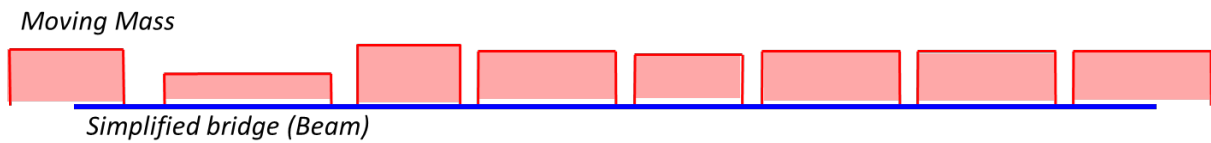
$$f_1 = \frac{\pi}{2L^2} \sqrt{\frac{EI}{\rho A}} \quad (10)$$

where ρA is the mass per unit length, E is Young's modulus, and I is the moment of inertia of the beam. Thus, EI is

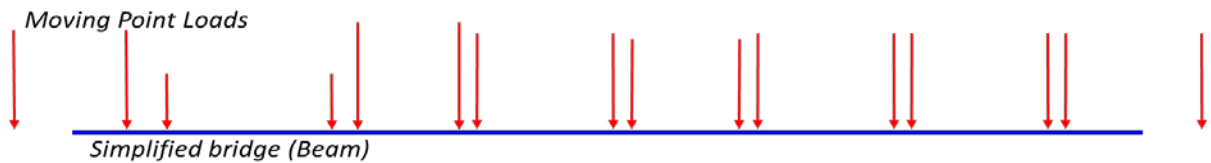
$$EI = \frac{4L^4 f_1^2 \rho A}{\pi^2} \quad (11)$$



(a)



(b)



(c)

Figure 4.7 Bridge and train model (a) FE model, (b) simplified beam and moving distributed-mass model, and (c) simplified beam and moving point-mass model

4.2.3 Comparison of Simplified Models

This section compares the moving distributed-mass model (see Figure 4.7b) with the point-mass model (see Figure 4.7c). Figure 4.8 provides a direct comparison between the two models. The two models produced essentially the same results. Due to better computational efficiency, the remainder of this report only uses the moving point-mass model.

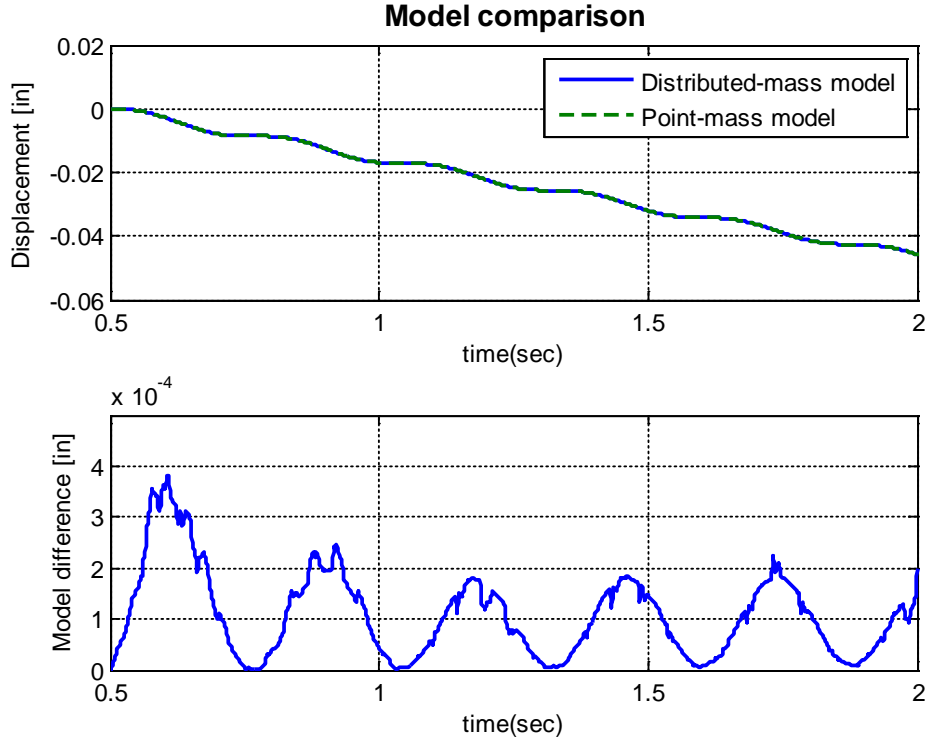


Figure 4.8 Distributed-mass model and Point-mass model comparison

4.2.4 Model Validation

The axial strain measured on the truss member L4-U5 is proportional to the shear load carried by the bridge at that location. Thus, to validate the moving-mass model, a comparison is made between the measured strain and the strain predicted by the simple beam model. The shear V in the beam is:

$$V = EIv'''(x, t) \quad (12)$$

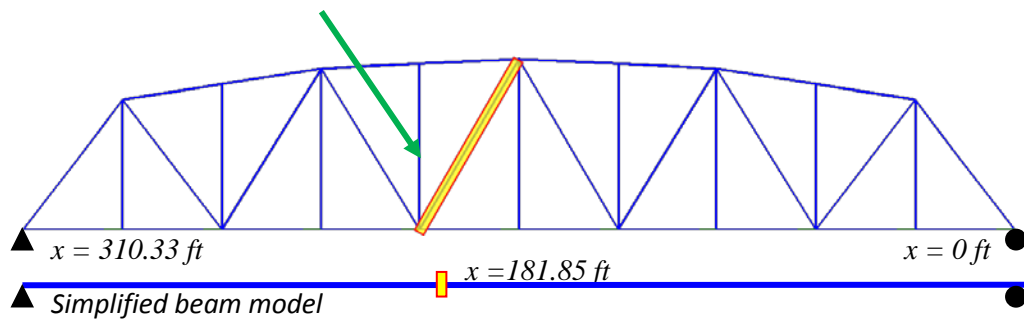
where $v = v(x, t)$ is the vertical displacement of the beam. Because of the truss geometry, the L4-U5 member carries the majority of the shear load in the truss. Thus, the shear load at this bay in the truss is:

$$V_{truss} = \varepsilon_{measured} EA \sin(63.4^\circ) \quad (13)$$

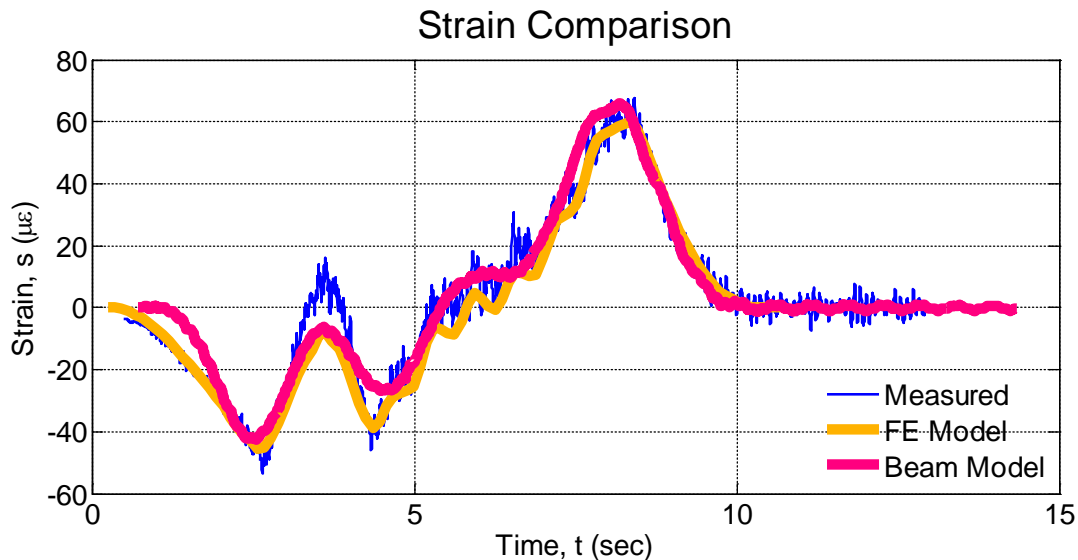
The strain estimated by the model is then:

$$\varepsilon_{estimated} = \frac{V_{beam}}{EA} \sin(63.4^\circ) \quad (14)$$

Using these equations, Figure 4.9b shows the strain in the L4-U5 member based on the simplified model. The signature of the strain in the simplified model matches well with the measured strain and the strain predicted by the FE model.



(a)



(b)

Figure 4.9 Strain estimation from the beam-mass model (a) instrumented element location, (b) strain comparison

This section compared the measured strain in the field with the FE model strain and the simple beam model strain. The results show that both models can predict the strain under known loads accurately and provide the foundation for using the simple beam model to predict the bridge response under trains running at faster speeds.

In conclusion, the Illinois research team has designed a new simple beam model that can estimate railroad bridge responses under load and factor the mass of the cars crossing the bridge into the bridge's response. The following sections show the potential of this model for several railroad bridge performance monitoring applications, including strain analysis, bridge resonance, and displacement estimations under trains.

4.3 Bridge Resonance

Resonance occurs when the train loading frequencies coincide with the bridge's natural frequencies, which causes the bridge's response to increase significantly. Therefore, estimating the critical speed of trains crossing existing bridges in shared corridors is an essential part of upgrading these bridges to higher speed trains. The Illinois team investigated bridge resonance

under various trains using the simplified moving-mass/load model. This section compares the traditional moving-load model with the moving-mass model to emphasize the effect of train mass on the bridge and provides further comparisons between the project's model and the method of calculating resonances traditionally employed by the railroad industry.

4.3.1 Vertical Resonance Under Work Train

To investigate bridge characteristics under resonance conditions, the Illinois research team compared acceleration and displacement time histories at specific train speeds. Figure 4.10 shows the acceleration and displacement responses at the mid-span of the bridge for various speeds. At 91 MPH (see Figure 4.10c), the dynamic responses increase as the car enters the bridge and reach the highest peak when the locomotive arrives the end of the bridge. The peak acceleration and the maximum displacement at the resonance speed are much larger than higher speeds such as 150 MPH (see Figure 4.10d).

Subsequently, the Illinois research team performed a dynamic analysis under the vertical work train loading, for speeds varying from 1 MPH to 200 MPH. A comparison was made between the moving mass model and the moving-load model. In examining the maximum RMS acceleration responses in Figure 4.11, the moving-mass model predicts the critical resonance around 90 MPH for the work train, while the moving-load model predicts the resonance to be approximately 20% higher. The test train speeds varied from 5 MPH to 50 MPH. Within these speeds, bridge responses in both vertical and lateral directions are within the linear range, as shown both in the measurements (see Figure 3.27) and in the analyses.

Figure 4.12 shows the maximum absolute displacement. Examination of this figure further demonstrates that the train speed does not affect the maximum vertical bridge displacement significantly. The dynamic displacements are equal to the total displacements minus the pseudo-static responses of the bridge. The dynamic displacements show resonance at speeds similar to those found in the RMS acceleration plots (see Figure 4.13).

These results show that for train speeds under 70 MPH, the moving-load model approximates well the maximum bridge responses. However, the two models identify different critical resonance speeds, with the moving load model providing unconservative results. The differences in estimating critical speeds using moving mass model and moving load model become larger with heavier trains.

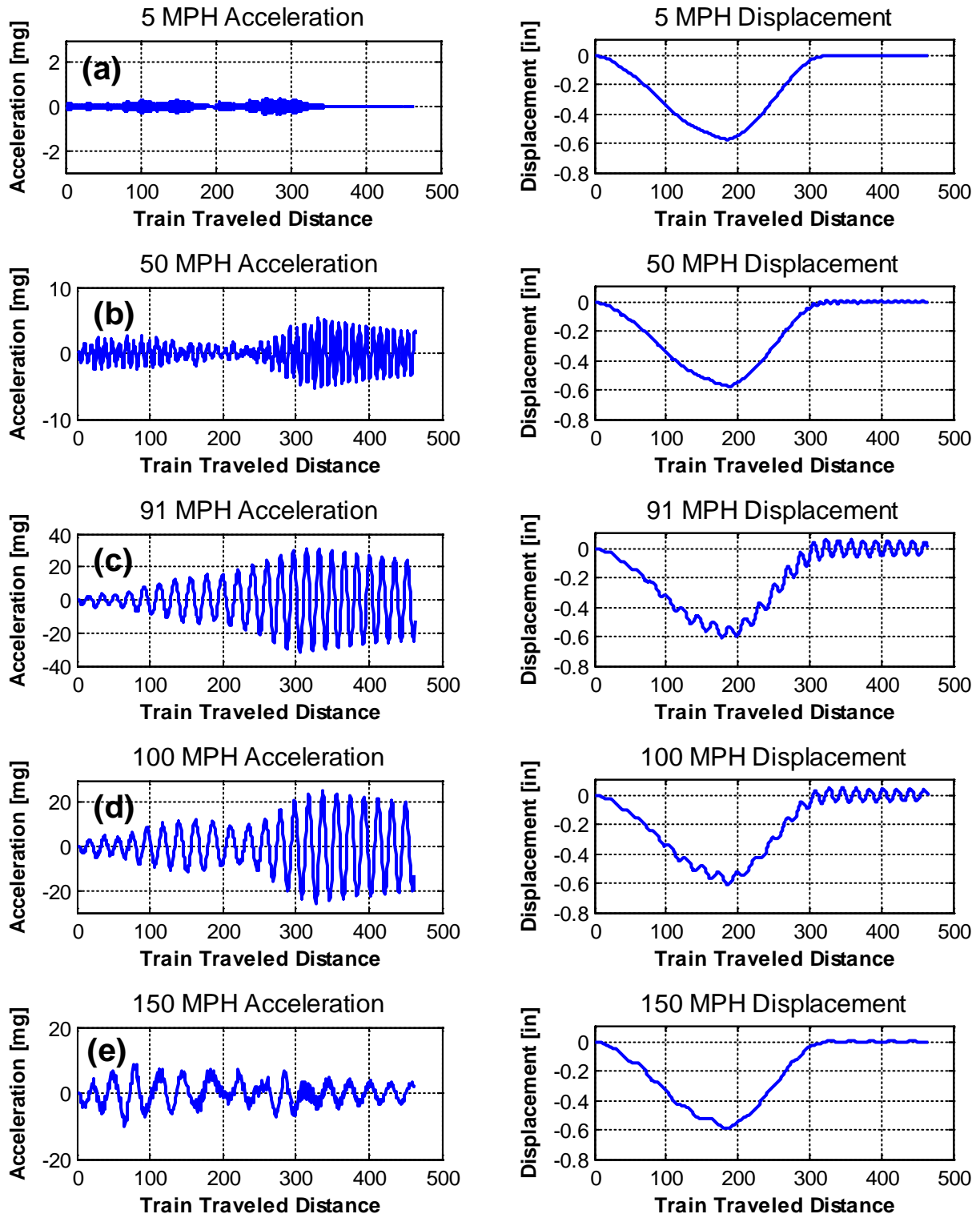


Figure 4.10 Examples of time history at mid-span of bridge at certain train speeds (Moving mass model); (a) train speeds at 5 MPH, (b) 50 MPH, (c) 91 MPH (Resonance speed), (d) 100 MPH, (e) 150 MPH

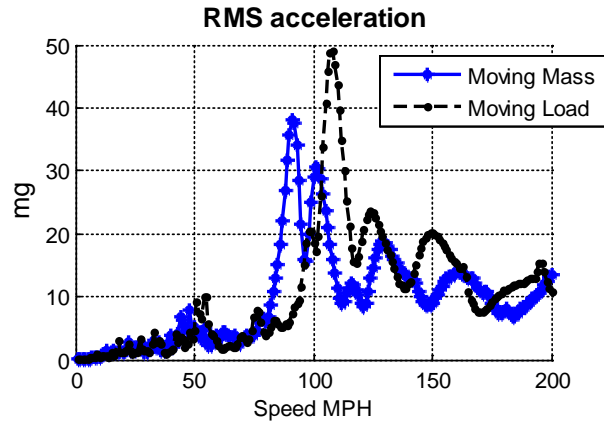


Figure 4.11 Vertical bridge response (RMS of acceleration) at mid-span of bridge for the work train

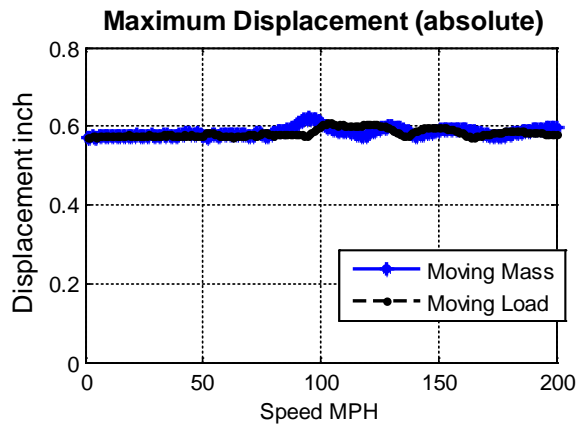


Figure 4.12 Vertical bridge response (maximum absolute displacement) at mid-span of bridge for the work train

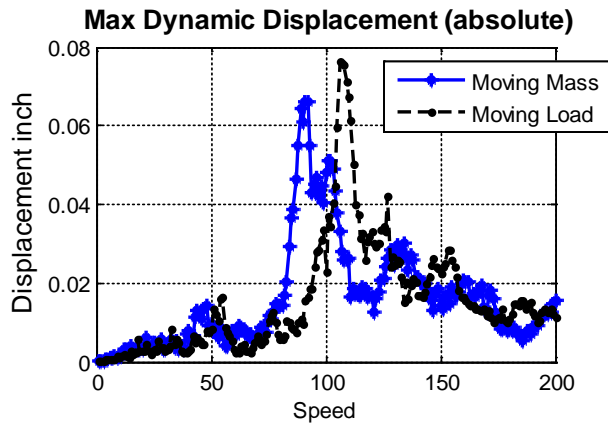


Figure 4.13 Vertical bridge response (maximum dynamic displacement) at mid-span of bridge for the work train

4.3.2 Lateral Bridge Resonance

The Illinois research team adjusted the stiffness of the simple beam model so that the first natural frequency matches the first lateral frequency of the bridge. The source of these lateral forces may come from the tilt of the bridge, the lateral wheel-rail contact forces, train hunting, track irregularities, wheel irregularities, car vibrations, etc. In this assessment, the research team assumed that lateral force is proportional to the vertical force. Figure 4.14 shows the maximum lateral displacement predicted by the moving-mass and the moving-load models.

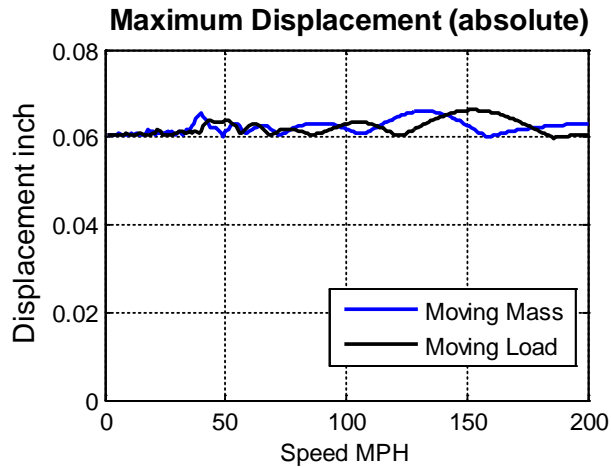
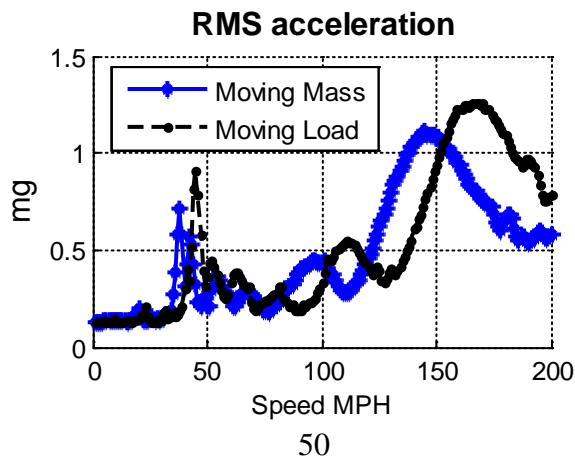


Figure 4.14 Maximum lateral displacement of the beam-mass model under various speeds at mid-span of bridge for the work train

Figure 4.15 shows the maximum acceleration for various speeds of the work train. The first critical speed for the lateral directions for moving mass case is around 38 MPH while critical speed for the vertical case was around 90 MPH. This result occurs because the bridge's first lateral natural frequency (1.5 Hz) is about 40% smaller than the first vertical frequency. Therefore, the critical speeds of the bridge are proportional to the fundamental frequency of the bridge, while the maximum responses are proportional to the weight of the train. Once again, the moving-load model provides unconservative results.



**Figure 4.15 Lateral response of the beam-mass model under the test train
(RMS of acceleration)**

4.3.3 Resonance Under Amtrak Train

Similar simulations using the moving-mass model predicted critical speeds under Amtrak traffic over the CN bridge. A typical Amtrak train contains eight cars, including the locomotive, and weighs approximately half of the tested work train. The speed under the Amtrak loading was also varied from 1 MPH to 200 MPH. Figure 4.16a shows the vertical RMS acceleration for different speeds for the Amtrak traffic. Because the cars of the Amtrak train are lighter than the cars from the tested worked train, the critical resonance speed is higher (185 MPH in the moving mass case).

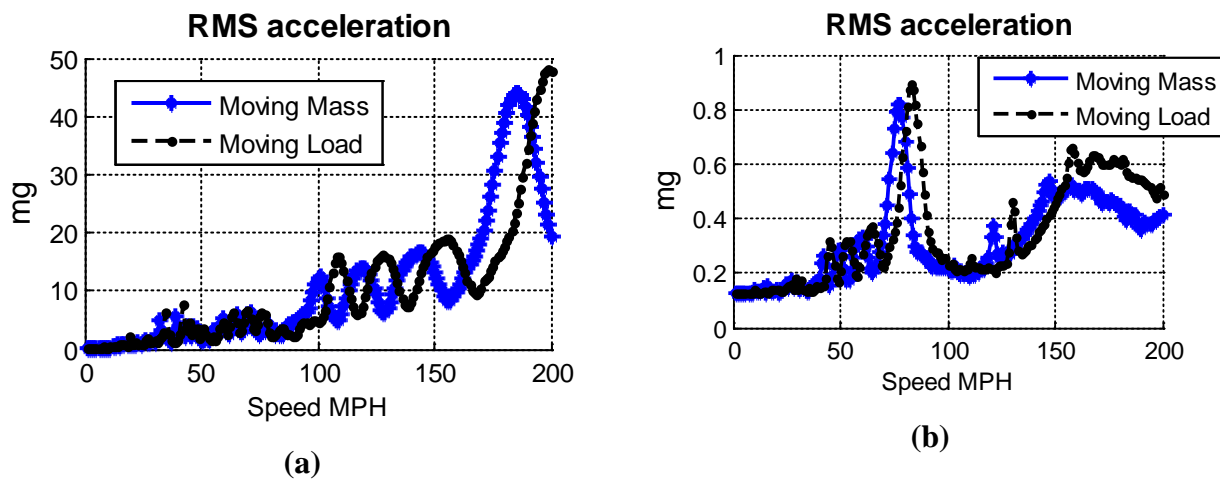


**Figure 4.16 Maximum vertical bridge response under Amtrak trains:
(a) vertical, (b) lateral**

The research team calculated lateral responses under the Amtrak traffic by applying a lateral force of about 1.8% of the vertical load. Figure 4.16b shows the results of these simulations. Because of the smaller first lateral fundamental frequency of the bridge, the resonance speeds occur at slower speeds (78 MPH for the moving mass case and 85 MPH for the moving load case) than those in the vertical direction.

4.3.4 Comparison with Traditional Approach to Estimate Bridge Resonance

An alternative approach to estimating resonance speeds relates the ratio between the spacing of the loads to the critical speeds; the critical speed is proportional to the load spacing and the frequency of the bridge, as shown in Equation (15) and in Figure 4.17:

$$\frac{d}{c} = \frac{k}{f_j} \quad , \quad \text{where } j = 1, 2, 3, \dots, \quad \text{and } k = 1, 2, 3, \dots, \frac{1}{2}, \frac{1}{3}, \dots \quad (15)$$

The first vertical and lateral natural frequencies of the bridge are 3.6 Hz, and 1.5 Hz, respectively. The main source of the resonance comes from the spacing of the loads applied to the bridge. The

dimensions of the last five vehicles of the work train are similar, while four cars have the dimensions of a 30000 series CN car (see Figure 4.18). The multiple distances between the loads (car-to-car distance, axle-to-axle distance, out-to-out distance between wheels) and their combinations can be entered into an equation (15), where the various associated critical speeds under the work train causing lateral resonance are proportional to the load excitation of the lateral frequency. Figure 4.19 compares this approach with the results of the vertical and lateral resonance estimation using the simple beam model. The dominant critical speeds estimated by the simplified beam model are 86 MPH and 38 MPH for vertical and lateral direction, respectively. Critical speeds estimated from the traditional method coincide with those found by the simple beam model; however, the traditional method cannot identify other critical speeds under this loading and in this direction. Furthermore, even if multiple load spacing vectors can determine different critical speeds, their relative severity to the excitation of the bridge response is not measured.

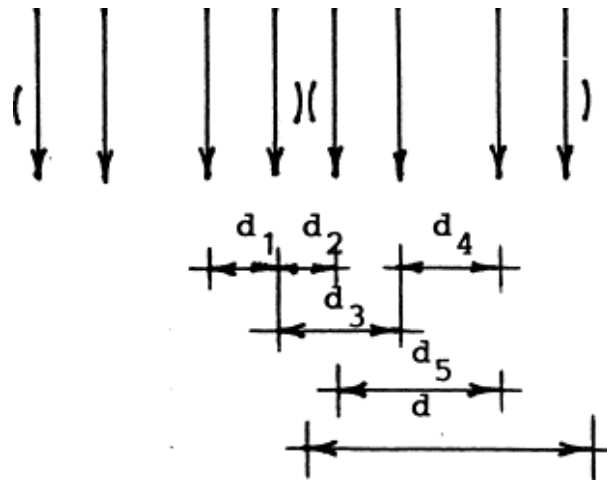


Figure 4.17 Loading distances potentially generating resonance in the bridge

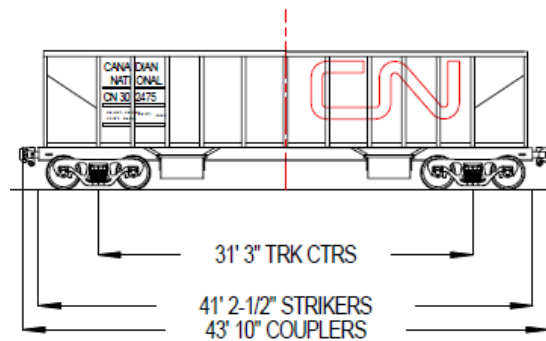
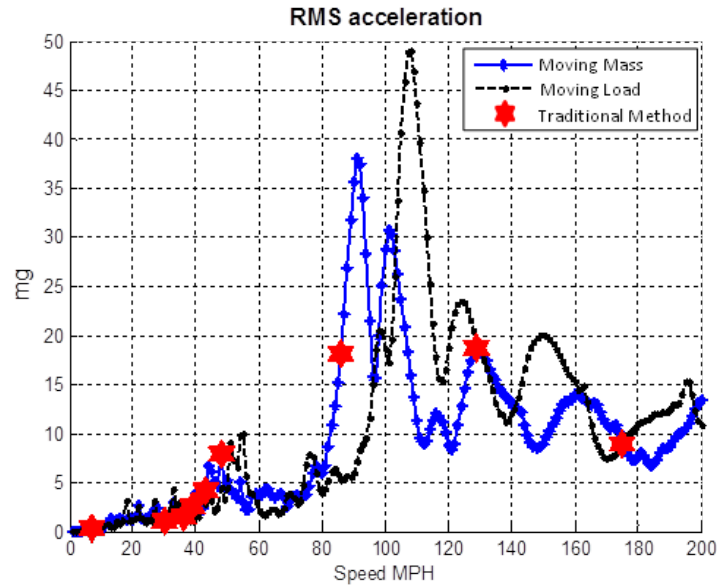


Figure 4.18 Car diagram for work train vehicle

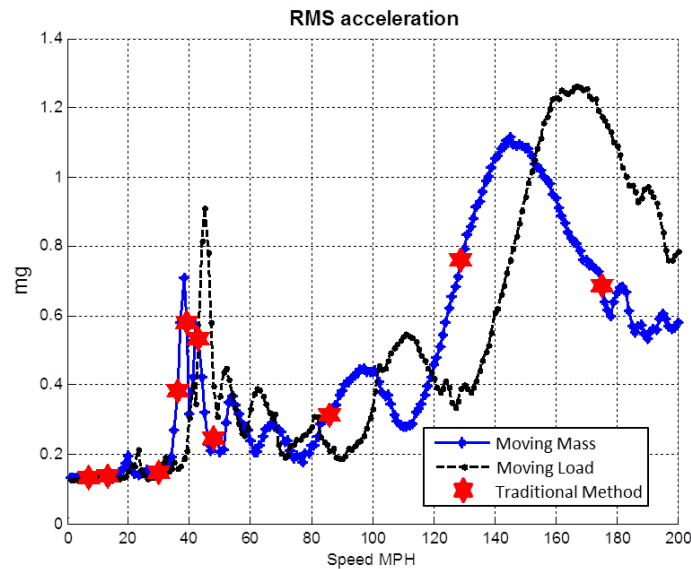
This section estimated the bridge resonance speeds under different traffic conditions using a moving-mass beam model and the input loading and spacing applied to the bridge. This research showed estimations for bridge resonance in both vertical and transverse direction for a range of train speeds from 1 to 200 MPH. This research also compared the critical speed results from this moving-mass beam model with traditional resonance estimations.

4.4 Reference-Free Displacement Estimation

One of the main research needs of the railroad bridge engineering community is the capability to easily estimate railroad bridge displacements under in-service train loads.¹ In past efforts, displacement has been estimated from acceleration measurements to provide a reference-free measurement of the bridge response. However, the available algorithms can only estimate zero mean displacements and, as has been shown earlier in this report, pseudo-static deformation levels are in general much larger than the dynamic displacements.



(a)



(b)

Figure 4.19 V_{cr} comparison for resonance under work train (a) vertical, (b) lateral

Preliminary research shows that displacement estimates using the Kalman Filter (KF) technique (see Figure 4.20) can determine responses in a system given different measurements (see Figure 4.21). To estimate the bridge displacement using multi-metric sensing measurements, the Illinois research team used the KF technique with the simple beam model. The KF estimator can predict displacements from any point of the model, without the need of a measurement reference.

The Illinois research team conducted experiments and calibration for this KF technique and included the results obtained from this approach in this project's final report. Then an assessment of railroad bridges to railroad traffic running at higher speeds could be done in reference to railroad bridge displacements under moving loads at different speeds by installing two sensors at the bridge in those locations of interest to the railroad (one at the mid-span and another one at the bridge approach). The multi-metric monitoring campaign can obtain and measure both the loads and bridge responses at these two locations in the field in real time. The predictive power of this simple beam model in the field can effectively inform the engineering team that is monitoring the bridge about the bridge's health.

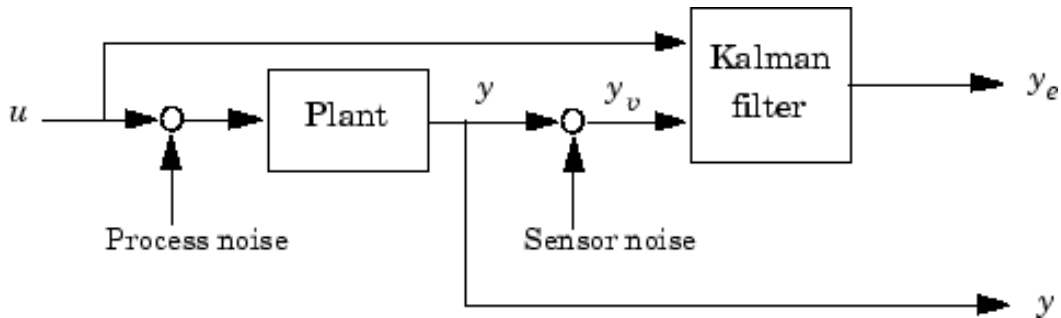


Figure 4.20 KF estimator

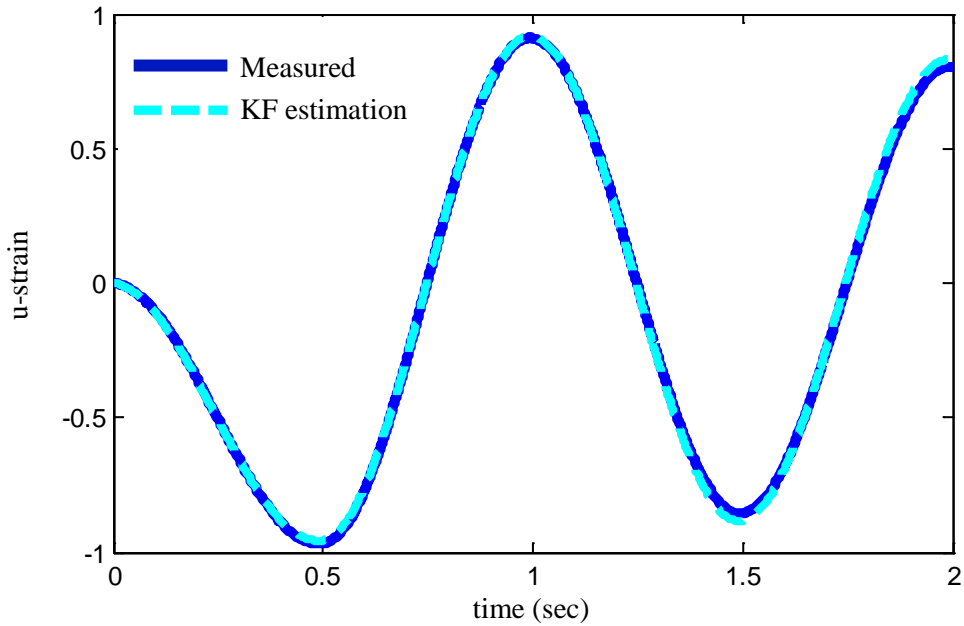


Figure 4.21 KF estimation¹⁶

The remote sensing system installed on the bridge can collect input loads and bridge responses (accelerations and strains) of specific points under train loading. Using that information as inputs, the KF estimation can provide displacement measurements under different traffic conditions to assess bridge performance.

The Illinois research team used the simple beam model to compare measured and estimated responses from the bridge, and they chose to measure the location within the CN model structure in the middle of the truss (see Figure 4.22). Applying the KF estimation technique, Figure 4.23 compares measured values and estimated values such as displacements, accelerations, and shears. The accuracy of the estimations shows that this tool can yield useful bridge displacement estimations under trains without a reference point.

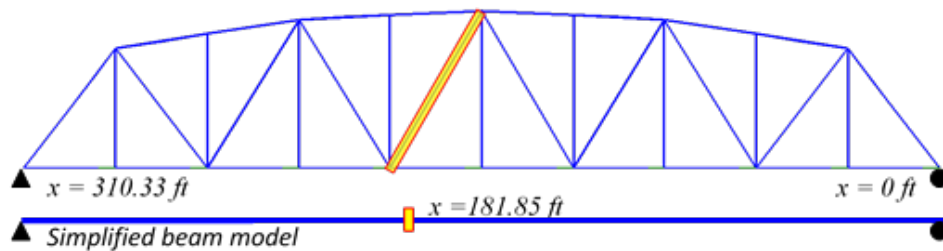


Figure 4.22 Simple beam model for KF displacement estimation

¹⁶ Jo & Spencer (2013). Multi-Metric Model-based Fatigue-Life Monitoring of Bridges. International Symposium on Innovation & Sustainability of Structures in Civil Engineering (ISISS-2013). July 6-7, 2013, Harbin, China.

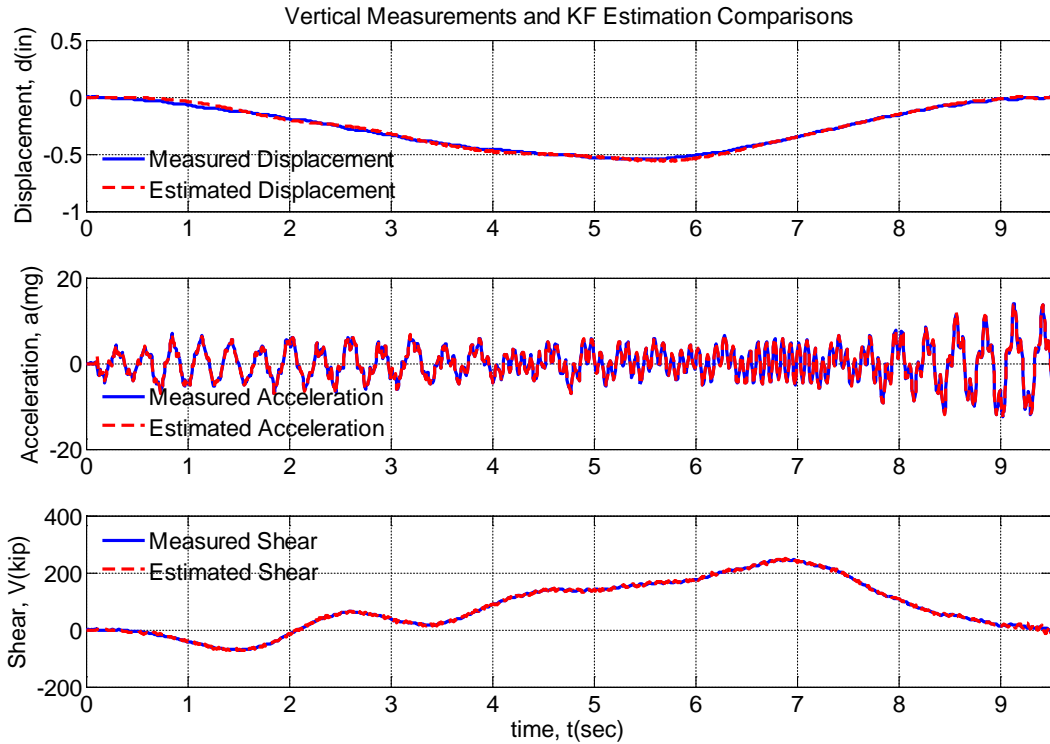
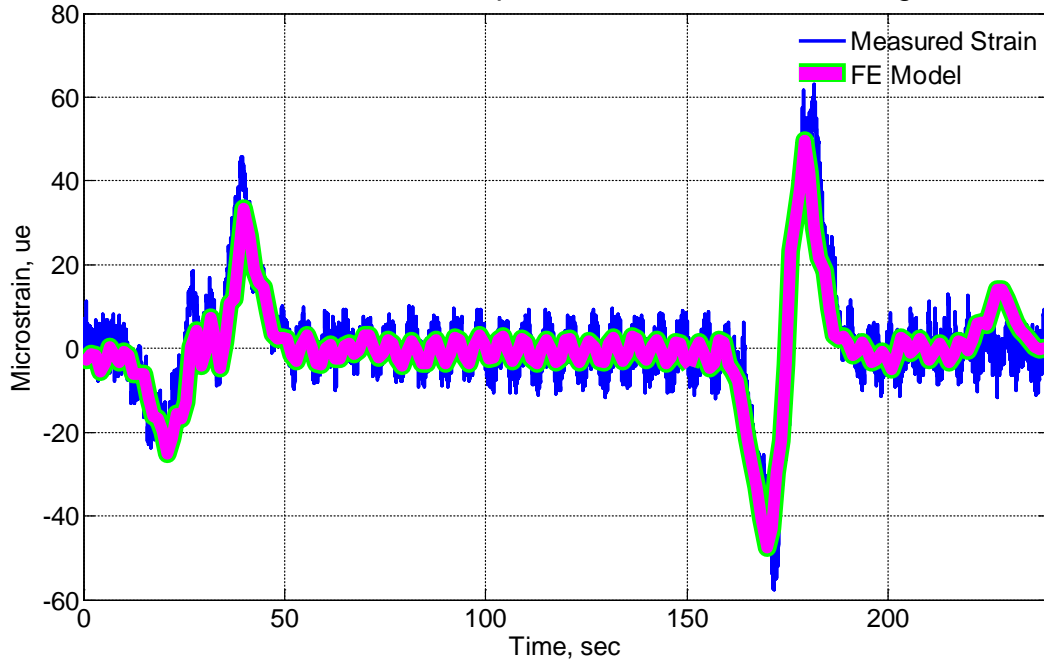


Figure 4.23 KF numerical example results

4.5 Sample Analysis of Autonomously Collected Data

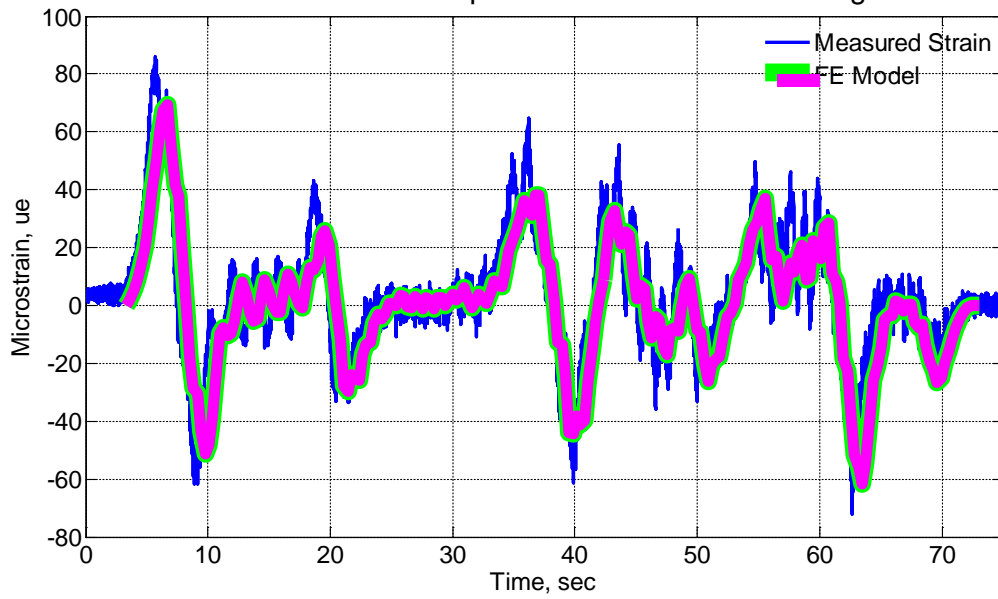
This section presents results from the analysis of data collected by the Auto Monitoring service. Figure 4.24 shows the measured strain data for two different trains that crossed the bridge while using Auto-Monitor, as compared with the estimated strain level. The strain comparisons show a high level of agreement, demonstrating again the predictive potential of the FE model. This tool was also used to predict the stress levels of all the members in the truss and compare them to the design unit stresses to ensure that the predicted stress levels are similar to the design unit stresses for live loading in the bridge. Figure 4.25 shows the labeling of the truss members. Figure 4.26a shows the maximum stress as a percentage of the design stress for each element in the truss under various train loads. Because this bridge has two tracks, the design assumes two trains are present on the bridge. Thus, Figure 4.26b shows the maximum stress as a percentage of the design stress, assuming there are two trains on the bridge. The results show that the stresses predicted by the FE model successfully estimate the stress levels stipulated in the design specifications.

L4U5 Structural Element Strain Comparison under Automonitoring NB Train 9 MPH



(a)

L4U5 Structural Element Strain Comparison under Automonitoring SB Train 33 MPH



(b)

Figure 4.24 Auto Monitoring validation (a) NB train 9 MPH, (b) SB train 33 MPH

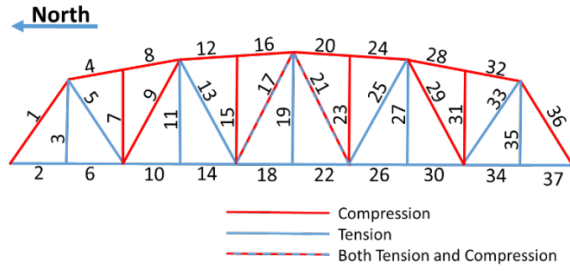
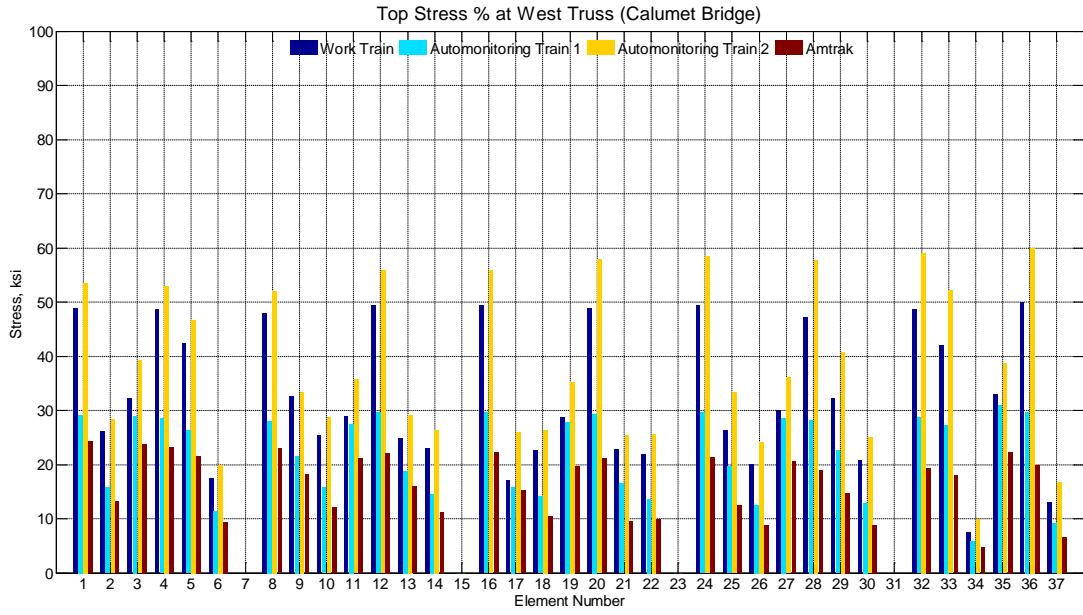
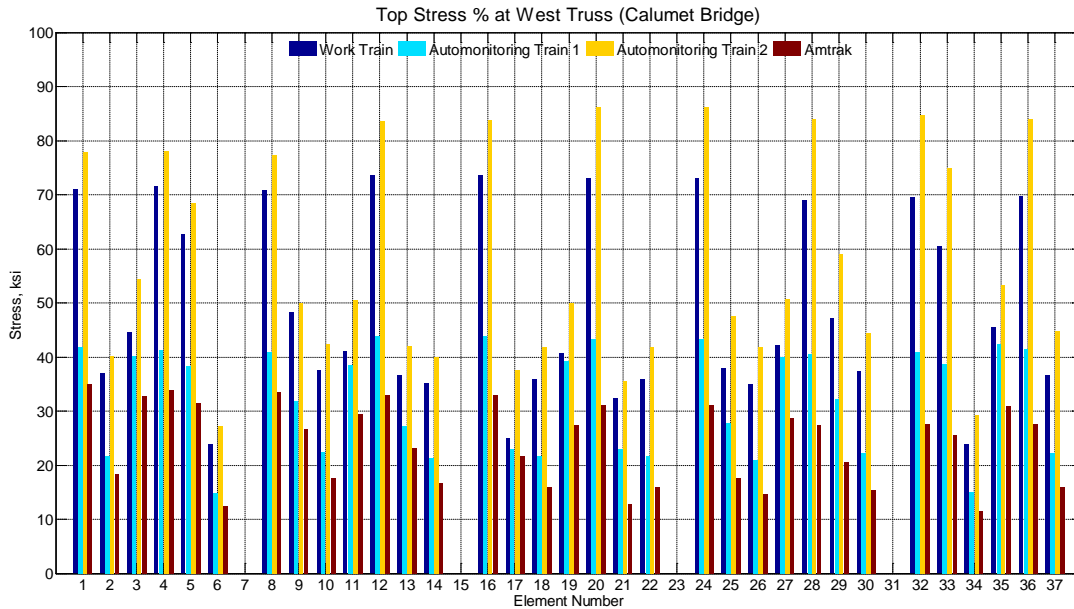


Figure 4.25 Truss element labeling



(a)



(b)

Figure 4.26 Predicted stresses percentages under open regular traffic (a) one train on West track, (b) two trains

4.6 Prioritization of Railroad Bridge Repairs and Replacement

This research provides a basis for developing a database of expected railroad bridge behavior based on measured bridge responses. Such a database would enable the following method for quickly measuring railroad bridge behavior under trains (see Figure 4.27):

1. Conduct multi-metric campaign monitoring of acceleration and strain responses to determine natural frequencies and strain ranges under train loads.
2. Develop and calibrate the FE model from these measurements (only during first inspection).
3. Assess global bridge responses using the FE model.
4. Establish a simple beam model that characterizes the bridge based on field measurements.
5. For bridges in shared corridors, perform a resonance study of the bridge and calculate critical speeds under various train loads.
6. Perform a detailed inspection of those elements with high stress levels as identified in the FE model and simple beam model.
7. Combine KF on both simple beam model and FE model to estimate strain and displacement responses of bridge members.
8. Compare data collected and update models as needed.
9. Write report summarizing the bridge performance level based on the campaign monitoring data.

Railroads can use this information to prioritize railroad bridge repairs and make replacement policies.

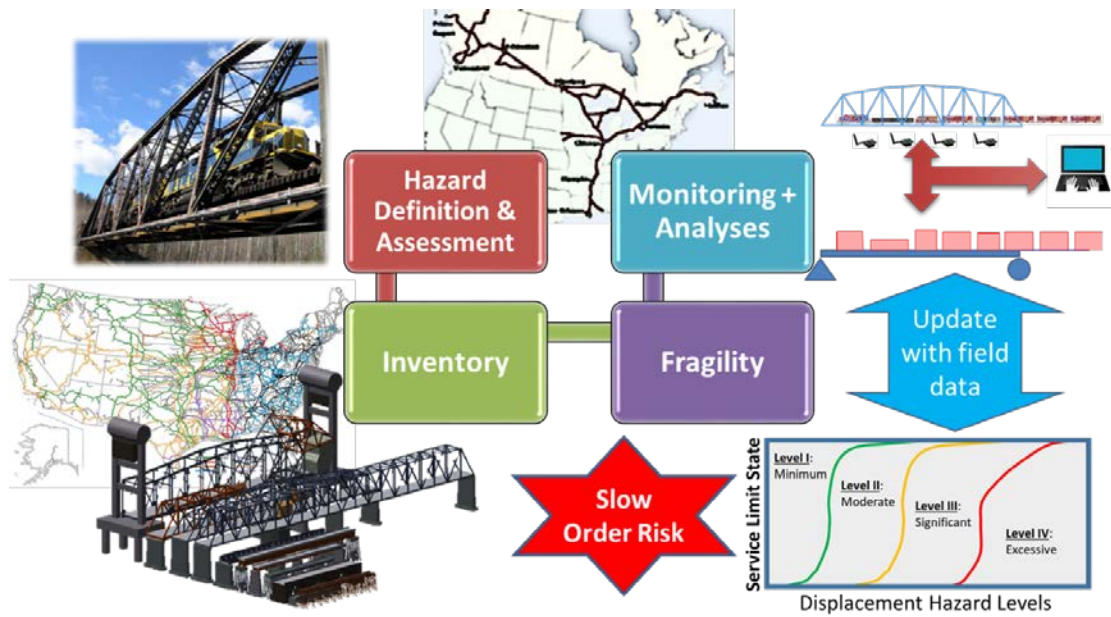


Figure 4.27 Simplified bridge campaign monitoring of railroad bridges

5. CONCLUSIONS

This research project has developed a portable, cost-effective, and practical SHM system for railroad bridges in North America using wireless smart sensors. The system has enabled campaign monitoring of in-service bridge responses and yielded new objective information about the performance of railroad bridges.

5.1 Summary of Achievements

- **Develop a framework for wireless monitoring of railroad bridges under train loads**

The Illinois research team adapted the wireless sensor technology developed by SSSL researchers into a framework for monitoring railroad bridge responses under train loads. They worked closely with CN personnel to understand the key concerns for railroad bridge performance in North America today and to tailor the system accordingly. The team deployed systems for both campaign and long-term monitoring on the CN bridge on the south side of Chicago and showed these systems to be appropriate for the harsh railroad environment and conditions.

The team also collected bridge responses under revenue service traffic (both freight and passenger [Amtrak] trains), including accelerations, structural strain, and rail strain. For example, researchers captured wheel-loading information at 280 Hz to estimate effectively wheel loads and speeds (even under Amtrak trains running at 65 MPH). Additionally, researchers verified the applicability of a magnetic strain checker for quick deployment and measurement of strains in both structure and rail in the railroad environment.

The team then used the data collected during the long-term monitoring of the bridge to validate the proposed methodology. The long-term monitoring deployment at the CN bridge allows multiple bridge responses under different trains to be automatically, continuously, inexpensively, and safely stored and sent to the University of Illinois. The researchers demonstrated the efficacy of new tools developed in this research, which can be used on different types of the bridges to enhance the applicability of the method and to help railroads develop databases of acceptable bridge responses. Finally, researchers installed a cellular internet connection for the bridge base station and implemented an autonomous email notification service that can alert railroad personnel of anomalous bridge behavior.

- **Ability to calibrate/validate current numerical approaches experimentally, turning these models from explanatory in nature to having powerful predictive capabilities**

The research team developed a preliminary FE model, used the CN bridge drawings to inform sensor placement, then used the information collected by the wireless sensor system to update the FE models that had been developed. The calibrated FE model closely matched the experimentally-derived natural frequencies and mode shapes, as well as the measured strains, from the work train experiments. The team developed a GUI for convenient data representation to the user. Subsequently, the model predicted bridge responses under revenue trains that compared well with the measured data. This research demonstrates that the proposed framework can quickly and easily collect railroad bridge responses under train loads and use it to predict railroad bridge responses with a calibrated FE model.

- **Ability to harvest objective information about the in-service performance of bridges, offering the potential to improve safety and reliability and provide early warning regarding potential problems**

Using the calibrated FE model, researchers generated the strain map for the entire bridge for in-service train loads. Due to the relatively slower speed of the trains, the measured data demonstrated that the primary response of the bridge was pseudo-static. Wheel loads, spacing, and speeds were determined from two strain sensors placed on the rail. Subsequently, the maximum stresses/strains at arbitrary locations on the bridge were determined from the pseudo-static response of the FE model. With this model, the Illinois research team can provide a strain map of the structural elements in the bridge under any given train load. Preliminary results show the potential use of this strain map for fatigue assessment of the bridge.

Researchers also developed and calibrated a new moving-mass beam model using the information collected from a limited number of wireless smart sensors. This simple beam model included the mass of the train crossing the bridge, while past models ignored the participation of the train mass in the response of the bridge. This model, combined with KF theory, provides the basis for developing a new reference-free displacement estimation method using wireless measurements. Note that the moving-mass model provides an example of how to extend the FE model to have full dynamic capabilities.

- **Identification of fundamental issues affecting the dynamic behavior of a railroad truss bridge in response to various train loads and speeds**

The research team used the simple moving-mass beam model developed in this research to estimate the resonances of the truss bridge (both in the vertical and lateral directions) and identify the critical speeds under two different train loads scenarios: freight trains and Amtrak trains. They also showed that the traditional moving-load model provides unconservative results as the differences in estimating critical speeds using moving-mass and moving-load models become larger with heavier trains. Combined with campaign monitoring using only two wireless sensor nodes to calibrate the proposed model, railroad personnel can estimate critical speeds for similar bridge types.

- **Ability to improve prioritization of railroad bridge repairs and replacement for HSR in shared corridors**

This research provides a basis to improve the prioritization of railroad bridge repairs and replacements by developing a database of expected railroad bridge behavior based on measured bridge responses.

5.2 Gap Analysis

This section identifies technological gaps that new research still needs to address. Research that fills these gaps will achieve the full potential of this technology for managing railroad bridge infrastructure.

- **Develop framework for wireless monitoring of railroad bridges under train loads**

Gap #1: Currently, the system automatically initiates long-term monitoring measurements when the acceleration or strain reaches a certain level. The result is that the measurements begin after the train enters the bridge. A method is needed to initiate measurement prior to the trains entering the bridge.

Gap #2: The research team needs to develop and deploy appropriate algorithms on the wireless smart sensors that can directly provide information of interest to the railroads in real time. For example, the researchers will develop a performance index that compares the expected behavior estimated from the FE model.

- **Ability to calibrate/validate current numerical approaches experimentally, turning these models from explanatory in nature to having powerful predictive capabilities**

Gap #3: The models developed are for specific steel truss bridges. To ensure the universal use of the developed methodology, researchers need to develop calibrated models for other bridge types.

- **Ability to harvest objective information about the in-service performance of bridges, offering the potential to improve safety and reliability and provide early warning regarding potential problems**

Gap #4: To enhance the predictive capability of the models, dynamic FE models that include the train mass must be created.

Gap #5: This research has verified accuracy of the proposed reference-free displacement estimation approach numerically, but the simulated results still must be validated against measured data.

Gap #6: Researchers need to extend the proposed approach to reference-free displacement estimation to other bridge types within the railroad's inventory.

- **Identification of fundamental issues affecting the dynamic behavior of a railroad truss bridge in response to various train loads and speeds**

Gap #7: Researchers need to extend the moving mass model to other types of bridges in railroad inventories.

- **Ability to improve prioritization of railroad bridge repairs and replacement for HSR in shared corridors**

Gap #8: The tools for development of such a database are now available and researchers need to realize their benefits.

In summary, the results of this project provide a strong foundation for developing simplified and effective campaign monitoring of railroad bridges using wireless smart sensors. The gap analysis demonstrates that expanding this project will enhance the applicability of the developed methodologies to HSR and to different classes of the railroad bridges. The next chapter details further research needed to fulfill the vision and realize the benefits of using wireless smart sensors for North American railroads.

6. VISION FOR THE FUTURE

6.1 Background

Today, freight transportation in North America is widely considered to be the best in the world,¹⁷ with 40% of the nation’s freight tonnage carried by railroads¹⁸. Because many parts of the current railroad networks are over 100 years old, railroads in North America have doubled capital investments in the last few decades. For example, Class I railroads invested over \$12B in capital expenditures in 2012,¹⁹ with \$600M of this amount dedicated to railroad bridges.²⁰ This investment, combined with innovations in freight technology, has doubled the average tons of freight per train load²¹ and lowered freight costs per ton-mile by roughly 50%.²² However, US railroads expect to reach capacity over the next 20 years at many locations within their network (see Figure 6.1).²³

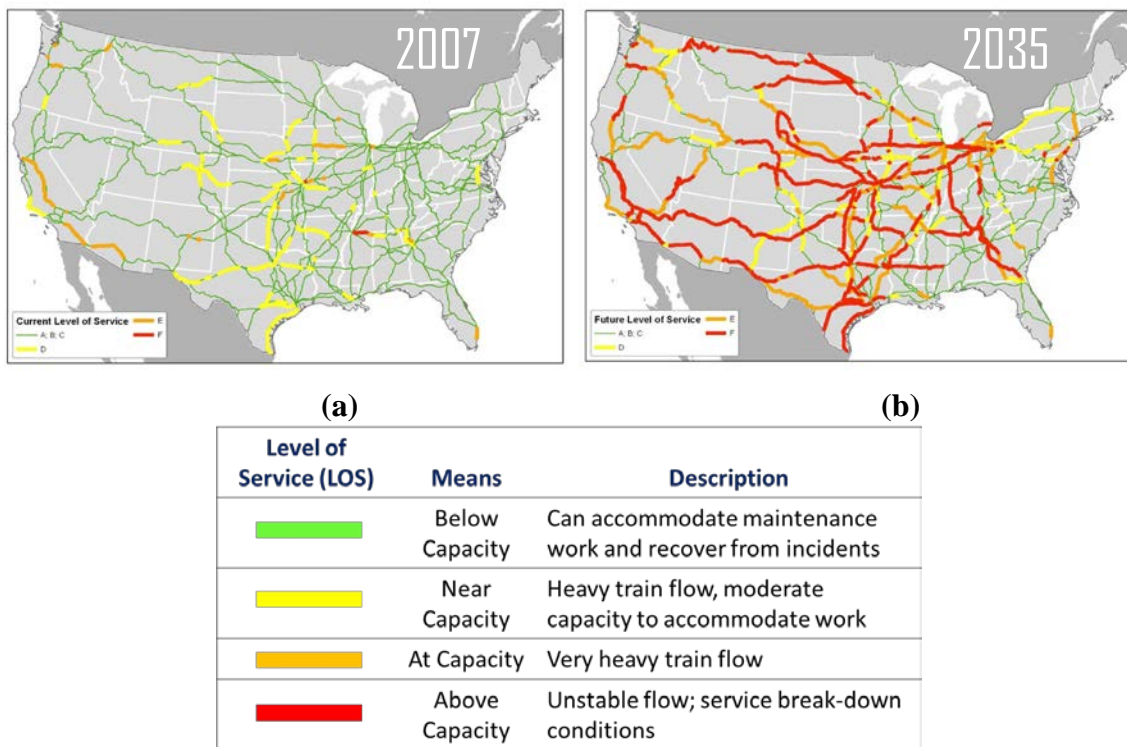


Figure 6.1 Railroad corridor capacities level of service: (a) in 2007 and (b) in 2035.

¹⁷ GeoMetrx. (2013, December 22) High Speed Rail: A Vision for the Future. geomtrx.com.

¹⁸ United States Government Accountability Office. (2007). Railroad bridges and tunnels; Federal Role in Providing Safety Oversight and Freight Infrastructure Investment Could Be Better Targeted.

¹⁹ Berman, Jeff, (2012, January 30) Class I railroads are on track to spend \$13 billion in 2012 capital expenditures, says AAR. Logistics Management.

²⁰ American Association of Railroads (AAR). (2013, December 22). <http://freightrailworks.org/>.

²¹ Weatherford, B. A., Willis, H. H., & Ortiz, D. (2008). The State of U.S. Railroads, a Review of Capacity and Performance Data. RAND Corporation.

²² Thompson, L. (2010). A vision for railways in 2050. International Transport Forum.

²³ Cambridge Systematics, Inc. (2007, September). “National Rail Freight Infrastructure Capacity and Investment Study”, prepared for the AAR.

The 2025 Vision²⁴ from the American Society of Civil Engineers (ASCE) predicts: “In 2025, intelligent infrastructure (embedded sensors and real-time onboard diagnostics) have led to this transformation of rapidly advancing and adapting high-value technologies in the life of a structure. Real-time monitoring, sensing, data acquisition, storage, and modeling have greatly enhanced the prediction time leading to informed decisions.” Further, this report states that engineers will be “relying on and leveraging real-time access to living databases, sensors, diagnostic tools, and other advanced technologies to ensure informed decisions are made” (see Figure 6.2). North American railroads need to move aggressively and implement this vision to meet future demands on its infrastructure.



Figure 6.2 ASCE 2025 Vision

6.2 Recommendations

Based on the outcomes of this pilot research effort, the gap analysis in Chapter 6, and the vision of the future put forth by ASCE, the Illinois research team recommends the following actions to realize of the full potential of wireless sensor technology in managing railroad bridge infrastructure:

- The technology, models, and algorithms developed and employed in the pilot study of the CN steel truss bridge should be extended to include other important classes of railroad bridges.
- The pseudo-static finite element model for railroad bridge, including the train mass, should be extended to include dynamic bridge response, further enhancing the predicative capability of these models.
- The simple moving mass model should be extended to include other types of bridges in the railroad’s inventory, which will provide a straightforward and accurate way to determine limiting speeds for railroad bridges.
- The proposed reference-free displacement estimation algorithms should be validated against measured data to further refine and demonstrate the potential of the approach. Additionally, this algorithm should be extended and demonstrated for other important bridge types within railroad inventories.
- The remote monitoring capabilities demonstrated in this pilot project should be further developed to allow for continuous monitoring of important bridge infrastructure.
- A living database of expected bridge responses should be developed for the benefit of the entire railroad industry.

²⁴ASCE. (2006). “The Vision for Civil Engineering in 2025.”

6.3 Proposed Research Tasks

In support of these recommendations, the following specific research tasks are proposed. Successful completion of these research tasks will constitute a major step toward realization of the full potential of the use of wireless sensor technology in the management of railroad bridge infrastructure.

Task #1: Inventory (Gap #3)

While the pilot research project successfully demonstrated wireless sensor technology for steel truss bridges, various types of railroad bridges exist in North America (see Figure 6.3), with 53% being steel, 23% being concrete, and 24% being timber.²⁵ The first task is to group bridges by type and specific performance concerns, then the research team will identify the bridges' relevance to the network. Further, they will assess which bridge responses are more important for each bridge type. Using this information, the team will choose the three most important bridge types for investigation in the follow-on research.

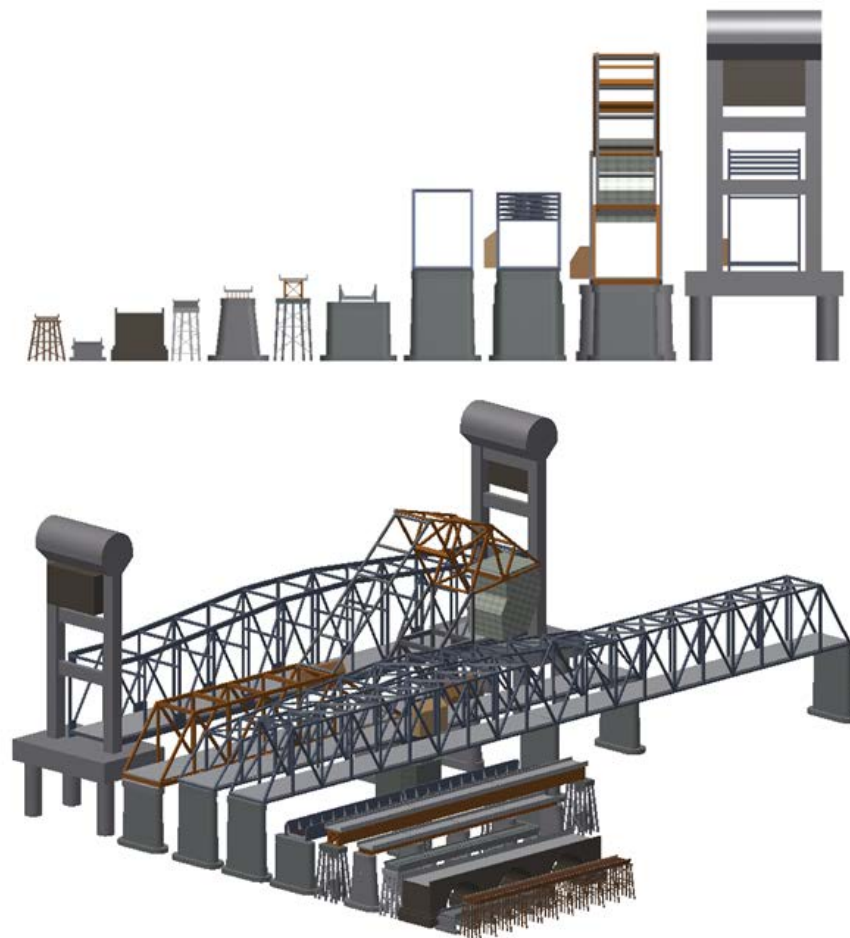


Figure 6.3 Railroad bridge classification towards campaign monitoring

²⁵AREMA (2008). Bridge Inspection Handbook© 2008

Task #2: Campaign Monitoring (Gap #3)

Researchers will conduct campaign monitoring for each of the railroad bridge types identified in the previous task. Campaign monitoring to assess bridge performance level under regular traffic will be conducted in coordination with the railroad (CN, Burlington Northern Santa Fe, and others). To confirm the predictive capability of the model for bridge condition, researchers in close coordination with the railroad will monitor three different bridge conditions of a similar bridge type.

Task #3: Dynamic FE Model (Gaps #3, 4)

Researchers will extend the FE model to be fully dynamic, incorporating the effect of the moving mass of the train. This new FE model will enable prediction of dynamic bridge responses using measured rail strain monitoring. The validation of this model will be a pivotal part of developing a library of bridge models, as described in the Task #5.

Task #4: Simplified Model (Gaps #3, 7)

Researchers will extend the moving-mass beam model to represent the behavior of the other bridges considered in this study.

Task #5: Bridge Model Library (Gaps #3, 4)

Researchers will develop a library of railroad bridge models based on the bridge types selected in Task #1. These structural engineering models will capture the main responses of interest to be tracked during campaign monitoring. The research team will determine the number and detail of the models iteratively. The models need to show predictive capabilities such as those of the pilot project.

Task #6: Performance Index (Gaps #2, 5, 6)

This task identifies the critical bridge responses under train loads for each of the bridge types described considered. Researchers will establish a performance index that compares the expected bridge response determined from the FE model for a given bridge type to the measured normalized quantity collected in the field in real time. The difference between measured and expected responses provides an assessment of the state of the bridge.

Task #7: Wireless Node Enhancements (Gap #1)

Based on the project's experience with wireless campaign monitoring, researchers will propose specific wireless node enhancements to improve monitoring activities. For example, to support autonomous monitoring, the research team will develop a strategy to initiate measurement prior to the trains entering the bridge. These enhancements will support the bridge model library.

Task #8: Database of Expected Bridge Responses (Gap #8)

The Illinois research team will create a database for assessing bridge performance. This database will be based on bridge type, dynamic models of bridge responses under trains, and data from bridge campaign monitoring.

APPENDIX: Abbreviations and Acronyms

| | |
|---------|--|
| AAR | American Association of Railroads |
| AREMA | American Railway Engineering and Maintenance-of-Way Association |
| ASCE | American Society of Civil Engineers |
| CN | Canadian National |
| FE | Finite Element |
| FRA | Federal Railroad Administration |
| GUI | Graphical User Interface |
| GAO | United States Government Accountability Office |
| HSR | High-Speed Rail |
| IF | Impact Factor |
| ISHMP | Illinois Structural Health Monitoring Project |
| IV | Superstructure-Vehicle Interaction |
| KF | Kalman Filter |
| LVDT | Linear Variable Differential Transformer |
| MPH | Miles per hour |
| NB | North Bound |
| NS | Norfolk Southern |
| PSD | Power Spectral Density |
| RailTEC | Rail Transportation and Engineering Center |
| RE | Vehicle Rocking |
| RMS | Root Mean Square |
| SB | South Bound |
| SHM | Structural Health Monitoring |
| SHM-A | Structural Health Monitoring – Accelerometer (sensor) |
| SHM-H | Structural Health Monitoring – High Sensitivity Accelerometer (sensor) |
| SHM-S | Structural Health Monitoring – Strain (sensor) |
| SSTL | Smart Structures Technology Laboratory |